GDR CNRS Pulse

Mesure *in situ* de la courbure: principe, limitations et étude de cas

Grégory Abadias

Professeur, Université de Poitiers, France

Institut P', Département Physique et Mécanique des Matériaux,

Outline

- ✓ Introduction
- ✓ Origins of residual stress in PVD thin films
- ✓ Mechanics of thin plates: curvature and stress
- ✓ Experimental determination of wafer curvature
- ✓ Selected examples
  - ➲ Multilayers
  - ➲ Epitaxial growth and stress relaxation
  - ➲ Stress evolution during Volmer-Weber growth
- ✓ Coupling with other *in situ* diagnostics
  - ➲ interface reactivity: Cu on *a*-SiOx and *a*-Ge
  - ➲ segregation in Au/Ni multilayers
  - ➲ phase transformation in Mo/Si

Introduction

Organic electronics and flexible electronic displays

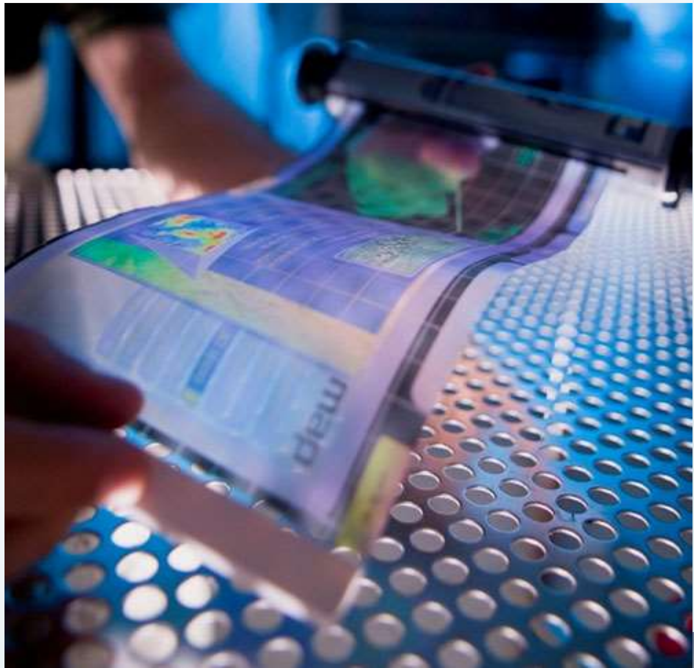

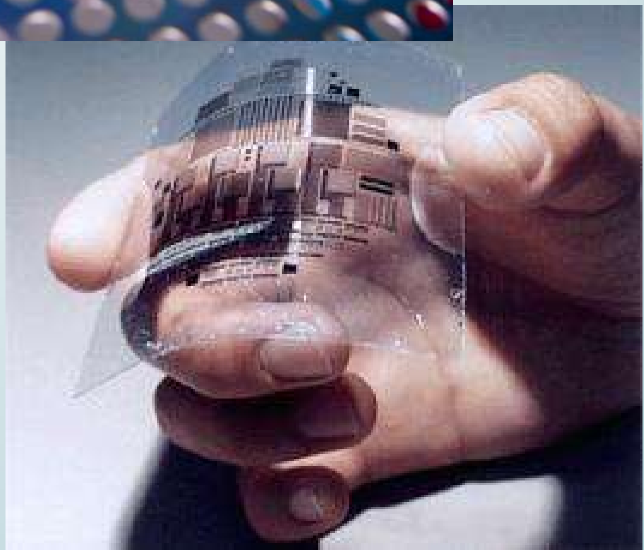

Thin film solar cells on flexible substrates

Amorphous Silicon (a-Si)
Cadmium Telluride (CdTe)
Copper Indium Gallium Selenide (CIGS)

Introduction

compressive stress

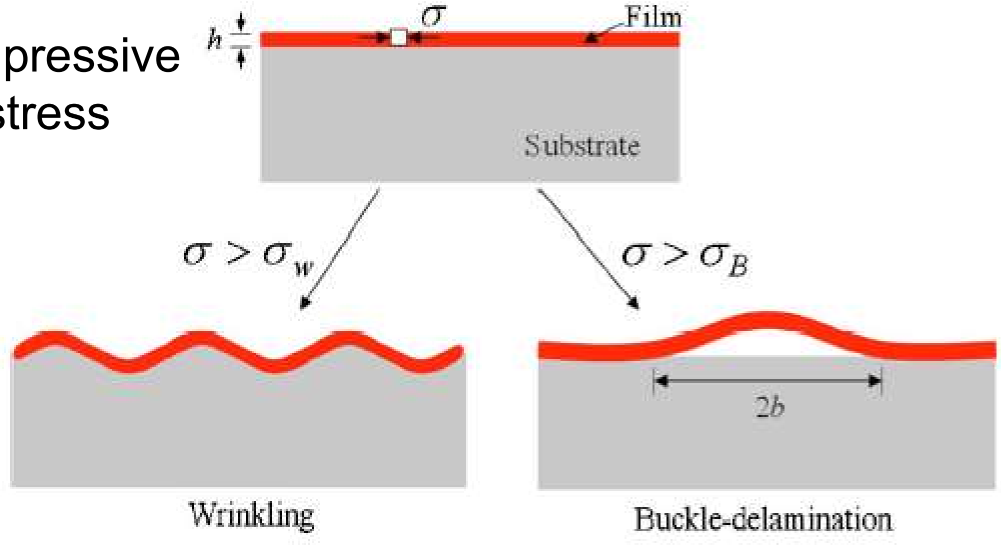

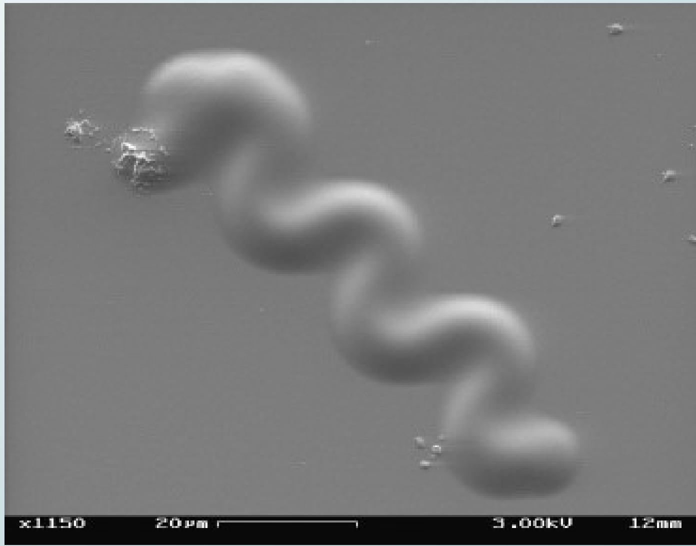

H. Mei et al., APL **90**, 151902 (2007)

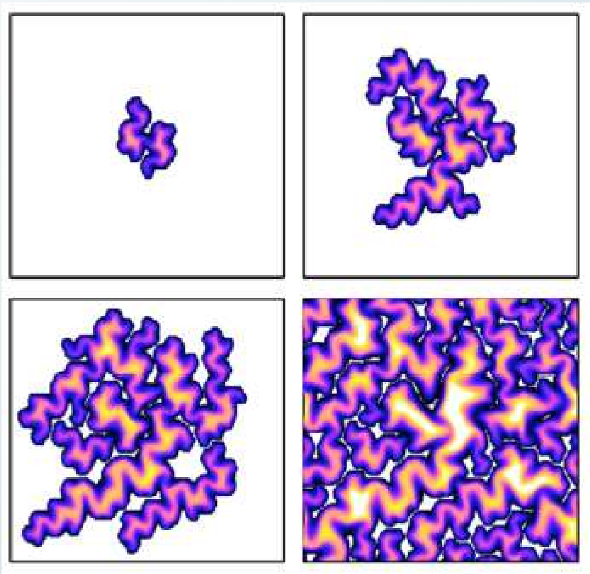

E.A. Jagla, PBR **75**, 085405 (2007)

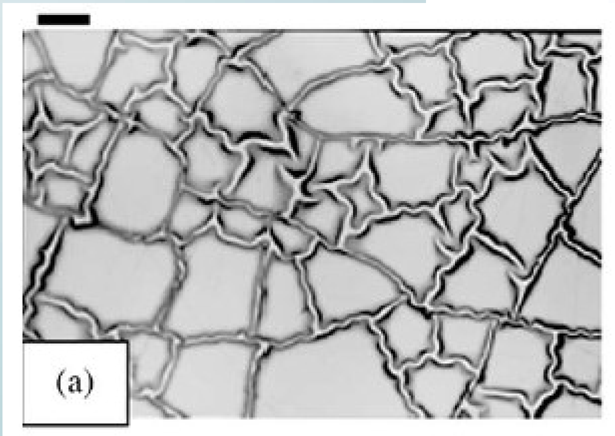

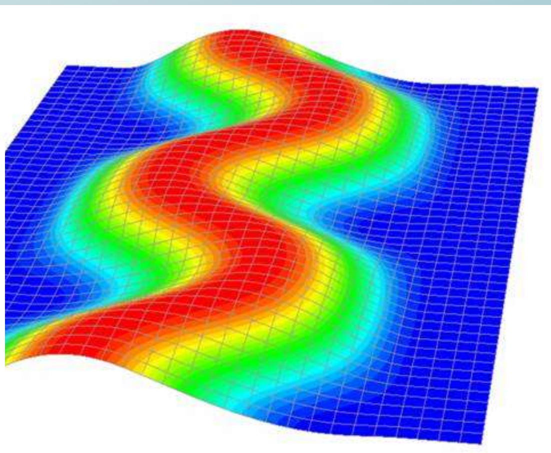

C. Coupeau , Thin Solid Films 406 (2002) 190–194

Introduction

tensile stress

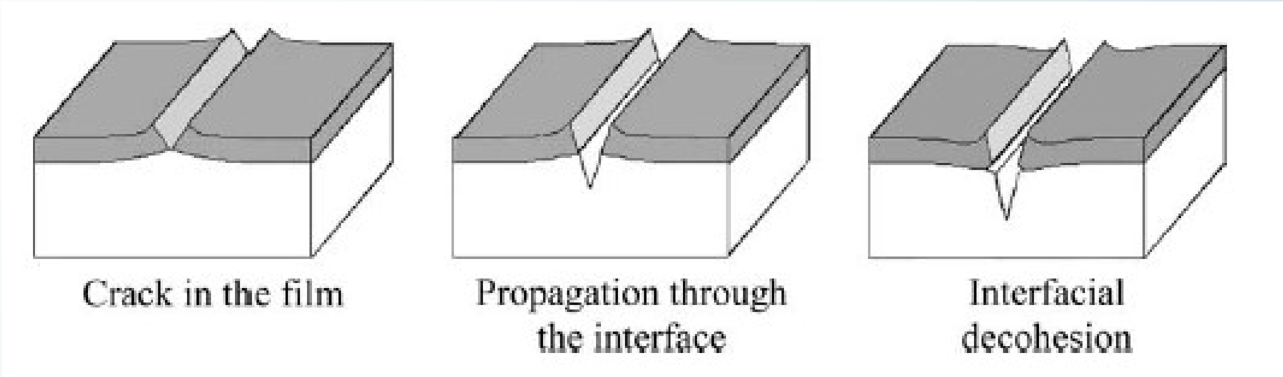

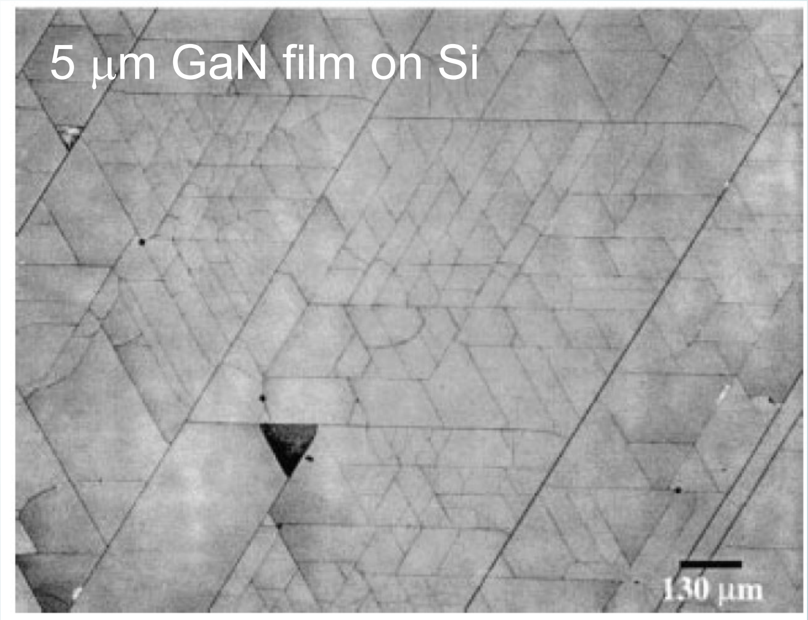

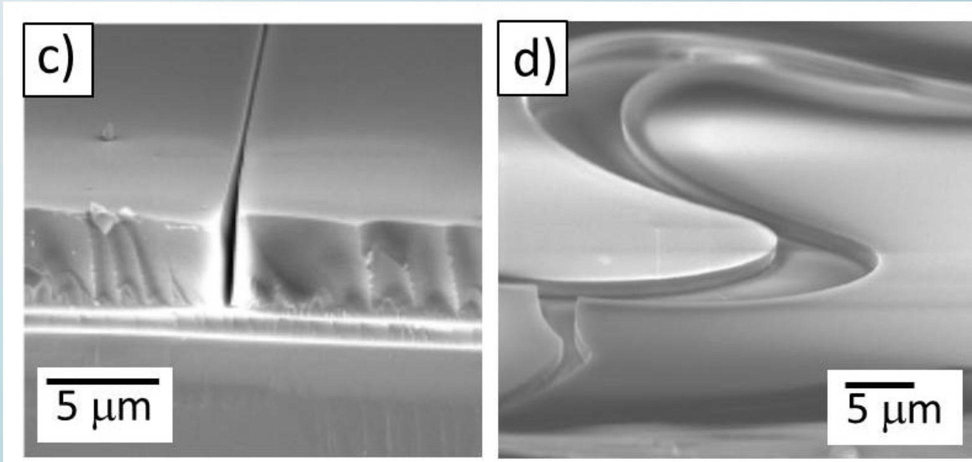

Marthelot et al, PRL **113** (2014) 085502

V.B. Shenoy, International Journal of Fracture **109:** 29–45 (2001)

Fabrication de micro-rouleaux ou d'origami

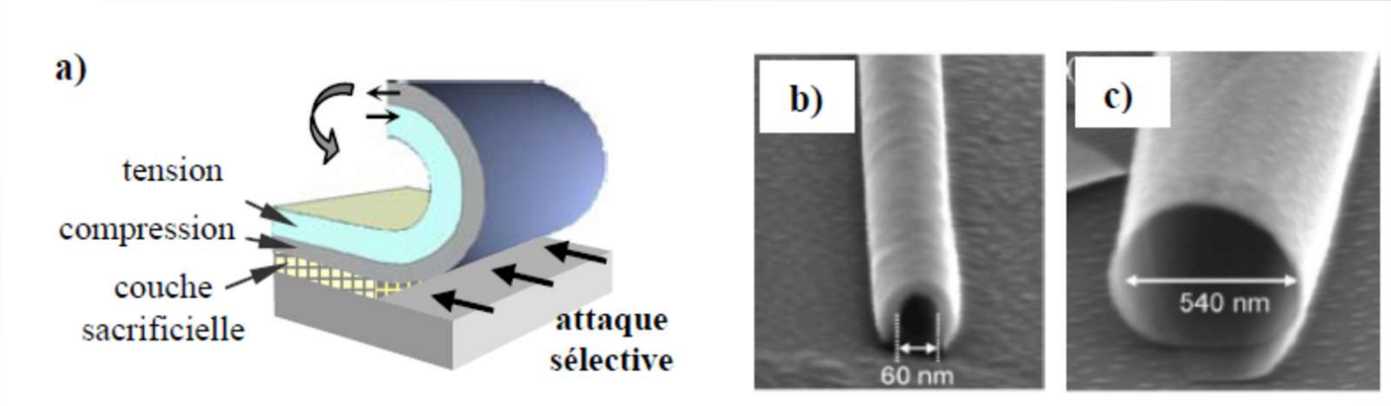

V. Prinz et al., Physica E ***6****, 828, 2000*
S. Golod et al., Appl. Phys. Lett. ***84*** *(17), 3391, 2004*

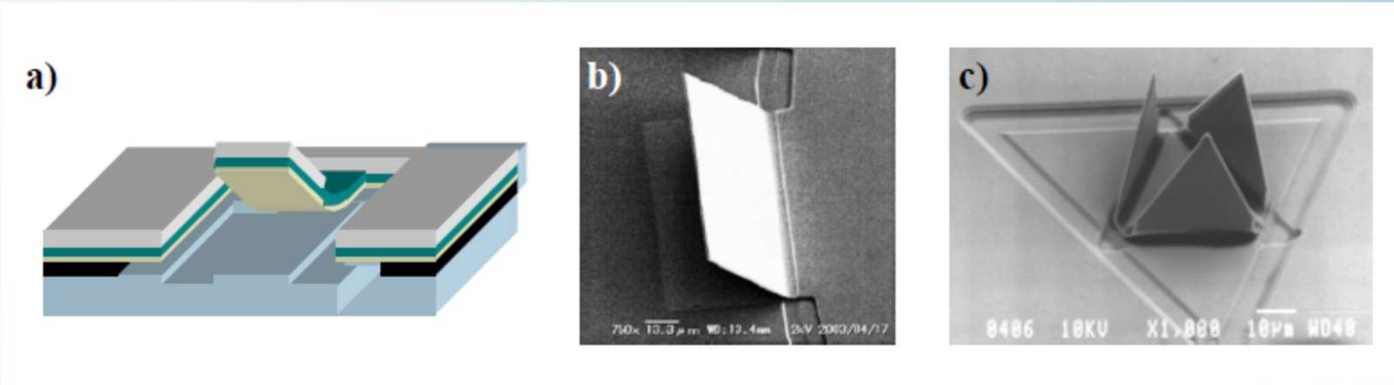

C. Fontaine, Chapitre 10, "Exploitation des contraintes dans les structures à base de semi-conducteurs" , Ed. Hermes (2006)

Why thin films are usually in a stressed state?

This is because the lateral dimensions of the layer are fixed by those imposed by the macroscopic (and infinitely rigid) substrate

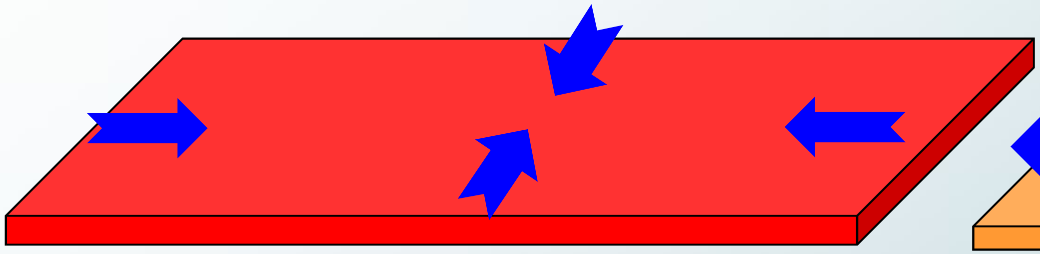

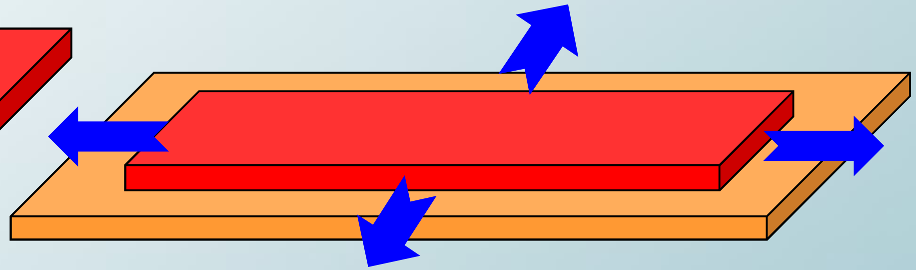

❶ layer > substrate

❷ layer < substrate

compressive stress state
$\sigma < 0$

tensile stress state
$\sigma > 0$

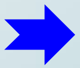 Force (in Newton) applied in the film plane

Definitions

- Definition: a stress (σ) is a force (F) per unit surface area (A): **σ = F/A**
- Unit: Newton per square meter: **N/m^2** or Pascal **(Pa)**
- A stress is therefore a quantity homogenous to a **pressure**
- It is a third order, 2^{nd} rank **tensor**

$$\overline{\overline{\sigma}} = \begin{pmatrix} \sigma_{11} & \sigma_{21} & \sigma_{31} \\ \sigma_{12} & \sigma_{22} & \sigma_{32} \\ \sigma_{13} & \sigma_{23} & \sigma_{33} \end{pmatrix}$$

- Origin: stress arises due to presence of (internal or external) forces which are generated in the deformed layer
- Characteristics:
  - For thin layers, the presence of a free surface sets that the stress generated in the layer is usually ***biaxial*** = in the film plane, i.e., the σ_{33} component is zero
  - If the substrate is sufficiently thin, then it can curve as a result of stress in the layer

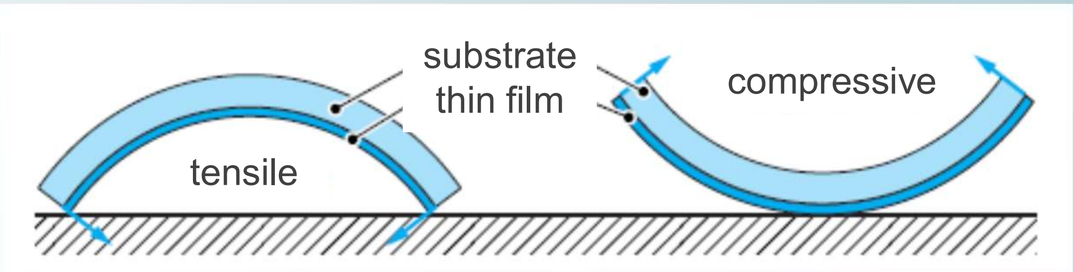

The curvature is κ=1/R given in m^{-1}

concave radius of curvature on the film side (R>0)

convex radius of curvature on the film side(R<0)

Stress and strain

- Characteristics (cnt'd): **stress** and **strain** in polycrystalline thin films

Schematic representation (cross-section)

Tensile stress

Compressive stress

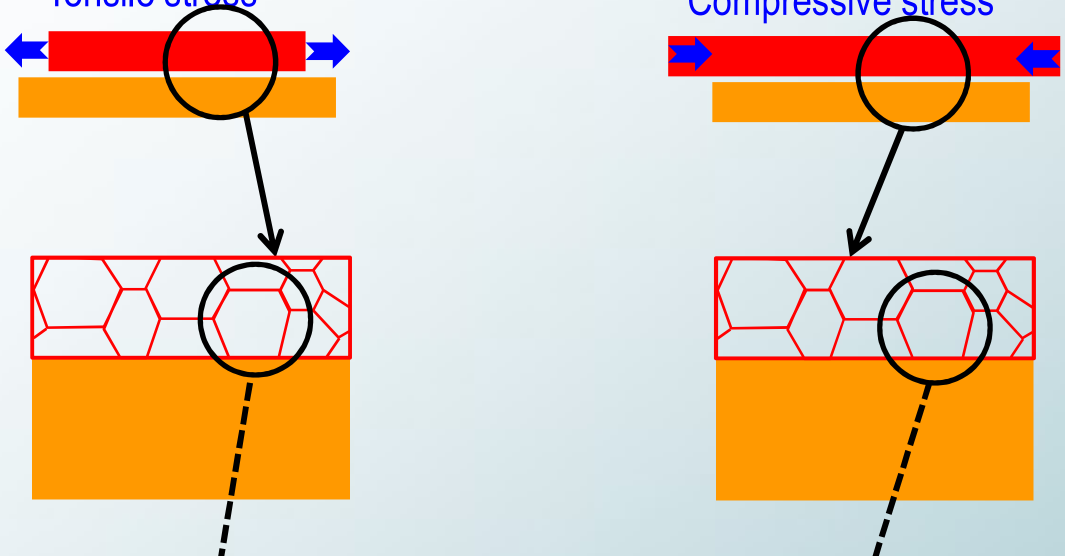

Gold layer (top view)

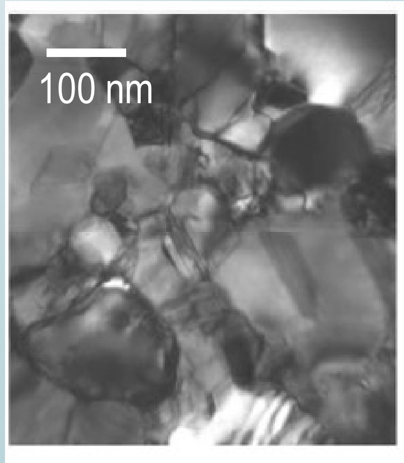

Lattice is **expanded** in the film plane: $\varepsilon_{//} > 0$
Lattice is **shrinked** along the film normal: $\varepsilon_z < 0$

Lattice is **shrinked** in the film plane: $\varepsilon_{//} < 0$
Lattice is **expanded** along the film normal: $\varepsilon_z > 0$

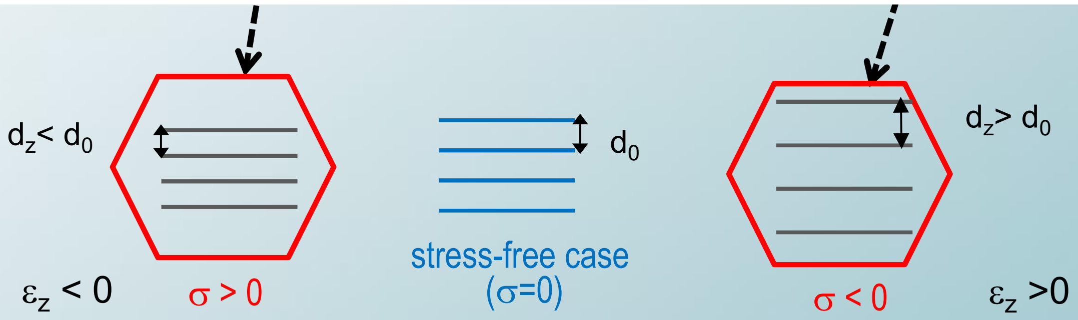

Elastic strain

$\varepsilon_z = \frac{d_z - d_o}{d_o}$ (out-of-plane)

$\varepsilon_\parallel = \frac{d_\parallel - d_o}{d_o}$ (in-plane)

Potentialities offered by curvature technique

- No need to know the elastic properties of the studied material
- Stress can be measured in amorphous (sub)layers
- In situ stress monitoring during growth
- Surface and interface stress can be uncovered
- Phase transition can be observed in real-time

Mo/Si multilayers

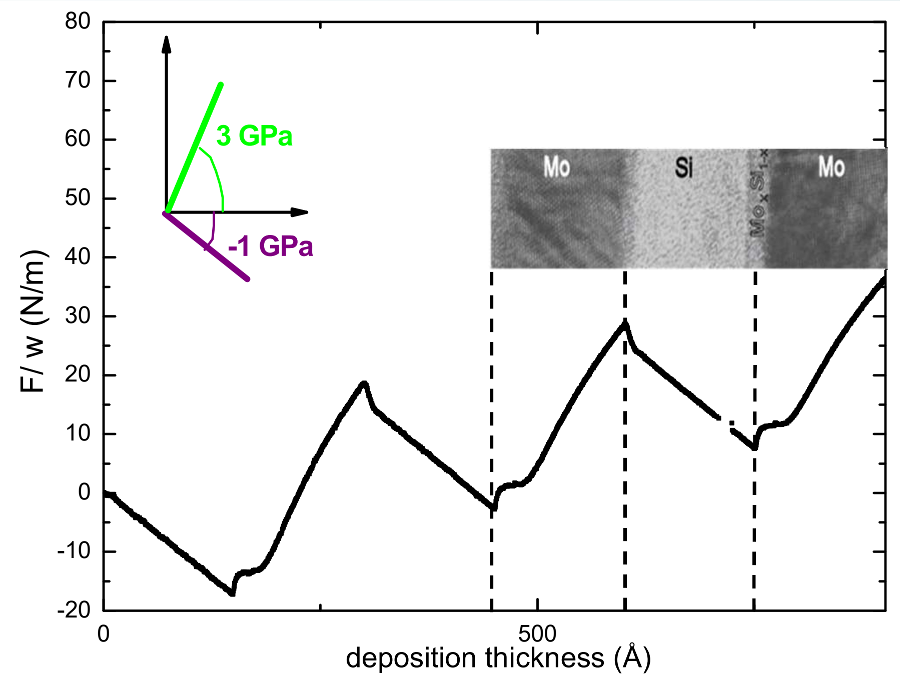

A. Fillon, PhD Thesis, Univ. Poitiers (2010)

Fe on Ir (001)

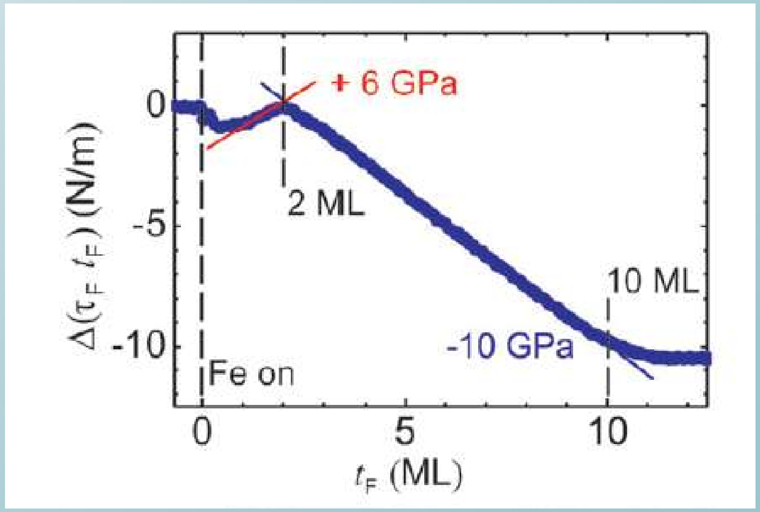

D. Sander et al., J. Phys.: Condens. Matter 21 (2009) 134015

Physical origins of stresses in thin films

Stress sources

- Usually, three stress components are distinguished

$$\sigma_{tot} = \sigma_i + \sigma_{th} + \sigma_{ext}$$

- Thermal stress σ_{th}

difference in thermal expansion coefficient between film and substrate and when $T_s \neq T_{amb}$

- Intrinsic stress σ_i

Stress source introduced during the PVD process: growth stress, coherency stress

- Extrinsic stress σ_{ext}

Induced by external factors: external loading, lifetime service, exposure to environment

Stress sources

- Usually, three stress components are distinguished

$$\sigma_{tot} = \sigma_i + \sigma_{th} + \sigma_{ext}$$

- Thermal stress σ_{th}

difference in thermal expansion coefficient between film and substrate and when $T_s \neq T_{amb}$

- Intrinsic stress σ_i

Stress source introduced during the PVD process: growth stress, coherency stress

- Extrinsic stress σ_{ext}

Induced by external factors: external loading, lifetime service, exposure to environment

Originates from strained regions
- ***within the film*** due to any micro-structural modification (grain boundaries, dislocation, voids), defects formation (point-defect, impurities, etc)
- *at the **film/substrate interface*** (lattice mismatch, intermixing, growth mode)
- *at the **film/vacuum interface*** (surface stress, adsorption)
- as a result of **dynamic** processes (interdiffusion, recrystallisation, etc…)

Stress sources

Possible mechanisms of intrinsic stress

- surface and/or interface stress,
- cluster coalescence to reduce surface area,
- grain growth, or grain boundary area reduction,
- vacancy annihilation,
- grain boundary relaxation,
- shrinkage of grain boundary voids,
- incorporation of impurities,
- phase transformations and precipitation,
- impurity adsorption or desorption,
- lattice mismatch strain in heteroepitaxy,
- structural damage (defect creation) as a result of energetic particle bombardment

Stress sources: thermal stress

- Thermal stress σ_{th}

difference in thermal expansion coefficient between film and substrate and when $T_s \neq T_{amb}$

$$\sigma_{th} = \frac{E_f}{1-\nu_f}(\alpha_s - \alpha_f)(T_{amb} - T_s)$$

TEC $$\alpha = \frac{1}{3V}\left(\frac{\partial V}{\partial T}\right)_P = \frac{1}{3\kappa}\left(\frac{\partial P}{\partial T}\right)_V = \frac{\gamma\, C_V}{3\kappa}$$

If $\alpha_f > \alpha_s$, tensile stress develops during cooling

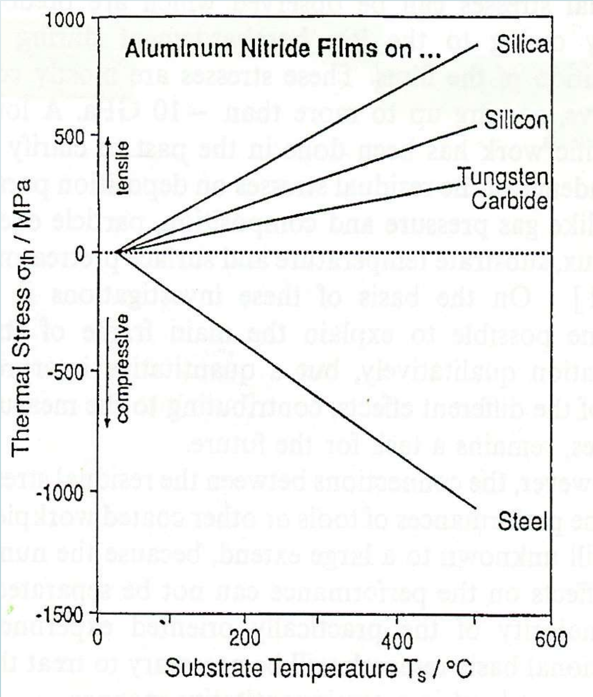

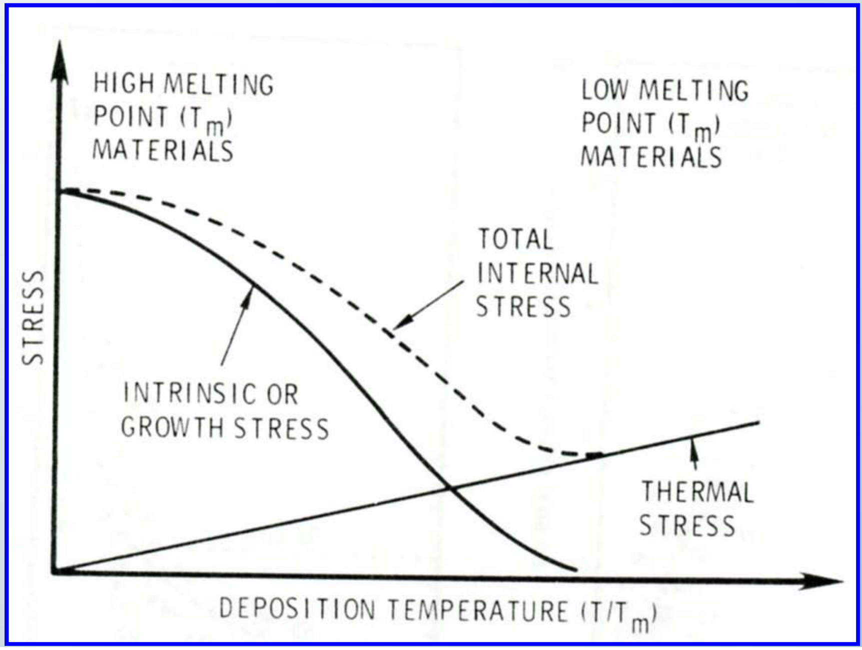

Stress sources: thermal stress

The slope of the σ(T) curve is the thermoelastic response of the film, provided that no microstructural changes had occurred on cooling and re-heating

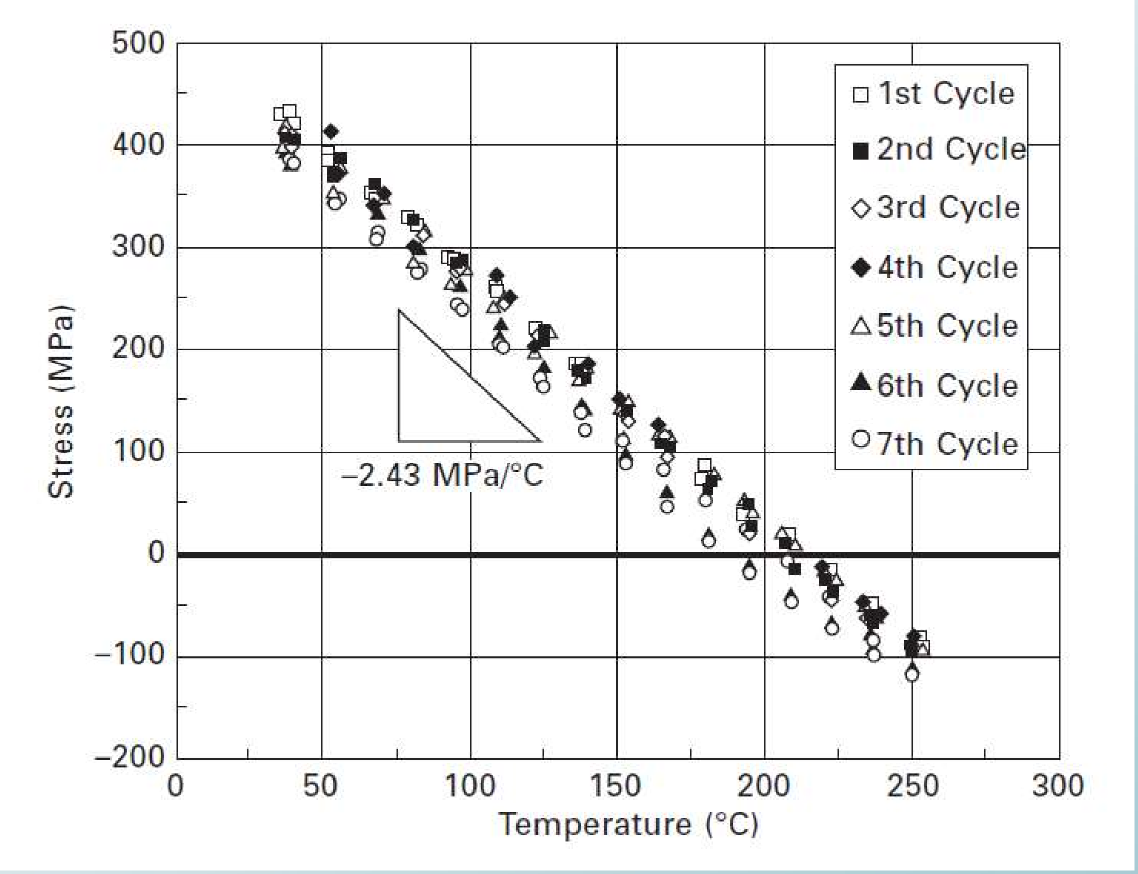

Biaxial stress in a 0.4 mm thick thin film of Al-1%Si-0.5%Cu on a silicon substrate during several thermal cycles from room temperature to 250°C

from Nix, Metallic thin films: stresses and mechanical properties, (K. Barmak and K. Coffey editors), Chap. 8, Woodhead Publishing, 2014

Stress sources: phase transformation

β to α phase transformation in Ta films subjected to vacuum annealing

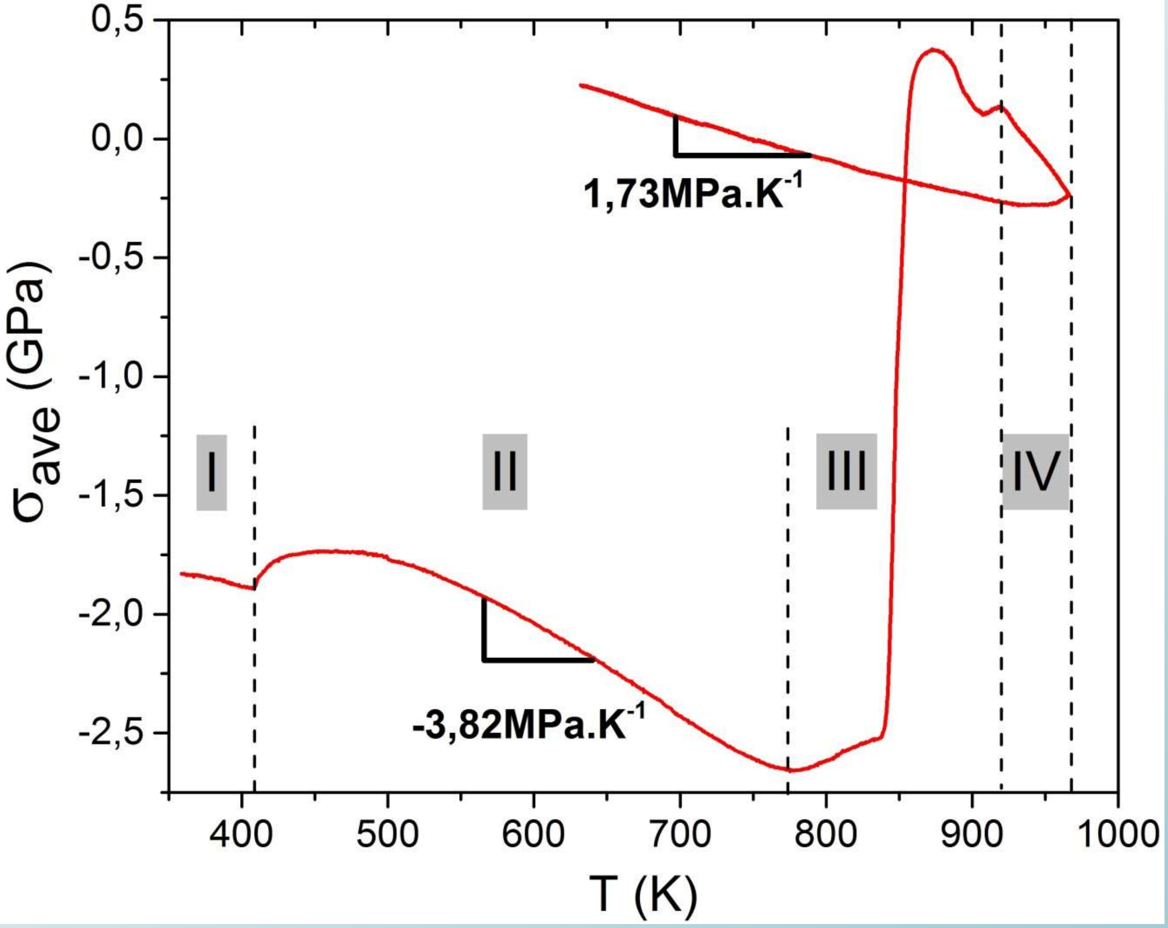

J. J. Colin et al., Acta Mater. 126 (2017) 481

Influence of microstructure on TEC

Magnetron-sputtered Cr films

- Manifest evolutionary growth regime (zone-T)
- Highest TEC for smallest grain size
- TEC is larger for GB region due to
- Weaker bonding of GB atoms (□ anharmonicity)
- Porosity
- Increased heat capacity (Debye model)

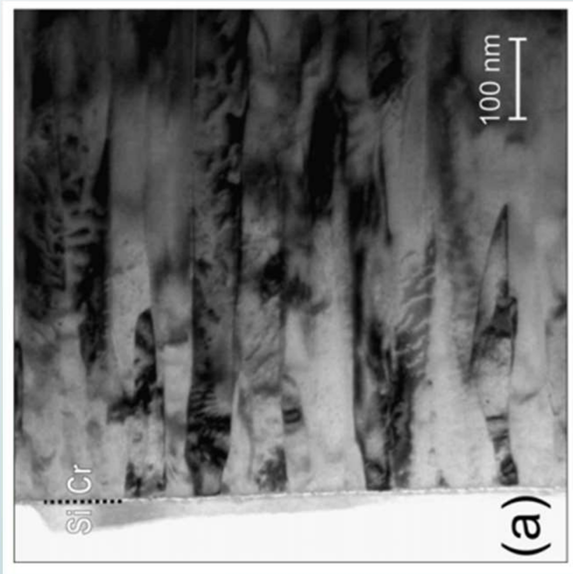

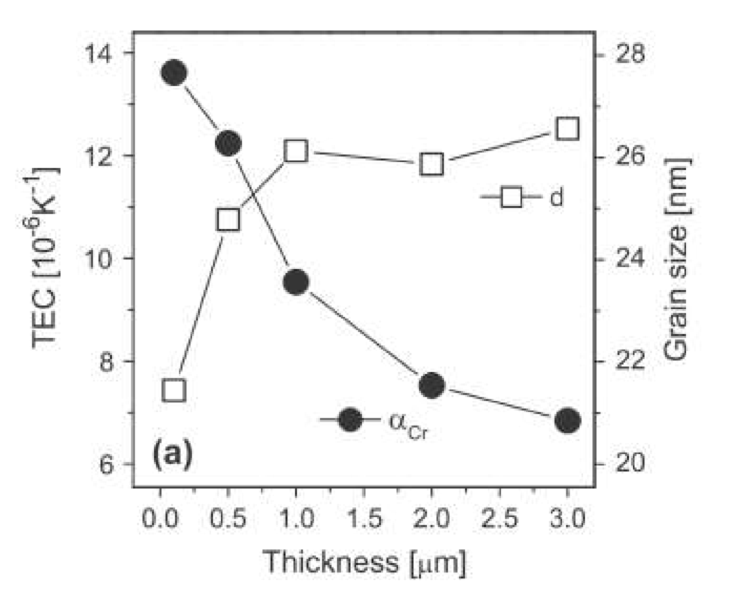

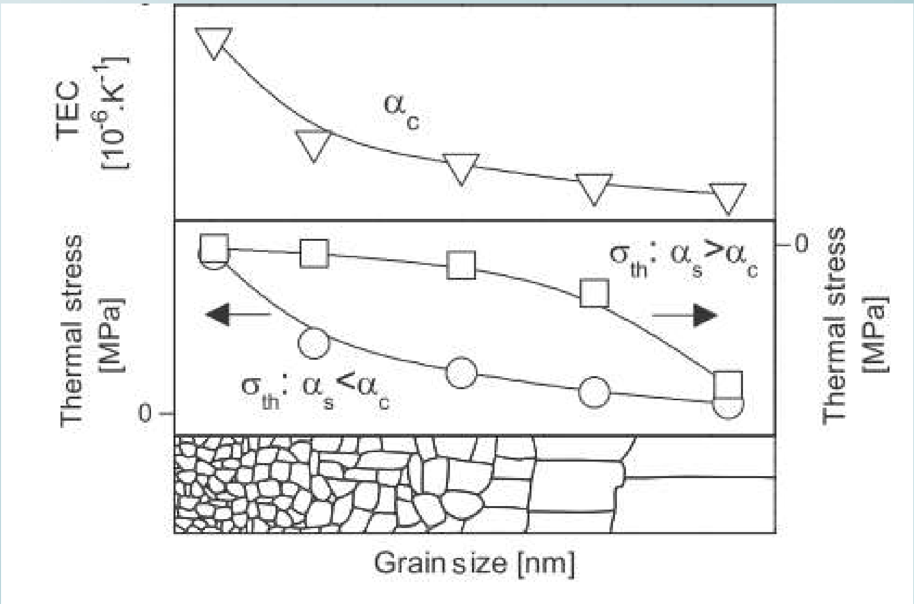

from Daniel et al., acta Materialia 59 (2011) 6631

Stress sources: epitaxial stress

- Coherence strains develop in thin films that growth epitaxially onto flat single crystal substrate, in a 2D growth mode (layer by layer)
- The lattice mismatch between film (a_f) and substrate (a_s) or **misfit** is accommodated by in-plane elastic strains, ε_1 and ε_2, resulting in a biaxial stress state

$$\varepsilon_{mis} = \frac{a_s - a_f}{a_s}$$

1) Cubic systems

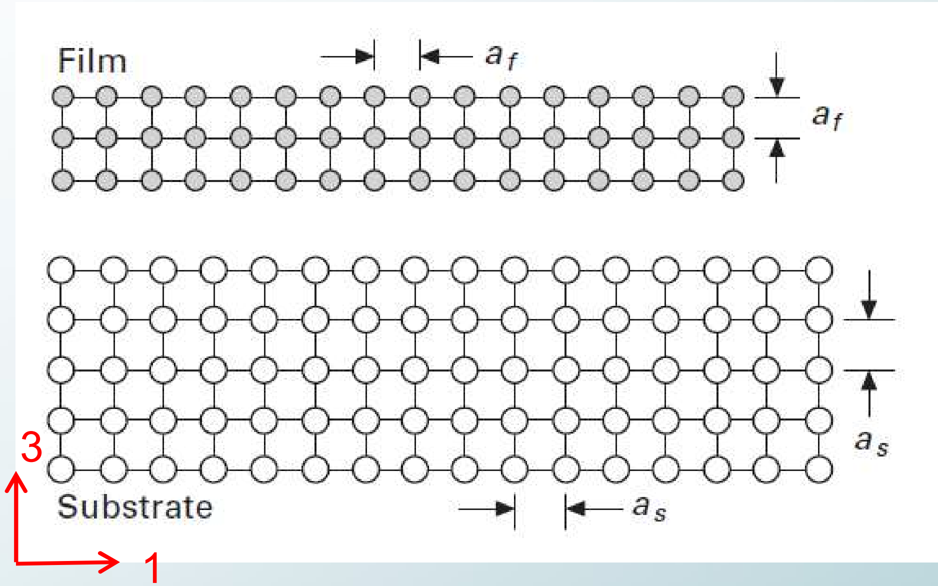

coherent growth
misfit is fully accommodated elastically

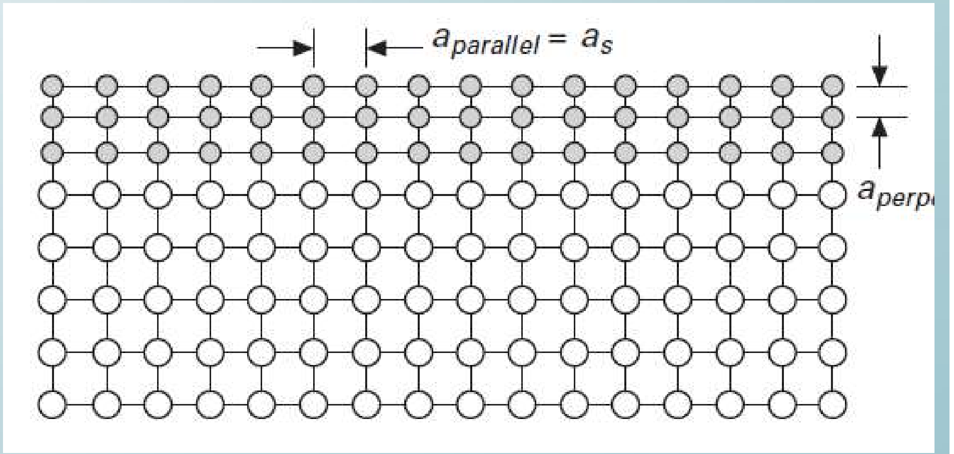

Here, $a_f<a_s$, elastic misfit strain ε_{mis} is positive, resulting in tensile stress $\sigma>0$

$$\varepsilon_1 = \varepsilon_2 = \frac{a_{parallel} - a_f}{a_f} = \varepsilon_{mis}$$

$$\sigma_1 = \sigma_2 = Y\varepsilon_1$$

Y= biaxial modulus

$$\varepsilon_3 = \frac{a_{perp} - a_f}{a_f} = -2\frac{c_{12}}{c_{11}}\varepsilon_1$$

Coherency stress

coherent growth

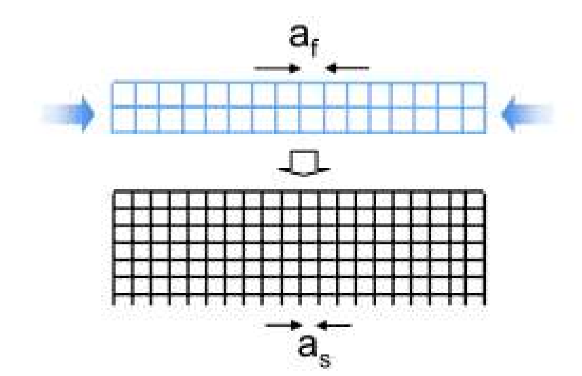

Misfit strain

$$\boxed{\varepsilon = \frac{a_s - a_f}{a_f}}$$

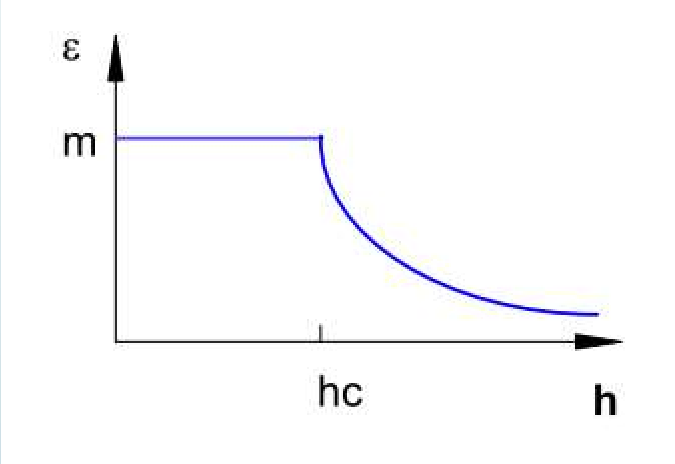

h_c= critical thickness for strain relaxation

incoherent growth

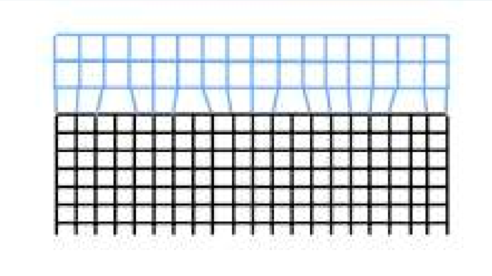

Model of Matthews et Blakeslee (1974) based on the balance of acting forces on a threading dislocation

Introduction of misfit dislocations to relax the misfit strain

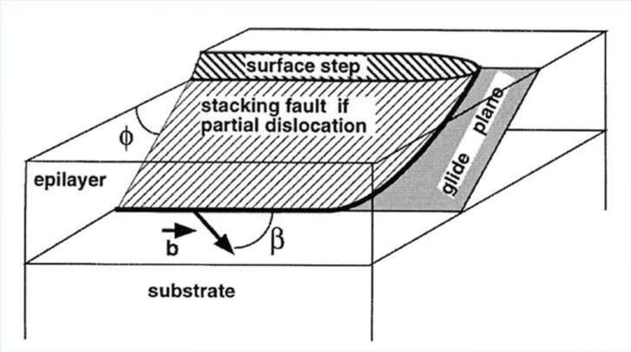

Stress and dynamics of film growth

during growth - surface different than eq. (much larger incoming flux than outgoing)

Ag: 23 C, 0.1 nm/sec → P(vapor)/P(equilibrium) = 10^{38}

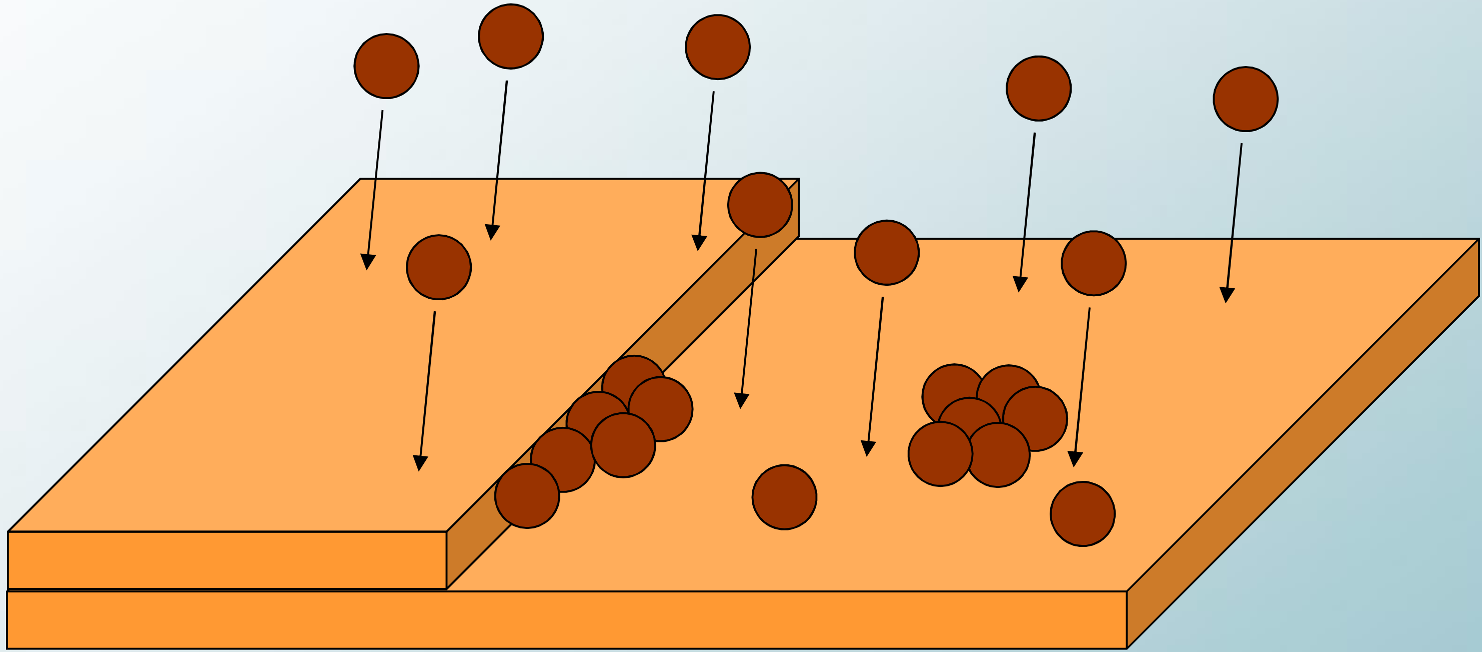

Supersaturation of adatoms during growth → *Higher chemical potential than equilibrium* → *High density of adatoms/clusters*

Growth modes at equilibrium (thermodynamic conditions)

The three growth mode categories are schematically shown.

- Frank-van der Merwe growth mode corresponds to a layer-by-layer (2D) growth
- Volmer-Weber growth mode corresponds to to an island (3D) growth.
- The Stranski-Krastanov growth mode is a mixture of the 2D and 3D growth modes, often observed for semi-conductor thin films

Stress and dynamics of film growth

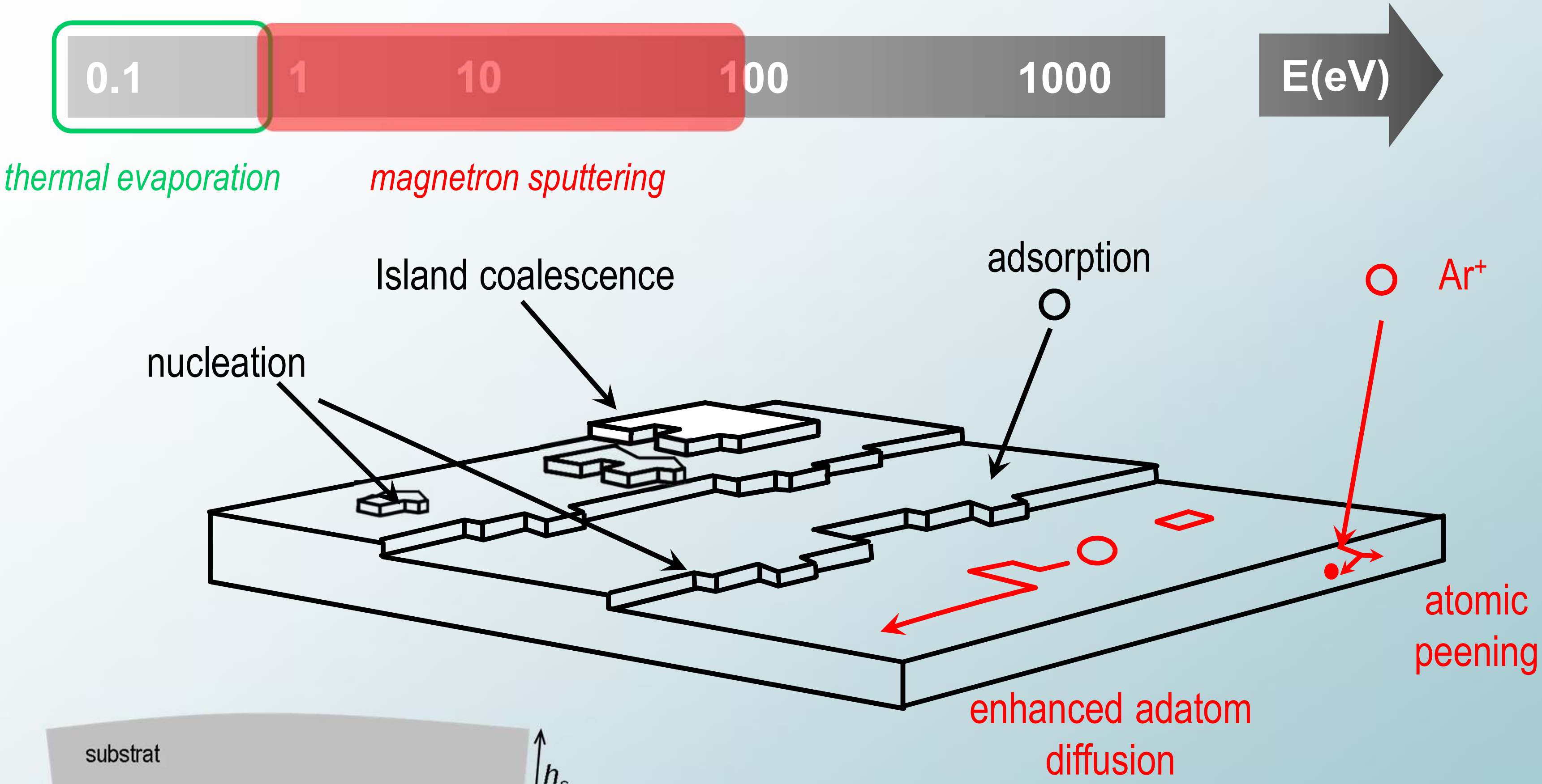

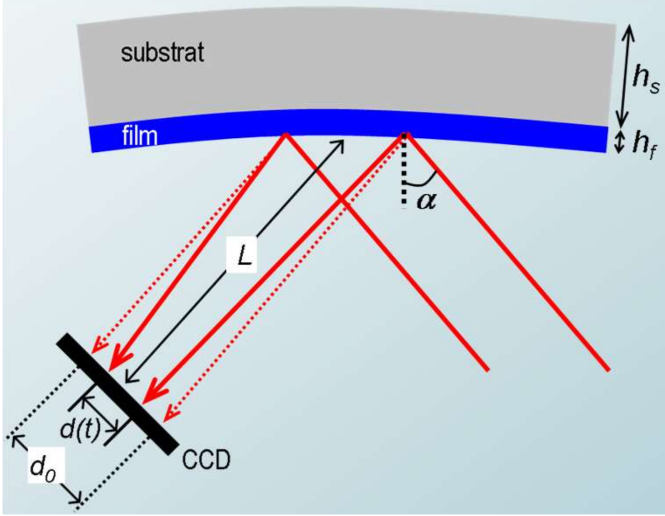

Fundamental understanding of growth mechanisms
- **early growth stages** (nucleation/coalescence)
- **growth dynamics using real-time techniques** (wafer curvature, surface differential reflectivity, RHEED, …

Mechanics of thin plates: curvature and stress

Bending of a thin plate

Biaxial bending of a thin plate, elastically isotropic

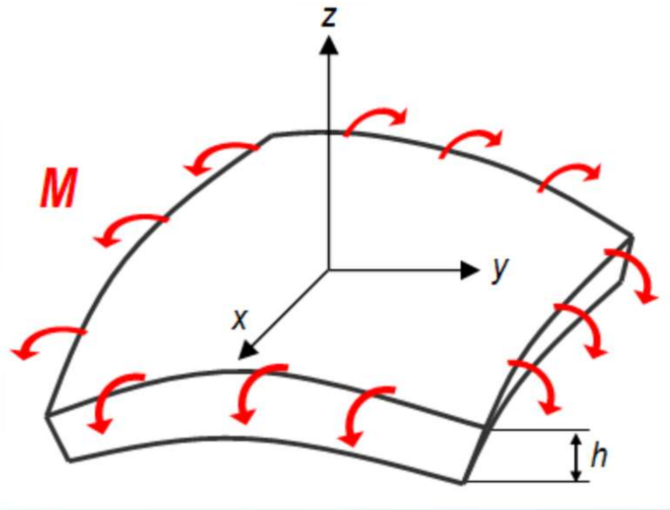

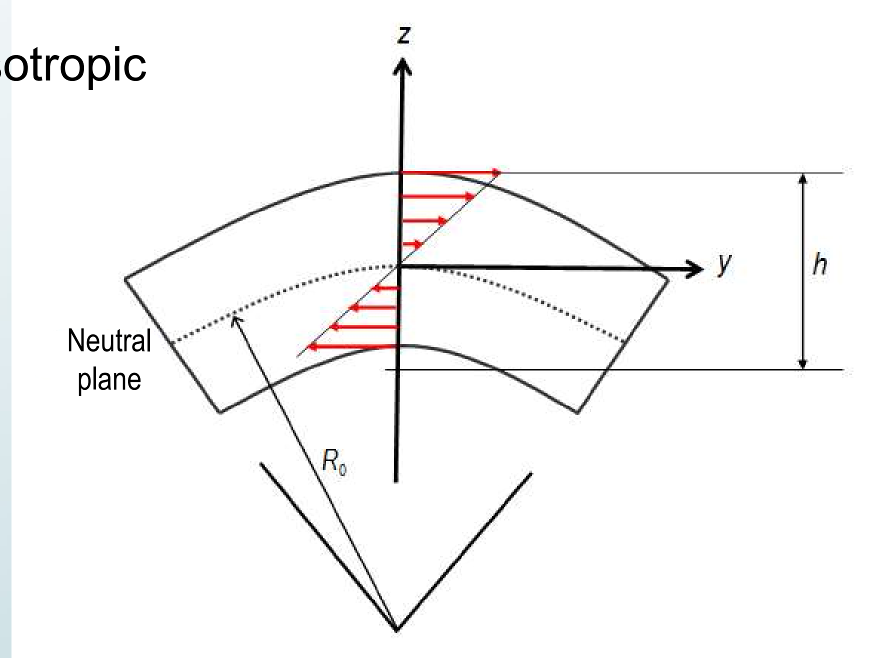

- In-plane biaxial stress $\sigma_{xx} = \sigma_{yy} = \sigma(z)$ and $\sigma_{zz} = 0$
- In-plane elastic strain $\varepsilon_{xx} = \varepsilon_{yy} = \varepsilon(z) = \frac{z}{R} = -\kappa z$ κ <0 in the figure

  reference (z=0) is taken at the ***neutral plane (z_0)***

- Hooke's law $$\varepsilon(z) = \frac{1}{E}\sigma_{xx} - \frac{\nu}{E}\sigma_{yy} - \frac{\nu}{E}\sigma_{zz} = \frac{1-\nu}{E}\sigma(z)$$

$Y = \frac{E}{1-\nu}$ Biaxial modulus $\sigma(z) = Y\,\varepsilon(z)$

Bending of a thin plate

- Bending moment per unit length $$M = \int_{-z_0}^{h-z_0} \sigma(z).z.dz = Y \int_{-z_0}^{h-z_0} \frac{z^2}{R} dz \qquad (1)$$

Origin of bending: stress in the film supplies a force that leads to a bending moment at the edges of the substrate and causes it to bend

Solving eq.(1) for $z_0=h/2$, one obtains $$M = -Y\frac{h^3}{12}\kappa \qquad (2)$$

However, one has $$\sigma(z) = -Y\kappa z \qquad (3)$$

$$\left.\begin{array}{l}(2)\\(3)\end{array}\right\} \quad \sigma = 12\frac{M}{h^3}z \qquad (4)$$

$\Rightarrow$ *Positive bending (M>0) produces tensile stress (σ>0) and strain for z>0*

$\Rightarrow$ *Negative curvature results from positive bending strain for z>0*

Curvature of a film/substrate plate

- Plate geometry

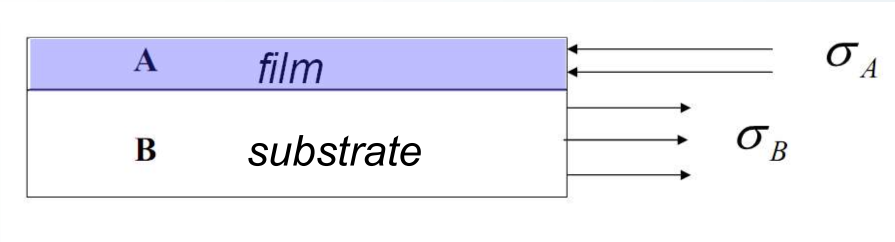

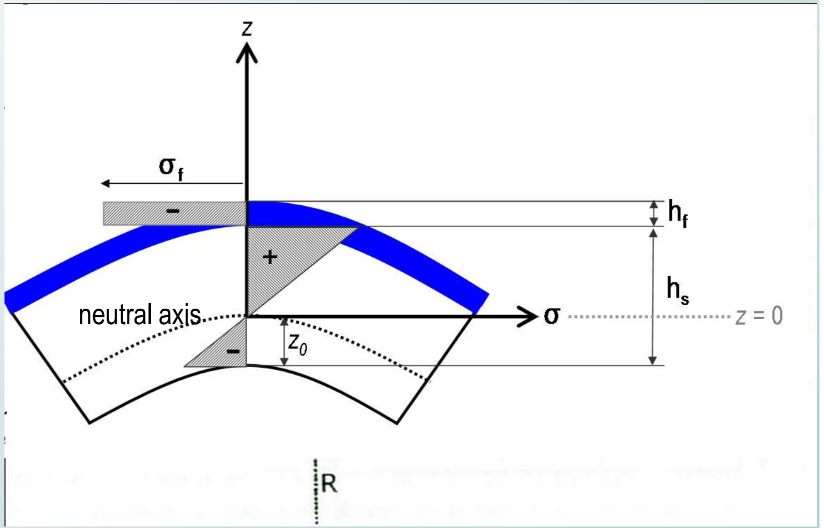

- Assumptions

☞ elastic, homogeneous and continuous materials
☞ isotropic elastic properties of film and substrate
☞ in-plane, **biaxial stress state** in the film
☞ $Y_f \sim Y_s$
☞ $h_f \ll h_s$
☞ tranverse cross-section remain plane during bending
☞ no interfacial delamination

- Equilibrium conditions (to be satisfied)

$$\sum F = 0 \quad \text{et} \quad \sum M = 0$$

$$F = \int \sigma(z)\,dxdz$$

$$M = \int \sigma(z)\,z\,dxdz$$

sum of longitudinal forces F = 0 *internal bending moment M = 0*

Curvature of a film/substrate plate

Let's assume the distance from neutral plane to the film surface is αh_s

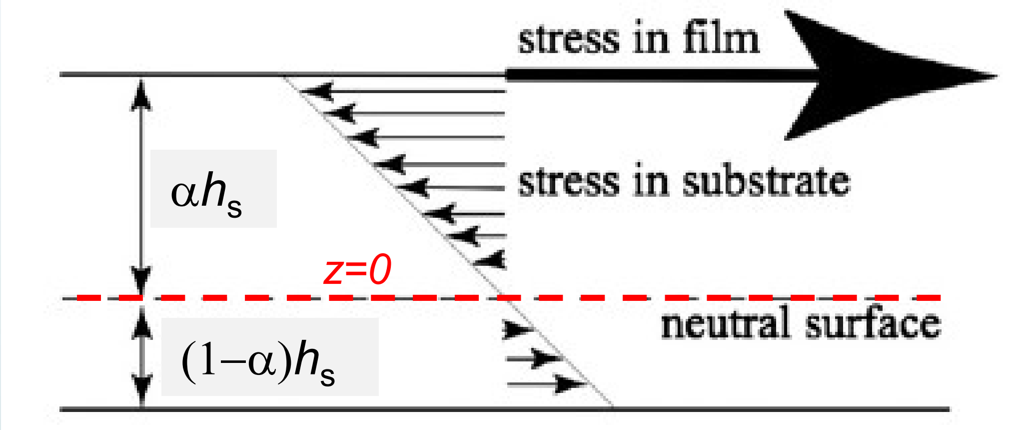

Solving equilibrum conditions yields

- $\int_{(\alpha-1)h_s}^{\alpha h_s} \sigma_{xx} dz + \bar{\sigma}.h_f = 0$ (5)
- $\int_{(\alpha-1)h_s}^{\alpha h_s} \sigma_{xx}\, z\, dz + (\alpha h_s)\bar{\sigma}.h_f = 0$ (6)

Inserting eq.(3) into eqs.(5) and (6) yields

$$-\frac{Y\kappa}{2}(2\alpha-1)\, h_s^2 + \bar{\sigma}.h_f = 0 \quad (7)$$

$$-\frac{Y\kappa}{3}\left(3\alpha^2 - 3\alpha - 1\right) h_s^3 + \alpha h_s\, \bar{\sigma}.h_f = 0 \quad (8)$$

Multipling eq.(7) by αh_s and subtracting it from eq.(8) yields

$$\boxed{\alpha = \frac{2}{3}} \quad \text{and} \quad \boxed{\bar{\sigma}.h_f = \frac{Y\kappa h_s^2}{6} = \frac{E}{(1-\nu)}\frac{h_s^2}{6R}}$$

Stoney equation

Note: Original Stoney equation was $\sigma.h_f = E\frac{h_s^2}{6R}$

Case of anisotropic single-crystal substrates

- (100) Si single-cristal

  Y_{100}=180.5 GPa

$$\sigma h_f = \left(\frac{1}{s_{11} + s_{12}} \right) \frac{h_s^2}{6R}$$

- (111) Si single-cristal

  Y_{111}=229.1 GPa

$$\sigma h_f = \left(\frac{6}{4s_{11} + 8s_{12} + s_{44}} \right) \frac{h_s^2}{6R}$$

Consequence of crystal elastic anisotropy:

For the same stress state in the W films, the substrate curvature is larger for (100) Si substrates

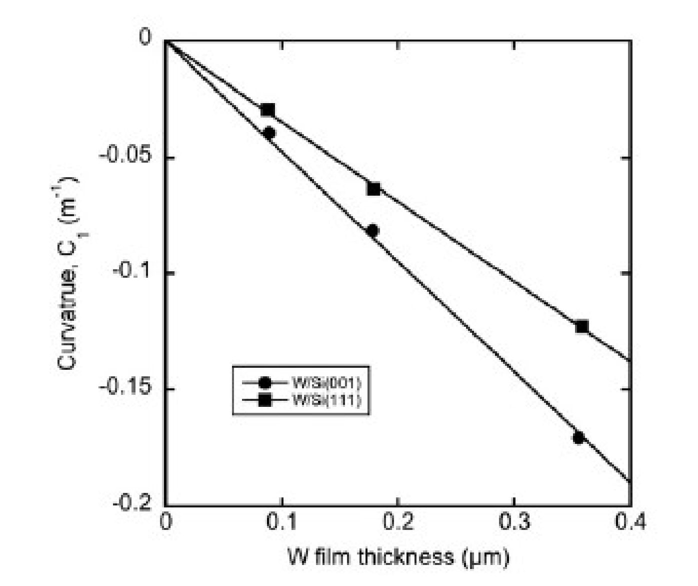

from Janssen et al., Thin Solid Films 517 (2009) 1858

Case of anisotropic single-crystal substrates

Note that the curvature measurements for both the bare and coated substrates must be measured along the same path

The in-plane stiffness of a silicon (001) wafer depends on the angular direction, $E_{[110]}$ =171 GPa and $\nu_{[110]}$ =0.26, while $E_{[100]}$ =130 GPa and $\nu_{[100]}$ =0.28

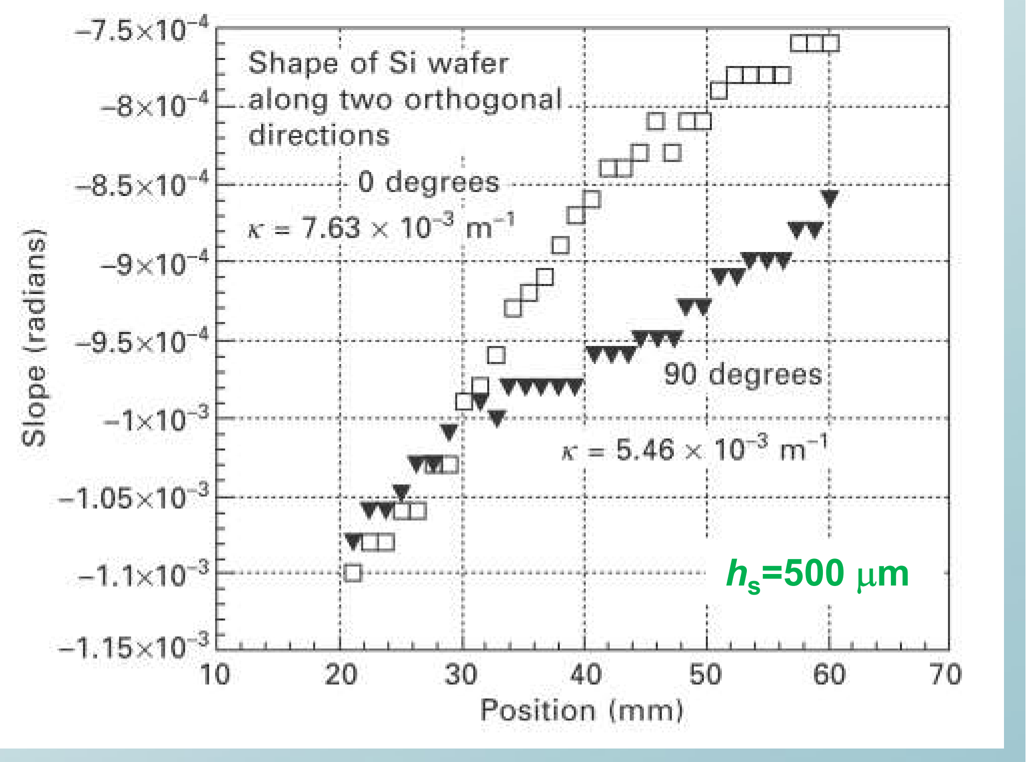

from Nix, Metallic thin films: stresses and mechanical properties, (K. Barmak and K. Coffey editors), Chap. 8, Woodhead Publishing, 2014

Bending induced stress in the film

The substrate bending creates a force which opposes to the intrinsic stress existing/developping in the film. This stress relaxation is however negligible in most cases, as $h_f << h_s$. Its expression can be derived according to

$$\sigma_f^{bend} = -Y_f \frac{z^{\max}}{R} = -\frac{2h_s}{3R}\frac{E_f}{1-\nu_f}$$

$$\delta = \frac{h_f}{h_s}$$

thickness ratio

$$\eta = \frac{Y_f}{Y_s}$$

biaxial modulus ratio

$$\sigma_f^{bend} = -4\,\sigma_f \frac{Y_f}{Y_s}\frac{h_f}{h_s}$$

or

$$\boxed{\frac{\Delta\sigma_f^{bend}}{\sigma_f} = -4\,\eta\delta}$$

Note that this bending induced change in stress is that expected for burried layers. This effect has to be bore in mind when growing multilayered systems!

Exercise: calculate for the stress induced by layer A (σ_A=–2GPa) in burried layer B using δ=0.15 % and η=2.3.

Answer: σ= *24 MPa*

What is the stress state in the substrate?

- For ***homogeneous*** thin layers, the stress in the substrate is usually negligible ~1-2% of the film stress
- This is no longer the case when the layer is ***inhomogeneous***, e.g. in trenches and vias of microelectronic devices (see below)

$$\boxed{\sigma_s^{\max} = -Y_s \frac{z^{\max}}{R} = -4\sigma_f \frac{h_f}{h_s}}$$

$$z^{\max} = 2\frac{h_s}{3}$$

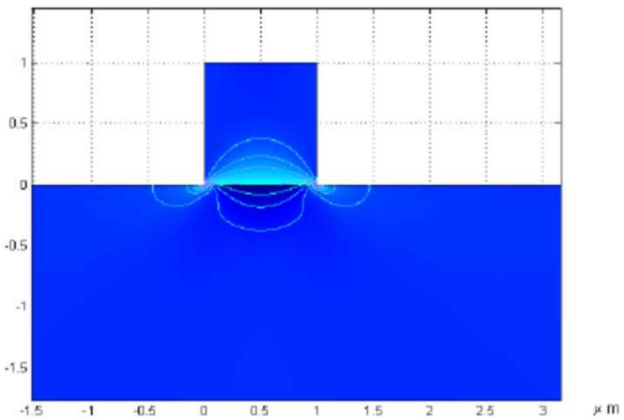

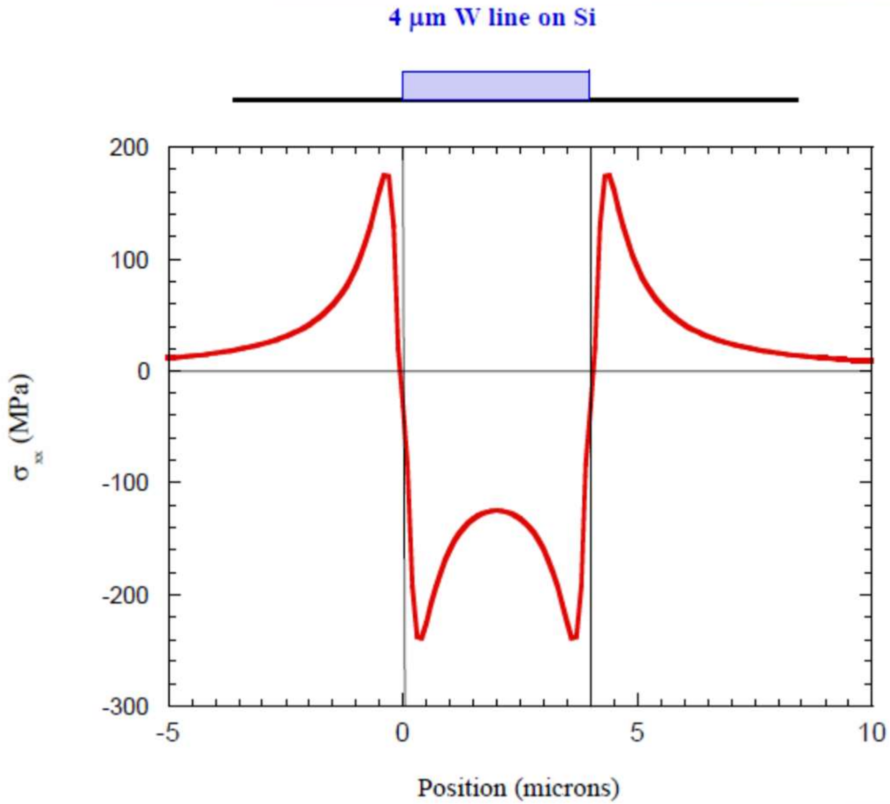

Stoney equation: summary

- Stoney equation

$$\boxed{\sigma\, h_f = \frac{1}{6} Y_s\, h_s^2\, \kappa_{stoney} = \frac{F}{w}}$$

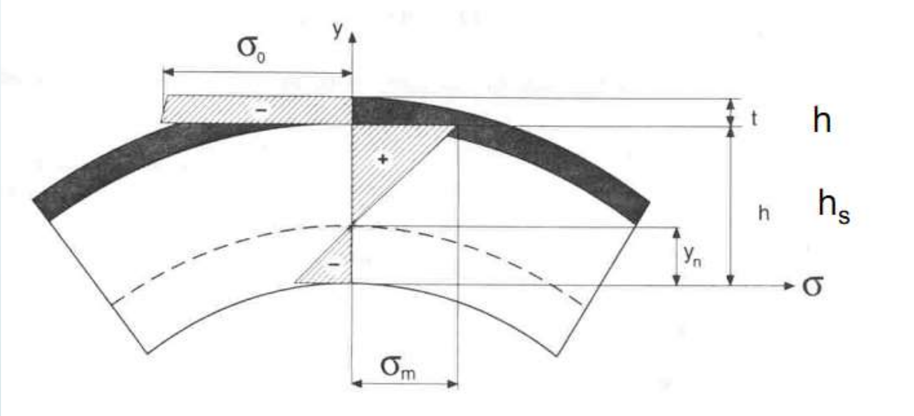

☞ Valid only for the assumptions described before
☞ No requirement of film elastic properties
☞ Relates the curvature κ (m^{-1}) to the "film force per unit width", F/w (N/m), which is equal to the film stress*thickness product quantity

- Numerical application: (001) Si wafer, Y_s=180.5 GPa

$$\frac{F}{w} = 10\ N/m, \quad h_s = 200\mu m \Rightarrow R = 120\ m$$

1 N/m = 10 GPa.Å

Stoney's equation: important aspects and limitations

$$\Delta\kappa = \kappa - \kappa_0 = \frac{6\,\sigma\,h_f}{Y_s\,h_s^2}$$

• One measures the **relative change** in curvature!
☞ for *post-deposition* determination of film stress, one needs to measure the absolute curvature both before and after deposition, along the same path
☞ for real-time measurement during growth, the change in curvature is obtained directly, once the reference curvature has been done on the initial substrate

• The curvature is inversely proportional to the **square of the substrate thickness**
☞ Maximum sensitivity requires very thin (100-200 μm) wafers; however, for deposition of thick coatings (several μm) with large stresses, thicker wafers should be used to avoid finite deflection effects (as discussed after)

• To derive stress from curvature measurement, the independent knowledge of **film thickness** is needed; accurate determination of the growth rate is required, e.g. using quart microbalances, post-growth XRR or profilommetry

Stoney's equation: important aspects and limitations

• elastic anisotropy

Angle dependent curvature for a 358 nm-thick W film on Si(111)

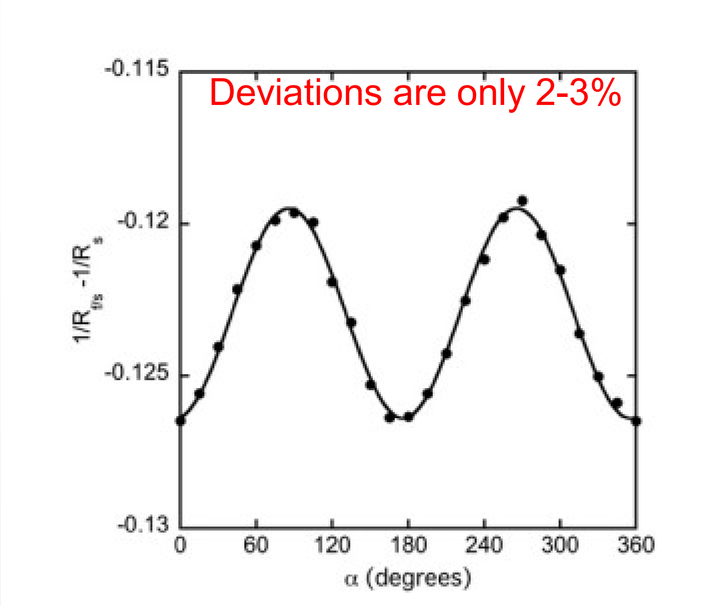

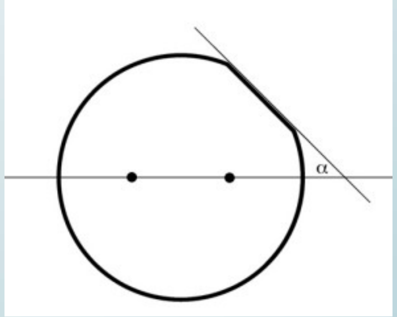

from Janssen et al., Thin Solid Films 517 (2009) 1858

Despite strong elastic anisotropy (30% for Si), the deformation of (111) or (100) Si substrates, is **radially symmetric** due to symmetry of constitutive strain-stress relationships. This is no longer the case for (110) orientation, or for stronger deflections (as discussed in the next slides).

Stoney's equation: important aspects and limitations

- Complete calculation: ~~$h_f << h_s$~~ and ~~$Y_f \sim Y_s$~~

$$\kappa = \frac{6\sigma h_f}{Y_s h_s^2} \frac{1+\delta}{1+4\eta\delta+6\eta\delta^2+4\eta\delta^3+\eta^2\delta^4}$$

$$\delta = \frac{h_f}{h_s}$$

thickness ratio

$$\eta = \frac{Y_f}{Y_s}$$

biaxial modulus ratio

$$\boxed{\frac{\kappa - \kappa_{Stoney}}{\kappa_{Stoney}} = \delta \ (1-4\eta)}$$

1st order

Error introduced when the thin film approximation is no longer valid

$$\delta \approx 3\%, \quad \eta = 1 \Rightarrow \frac{\Delta\kappa}{\kappa} \approx 10\%$$

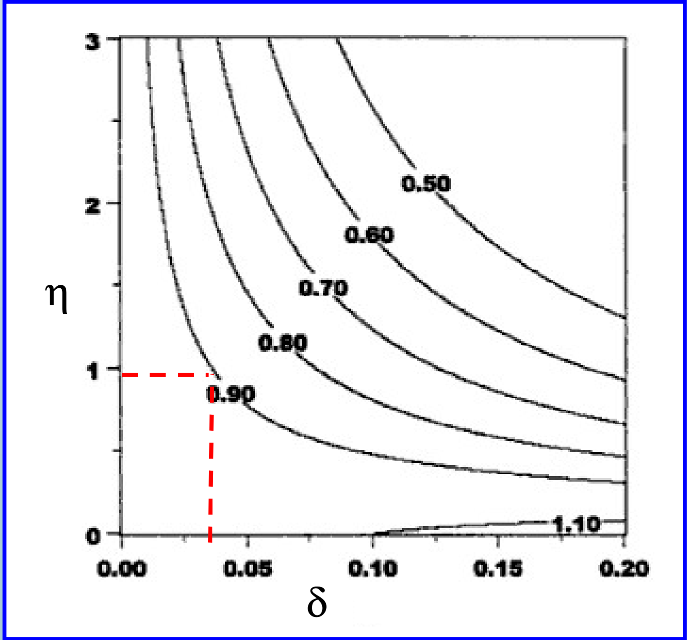

Stoney's equation: important aspects and limitations

The error in using Stoney equation when the thin film approximation is relaxed

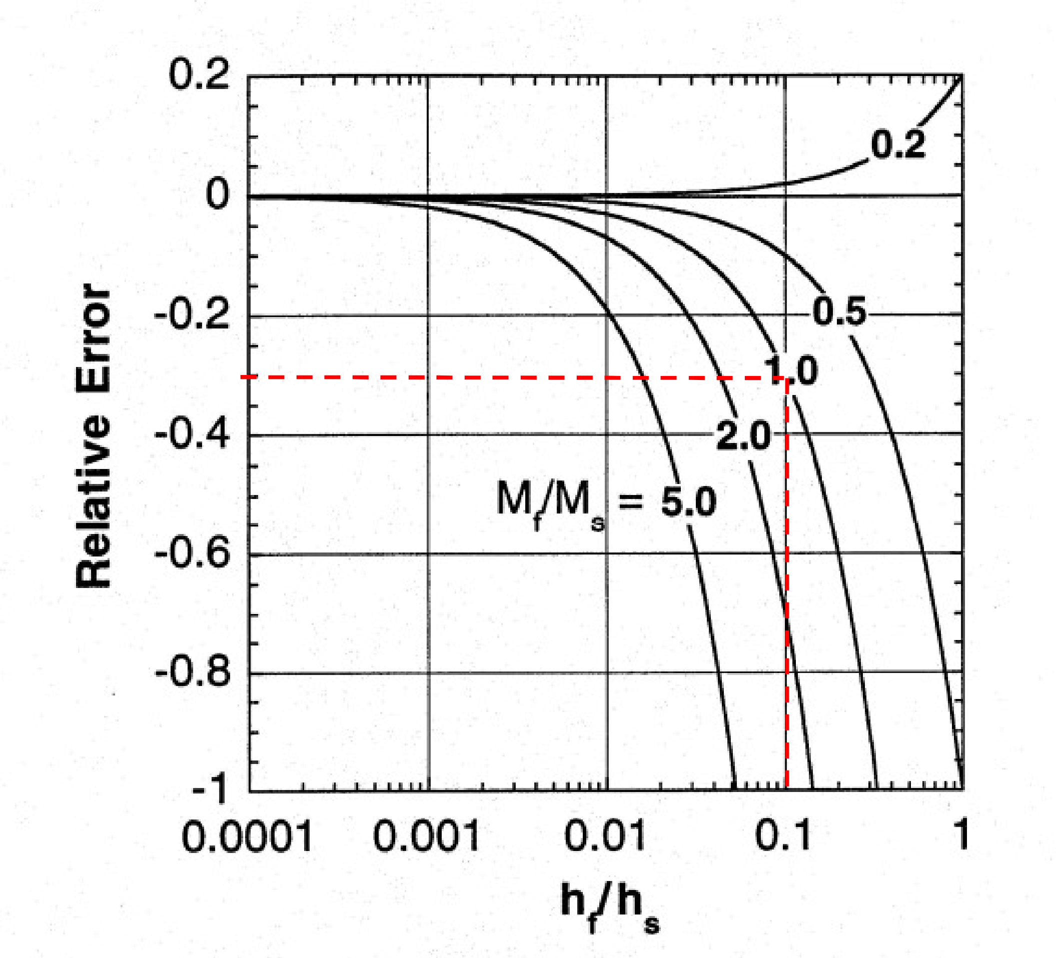

from Floro and Chason, Technical notes

Case of strong deflections: non-linearity and bifurcation

1st case: axially symmetric deformation in the nonlinear regime

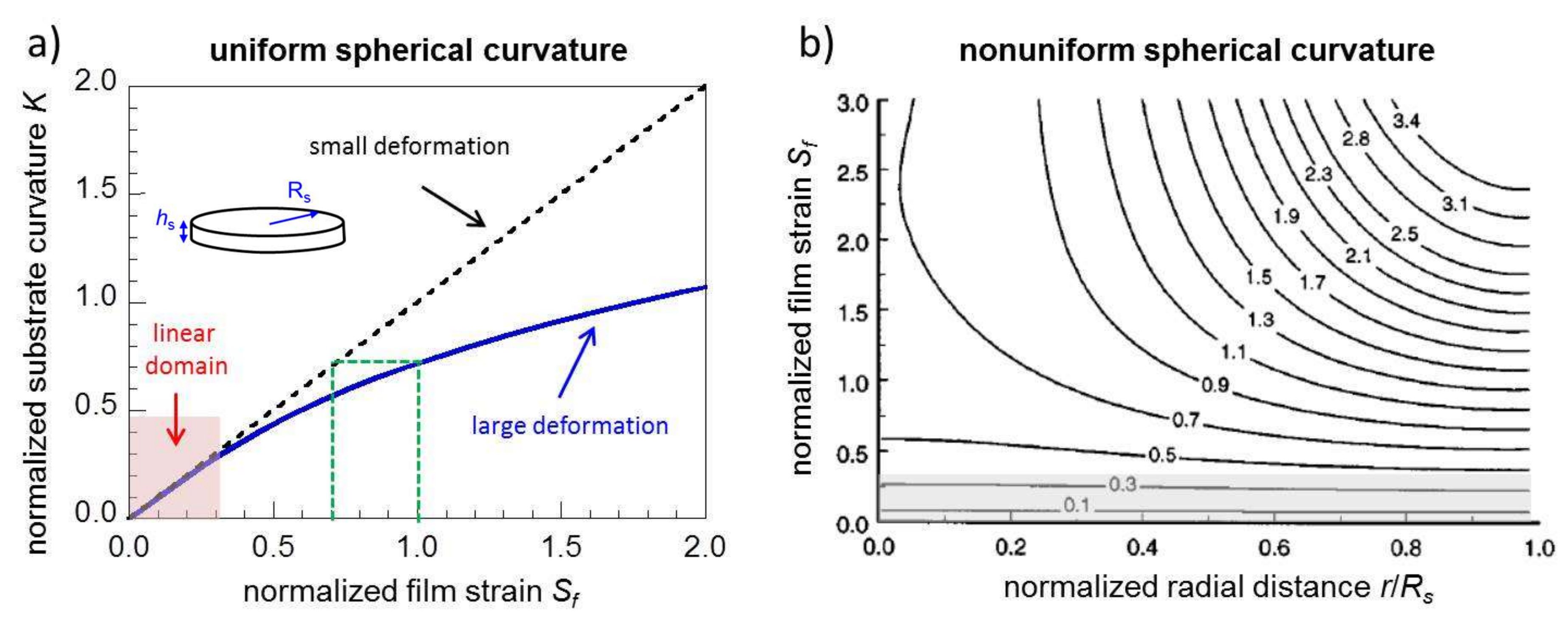

Freund et al. have introduced the normalized film strain parameter S_f and normalized curvature K

$$S_f = \frac{3}{2}\left(\frac{R_s}{h_s}\right)^2 \frac{\sigma_f}{M_s}\frac{h_f}{h_s} \qquad K = \frac{R_s^2}{4h_s}\kappa$$

For large substrate deflections, the use of Stoney equation is inadequate and will lead to an underestimate of the film stress

L. B. Freund, J. Mech. Phys. Solids. 48 (2000) 1159

Case of strong deflections: non-linearity and bifurcation

2nd case: bifurcation of equilibrium shapes

strong plate deflections: $\cancel{Z \ll h_s}$

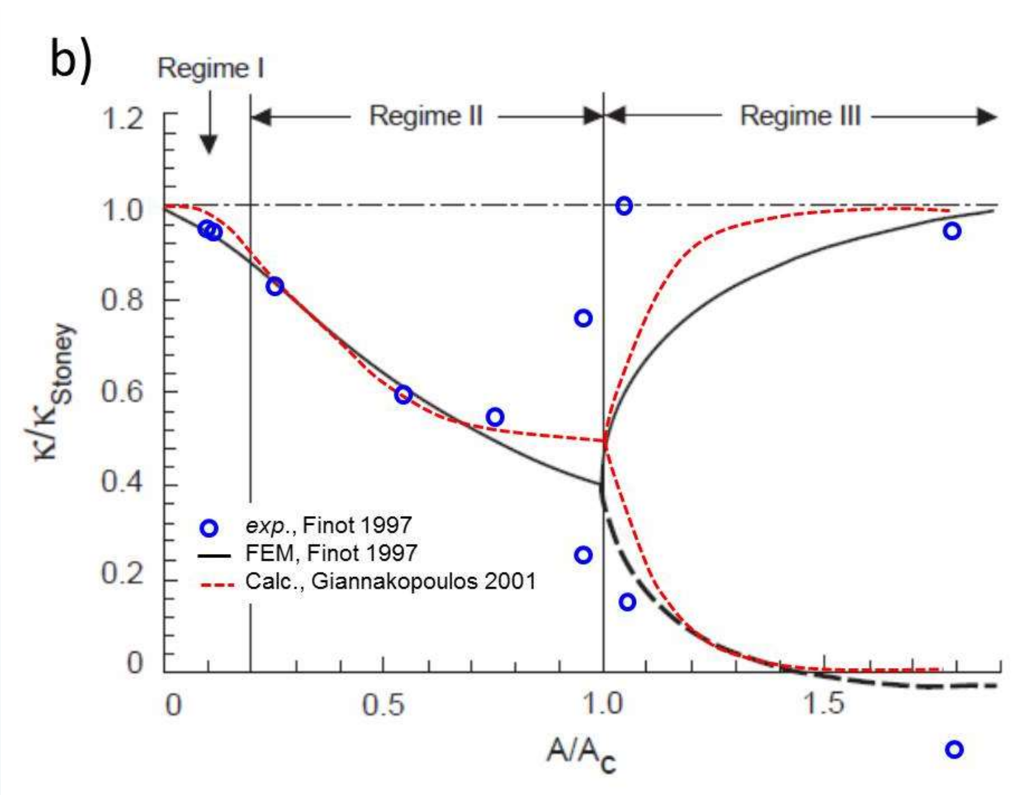

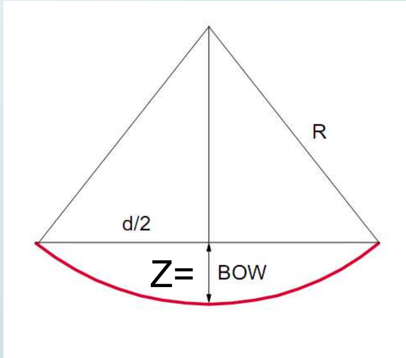

$$\frac{Z}{h_s} = \frac{3}{4}\frac{F}{Y_s}\frac{d^2}{h_s^3}$$

two principal in-plane curvature

$$(\kappa_x - \kappa_y)\left[\kappa_x \kappa_y R_s^4 (1+\nu) - 16\left(h_s + h_f\right)^2\right]$$

The mode of deformation is determined by the parameter A

$$A = \frac{D_s^2}{h_s^3}\sigma_f h_f$$

from Finot et al, J. Appl. Phys. 81, 3457 (1997)

Case of strong deflections: non-linearity and bifurcation

2^{nd} case: bifurcation of equilibrium shapes

For R_s/h_s>25, the critical parameter is A_c=680 GPa for Si substrate

- For A< 0.2 A_c, the use of Stoney equation is correct within 10%
- For 0.2 A_c < A< A_c, the deformation is still axially symmetric but the curvature is significantly lower than that predicted by Stoney equation
- For A > A_c, then bifurcation will occur with a large curvature in one direction and almost no curvature in the perpendicular direction

The requirement A<0.2 A_c leads to maximum force per unit width for 90% accuracy of the Stoney Equation of

$$d = 1\ \text{cm},\ h_s = 100\ \mu\text{m},\ F = 1.36\ \text{GPa}.\mu\text{m} = 1360\ \text{N/m}$$
$$z = 56.6\ \mu\text{m}$$

In practical cases, film force up to 500 N/m, so A=50 GPa i.e., A/A_c= 7.3 %

Be aware of what you measure!

Influence of plastic deformation of the substrate

TiAlN coatings on Si(001) substrate

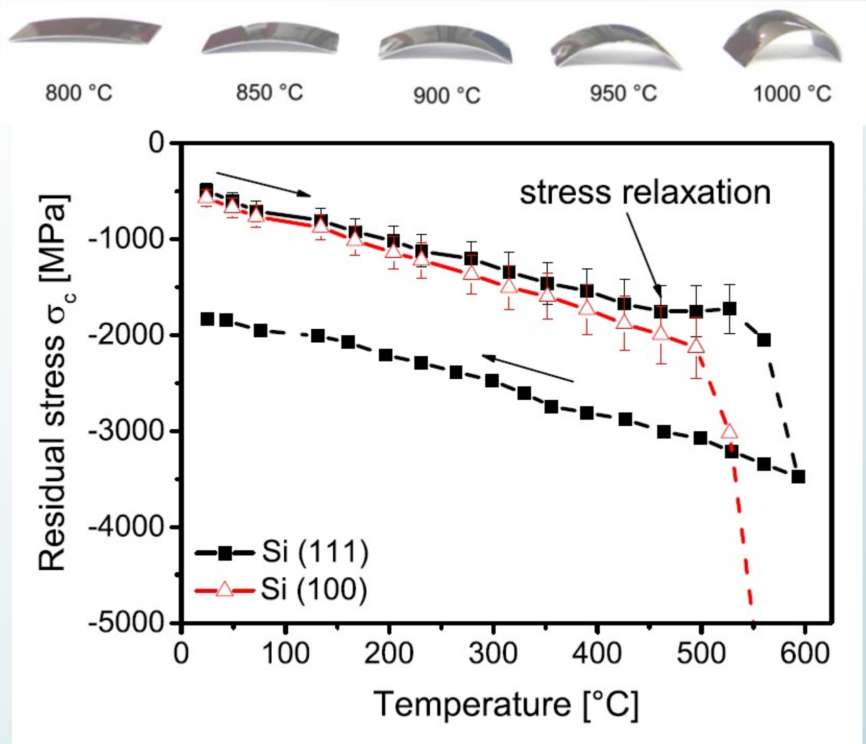

t= film thickness; d= substrate thickness

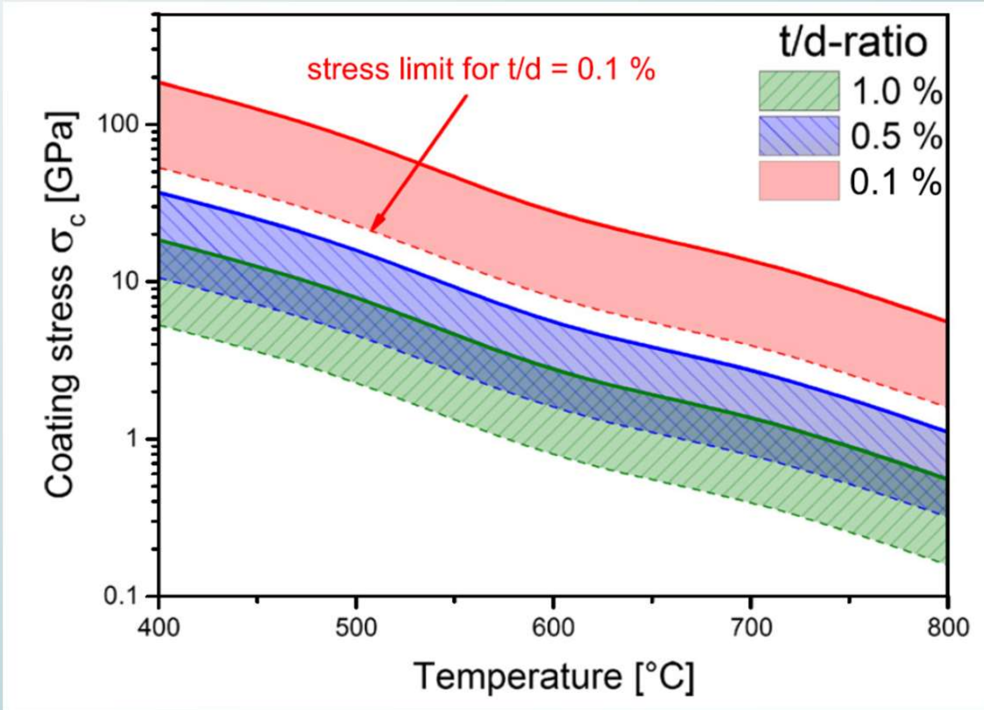

Apparent stress increase upon heating, but due to plastic deformation in the Si substrate

- brittle to ductile transition of Si starts between 400 and 500 °C
- critical resolved shear stress for Si around 20-30 Mpa at 600°C

from Saringer et al., Surf. Coat. Technol. 274 (2015) 68

Experimental determination of wafer curvature

How measuring residual stress (or strain) in thin films ?

'wafer curvature' method

⇒ integrated (macroscopic) stress
⇒ in-situ diagnostic

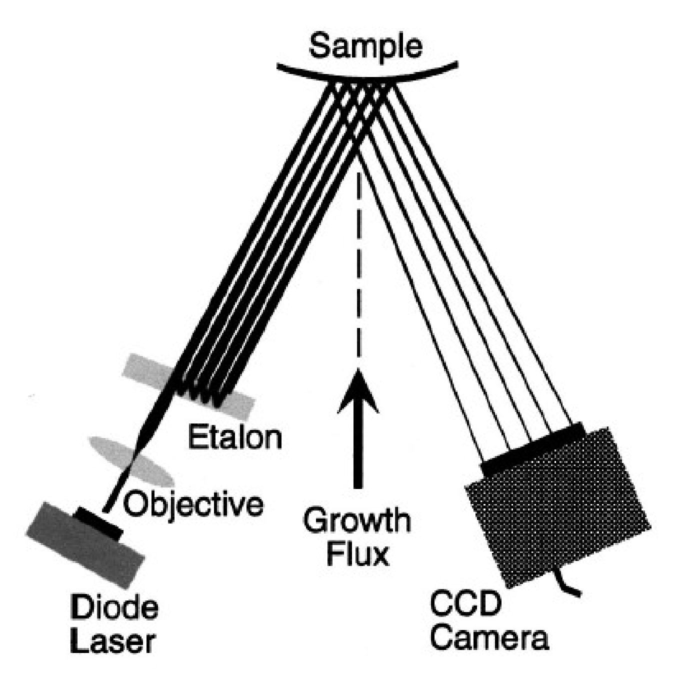

Floro et al., JAP 89 (2001) 4886

X-ray Diffraction

⇒ internal (microscopic) strain gauge
⇒ in-situ diagnostic
⇒ limited to crystalline materials

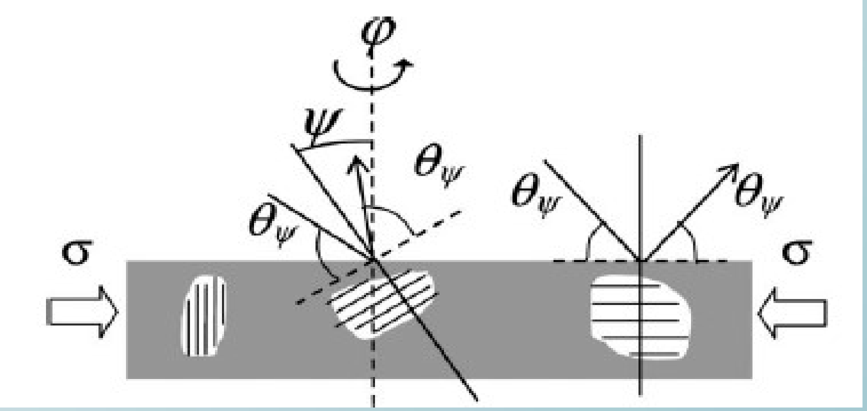

Welzel et al., J. Appl. Crystal. 38, 1 (2005)

Techniques for *real-time* stress measurements

• XRD
⇒ *time-resolved strain measurements only possible with bright sources such as the synchrotron (Lairson et al. 1995)*

• RHEED : Reflection High Energy Electron Diffraction
⇒ *lattice constant at the surface during epitaxial growth*
⇒ *limited to high-vacuum environment*

• Vibrating membrane technique
⇒ *film internal friction can be obtained*
⇒ *only tensile stress are measured*

• Raman spectroscopy
⇒ *during annealing and external stress loading of dielectric films*

Wafer curvature-based techniques offer the best overall compromise between versatility, simplicity, sensitivity and compatibility with a variety of film deposition processes.

Methods for curvature measurements

• point deflection : rectangular strip clamped substrate
Measured by capacitance change, interferometric method, CCD camera

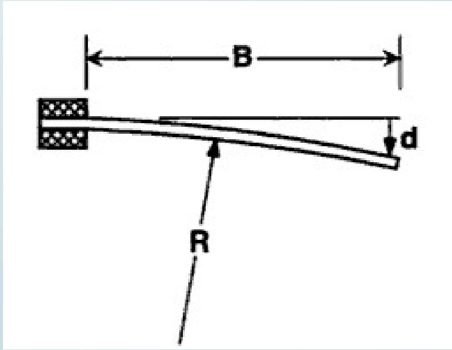

• height analysis:
Stylus profilometer or optical interferometry z(x,y)
(poor sensitivity)

• lattice bending
XRD on single crystal substrate (Segmuller et al. 1980)

• laser deflectometry
Translational or rotational scanning; good sensitivity (40 km),
1 km in deposition chamber (with vibrating noise)

Problem overcome with multipoint illumination (MOSS)

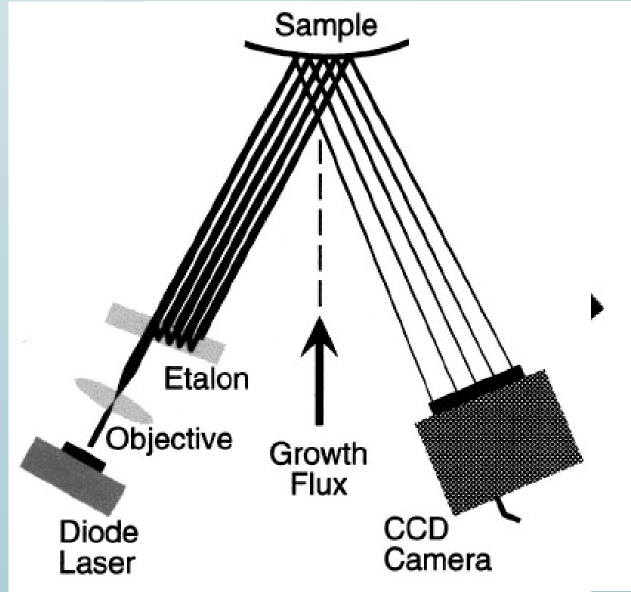

Sample rotation (uniform thickness or stoechiometry)
⇒Synchronous trigger

XRD lattice bending

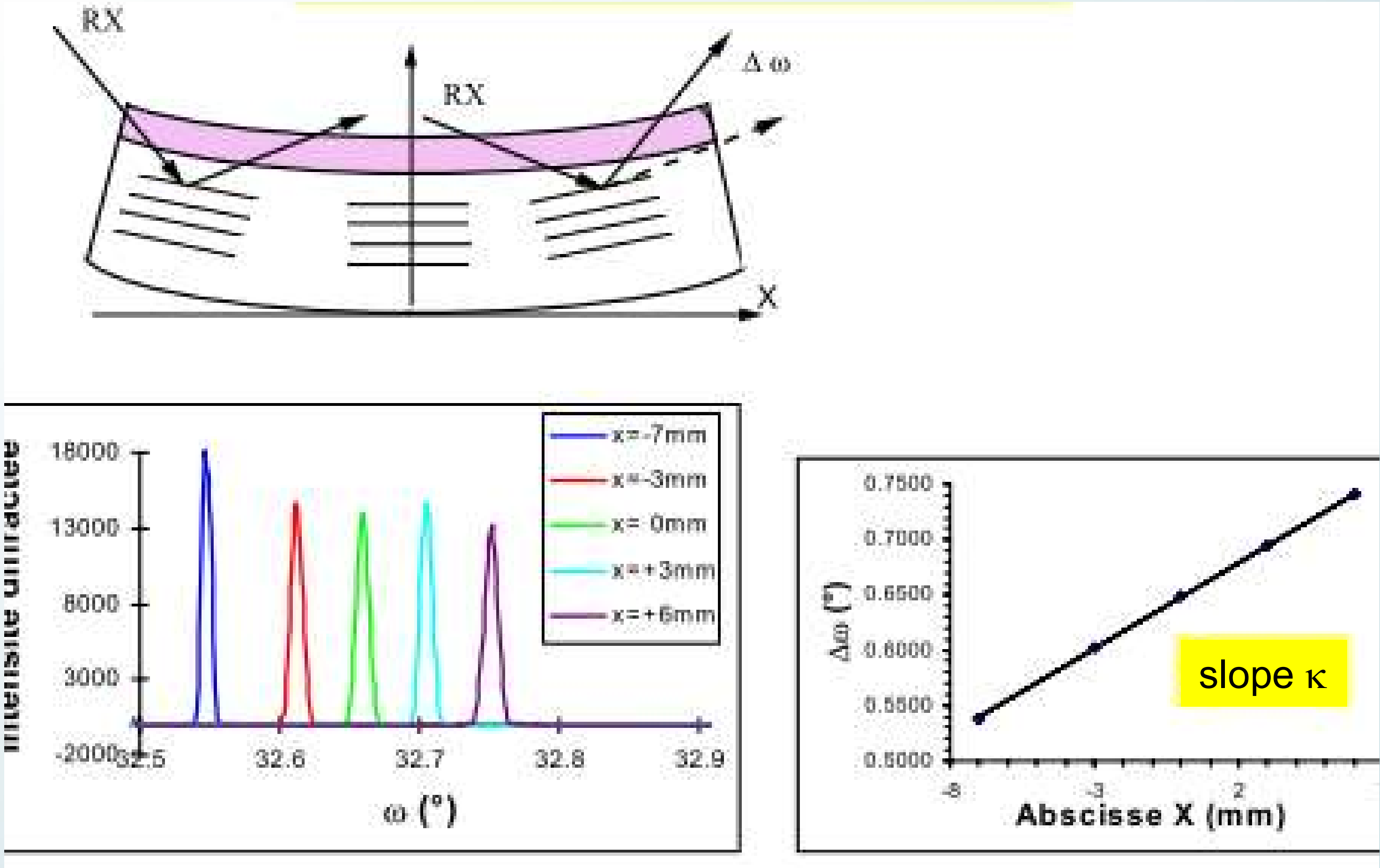

Cantilever technique

$$\kappa = \frac{1}{R} = \frac{2}{\sqrt{(l^2 - d^2)}} \sin\left[\tan^{-1}\left(\frac{d}{l}\right)\right]$$

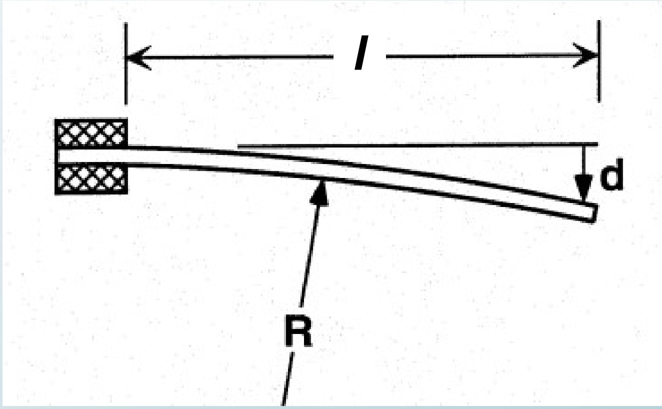

- The deflection can be measured using a microscope or video camera
  It suffers from a lack of sensitivity: 10 GPa.Å
- Restoring methods, in which a known force is applied to the end of the beam so as to balance out the deflection of the beam due to the stress
- Optical measurement of the end point deflection *d* or curvature κ using laser beam; well adapted for in situ monitoring
- Capacitive measurement of the end point deflection *d*; not particularly suited for curvature monitoring in constrained space

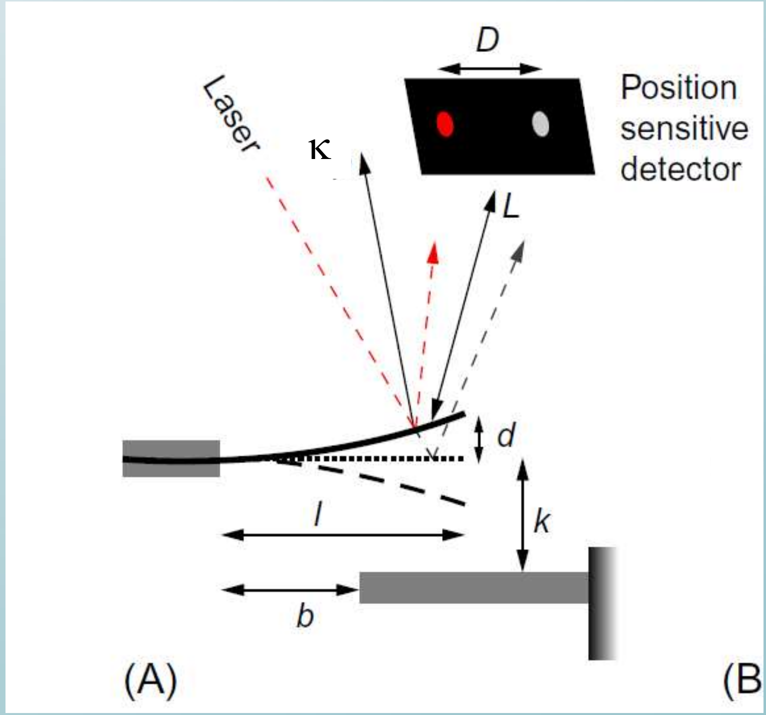

Fluri et al., Elsevier book (2018)

Cantilever technique

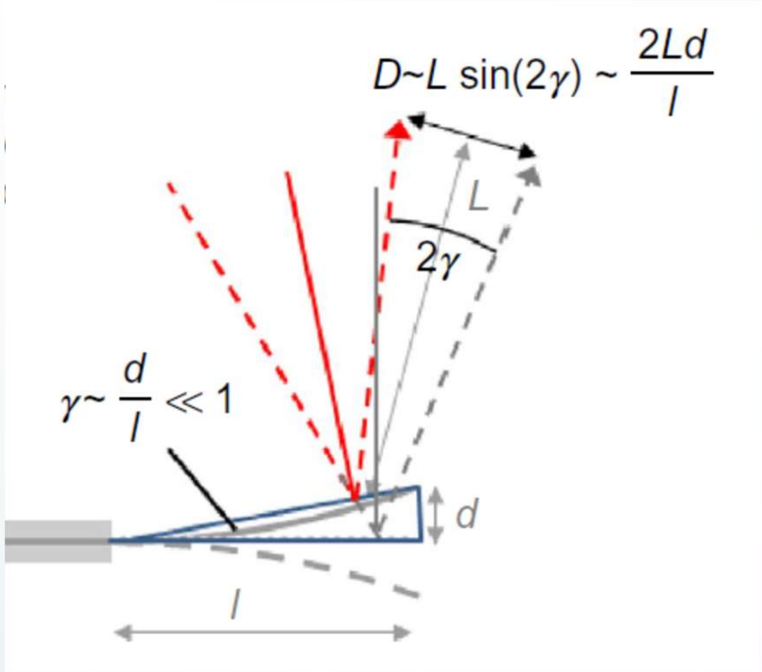

d= end point deflection
D= distance between the reflected beam positions
L= substrate-detector distance
l = cantilever length

curvature $\boxed{\kappa \sim \frac{2d}{l^2}}$

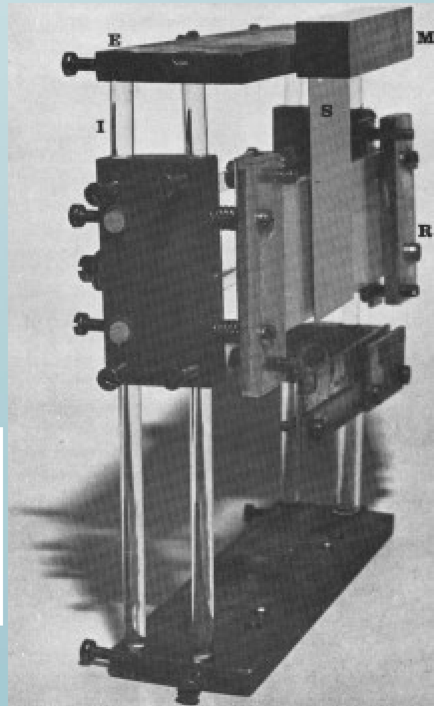

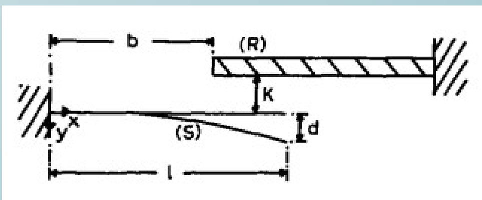

Initial capacitance $C = \frac{(l-b)w}{4k\pi}$

Change in capacitance $\boxed{d = \frac{3w(l-b)l^2}{4\pi C^2(l^2+bl+b^2)} \cdot \Delta C}$

w= substrate width

from Wilcock, Thin Solid Films 3 (1969) 3

Deflection and bowing

- End deflection δ

Let's consider a substrate in the form of a cantilever beam of length *L*, width w, and thickness t_s such that L >> w >> t_s, clamped at one end as shown in the figure

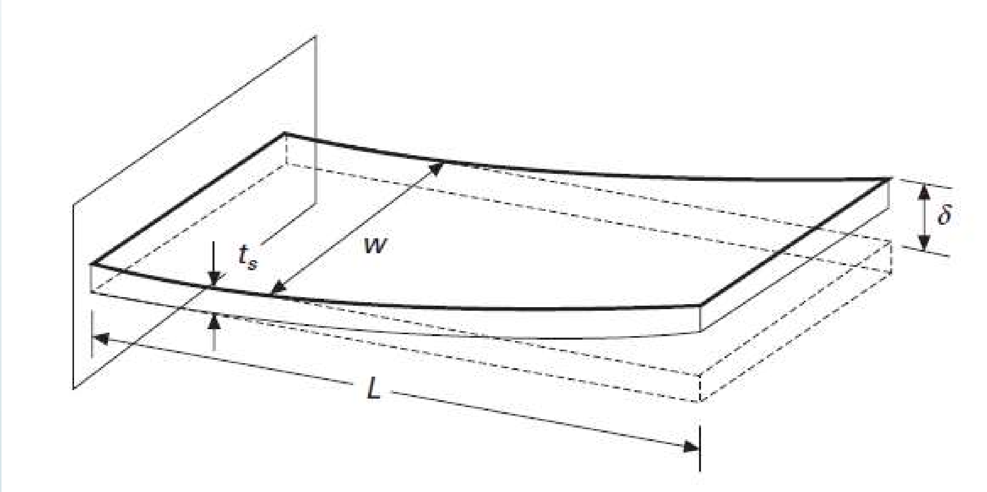

$$\boxed{\sigma h_f = \left(\frac{E}{1-\nu}\right)\frac{h_s^2}{3L^2}\delta}$$

eq. valid for biaxial bending

- Substrate bowing

☞ Valid if Z<<h_s

$$\boxed{Z = \frac{d^2}{8R}}$$

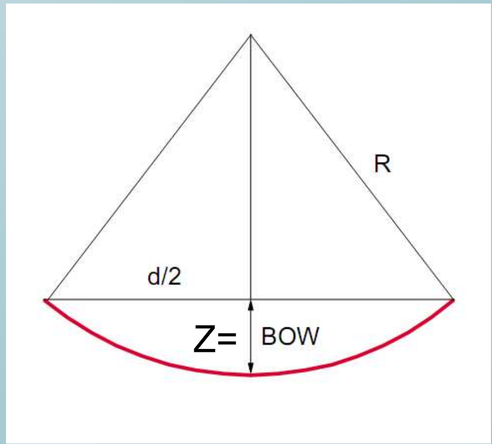

R=1 km

d (cm)	Bow (μm)
1	0.0125
10	1.25

R=100 m

d (cm)	Bow (μm)
1	0.125
10	12.5

Cantilever technique: two-beam setup

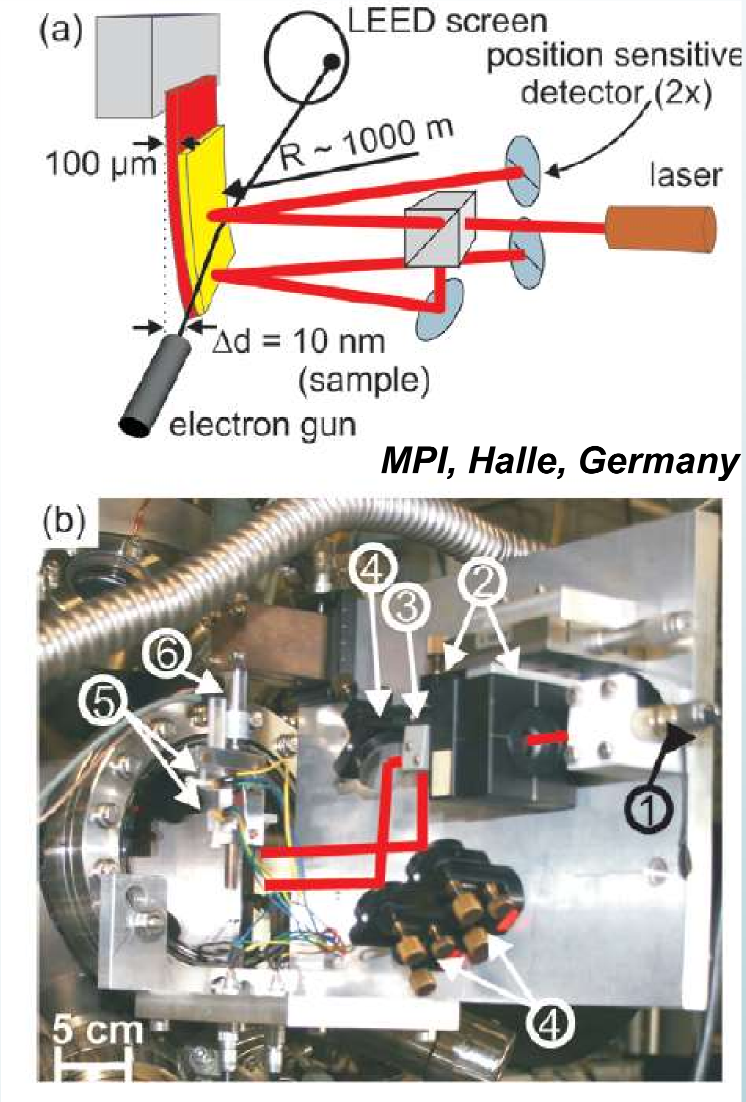

An order of magnitude for the surface stress change of a monolayer coverage is 1 N.m^{-1}, and a stress sensitivity better than 0.01 N.m^{-1} can be easily obtained

D. Sander et al., J. Phys.: Condens. Matter **21** (2009) 134015

Cantilever technique: multi-beam optical stress sensor (MOSS)

MOSS offers simultaneous multipoint illumination and detection

It consists of the following different optical elements

- **Laser source**: standard diode laser (658 nm) with Peltier cooling system
- Two **etalons**: piece of glass with parallel faces of high reflectivity, allowing to split the laser into parallel beams in X and Y directions
- A servo-controlled **mirror** allowing automated tracking capability of deflected beams for data acquisition
- A **CCD video camera**: standard (480x640 pixels) or high resolution (1300x1030 pixels), acquisition time of 8 ms; dimension of 0.8x1 cm

Possibility to trigger the CCD acquisition with rotation of the substrate, as small wobbles aorund the rotation axis can cause very large mouvements of the MOSS beam

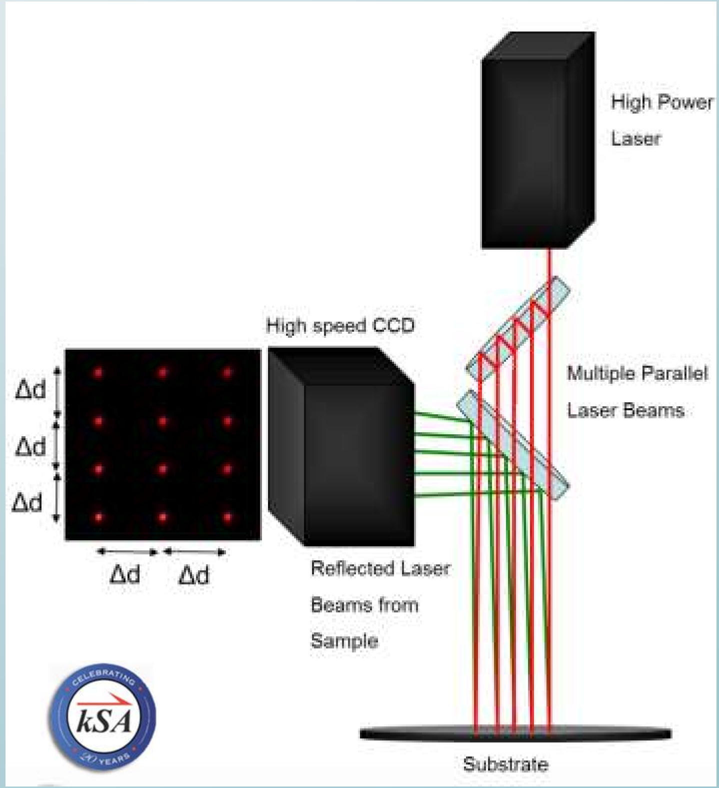

designed by kSA

MOSS: principle of measurement

Multi-beam optical stress sensor (MOSS)

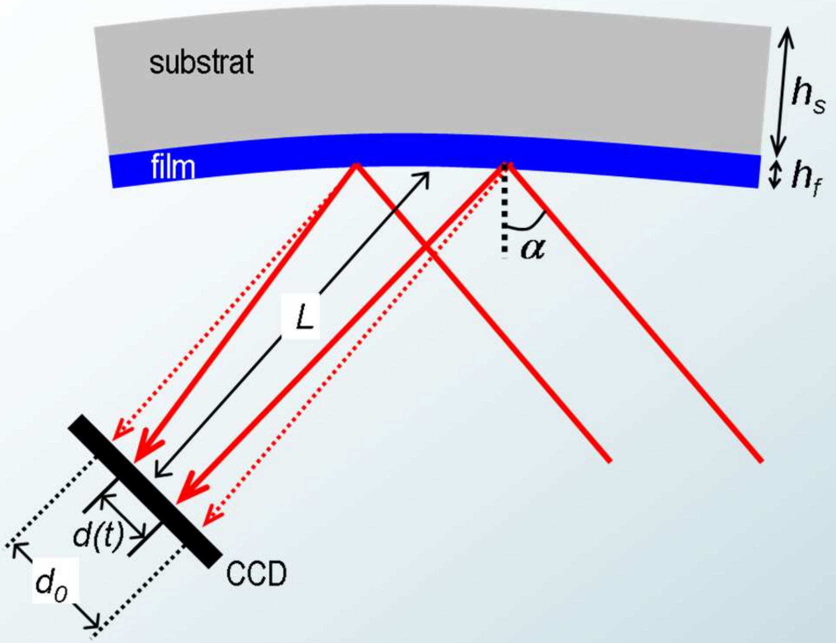

acquisition camera

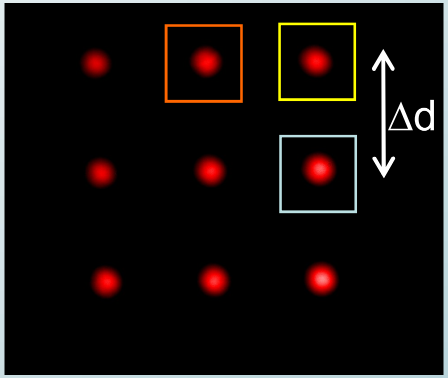

Relative spot spacing

⇨ *Curvature*
$$\Delta\kappa(t) = -\frac{\delta d(t)}{d_0}\frac{\cos\alpha}{2L}$$

⇨ *Stoney equation*
$$\Delta\kappa \cong \frac{6\ F/w}{M_s h_s^2}$$
if $h_f << h_s$

$$\boxed{\sigma h_f = \left[\frac{\delta d}{d_0}\right]\frac{M_s h_s^2 \cos\alpha}{12L}}$$

J. A. Floro et al., J. Elect. Mat. 26, 969 (1997)

MOSS: data acquisition

computer controlled detection system combined with proven fitting algorithms result in typical radius of curvature detection of 4 to 50 kilometers depending on system geometry.

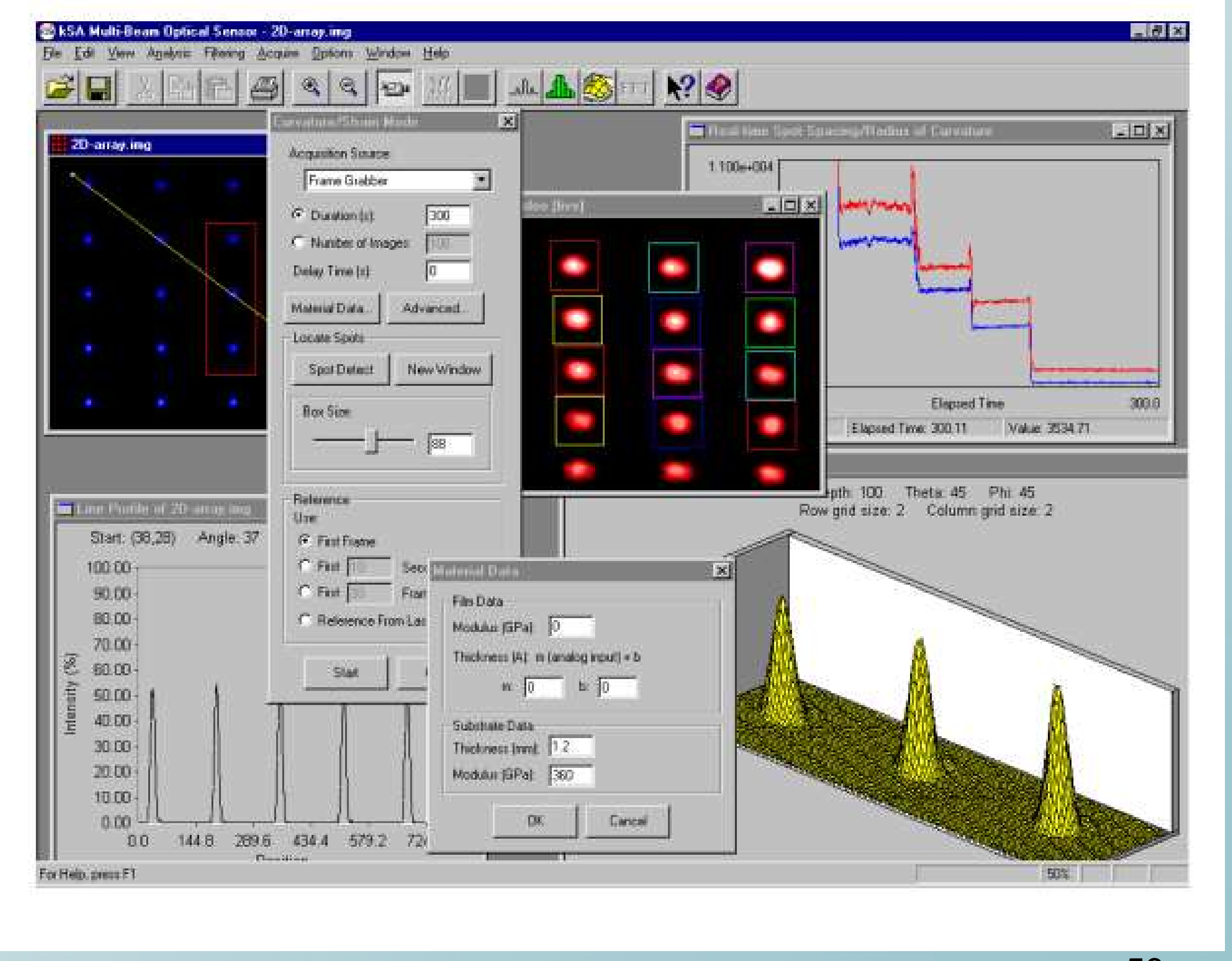

Conversion of beam deflection measurement to curvature

1) Vertical beam array geometry

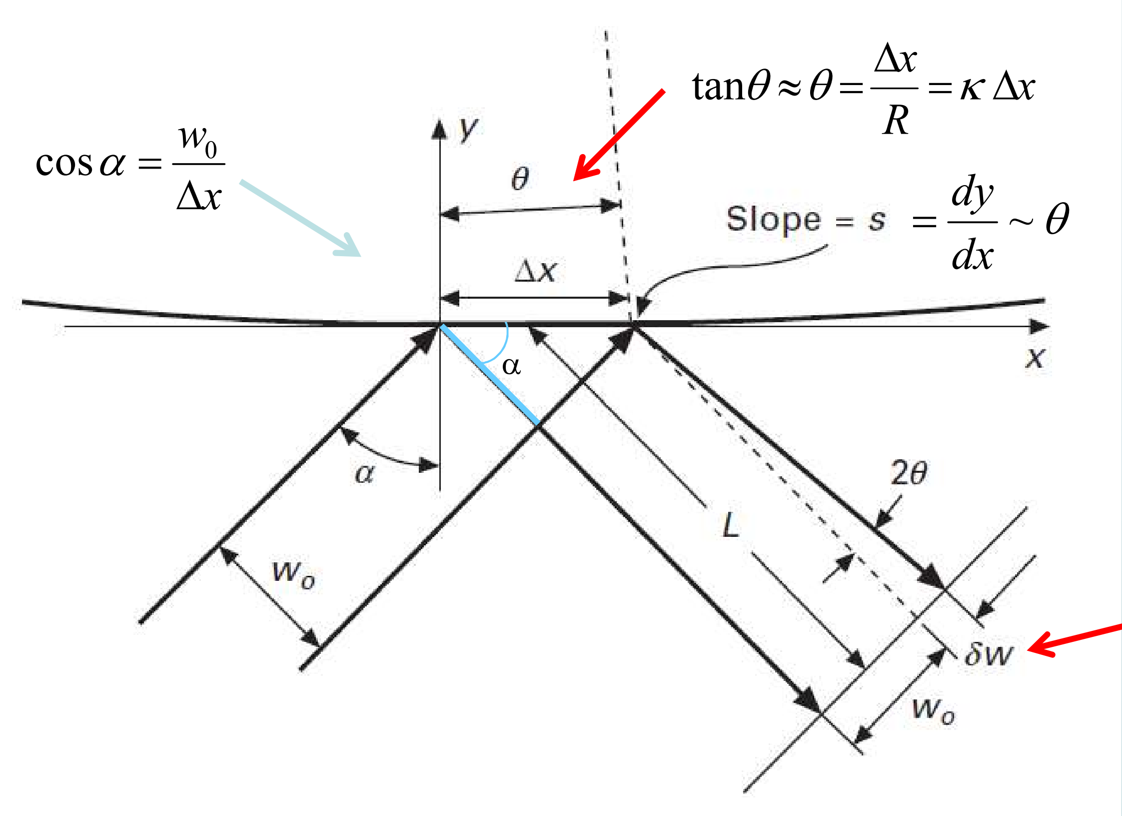

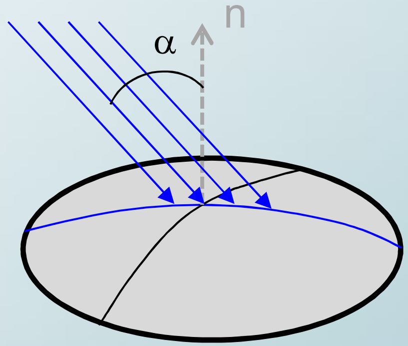

$$\tan 2\theta = \frac{\delta w}{L}$$

$$\kappa = \frac{d^2 y}{dx^2} = \frac{ds}{dx}$$

$$\boxed{\kappa = \frac{s}{\Delta x} = \frac{\delta w}{w_0}\frac{\cos\alpha}{2L}}$$

2) Horizontal beam array geometry

$$\boxed{\kappa = \frac{\delta w}{w_0}\frac{1}{2L\cos\alpha}}$$

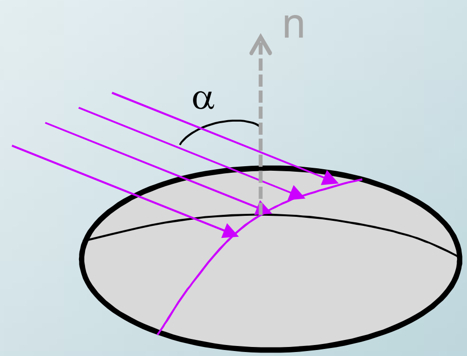

Summary

• The conversion factor between surface curvature and mean differential spacing depends on the incident angle α and distance from sample to detector *L*

• It is different by a factor $\cos^2\alpha$ for arrays of beams that are separated along the direction of the beam propagation(vertical array) and those normal to the direction of propagation (horizontal array)

e.g., at α=60 deg, the deflection of beams is 4 times larger for a vertical array than for a horinzontal array

Influence of sample mounting on bending

- One side clamping
  - $\rightarrow$ Biaxial stress for large *L*/*w* ratio

L/w > 3

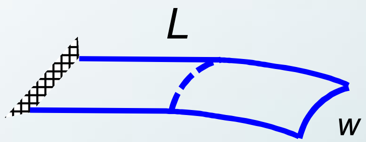

$$\bar{\sigma}.h_f = \frac{E}{(1-\nu)}\frac{h_s^2}{6R}$$

- Two sides clamping
  - $\rightarrow$ Uniaxial stress

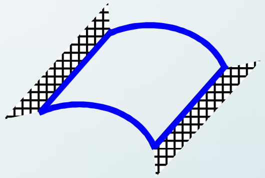

$$\bar{\sigma}.h_f = \frac{E}{(1-\nu^2)}\frac{h_s^2}{6R}$$

Dimensionality of the bending

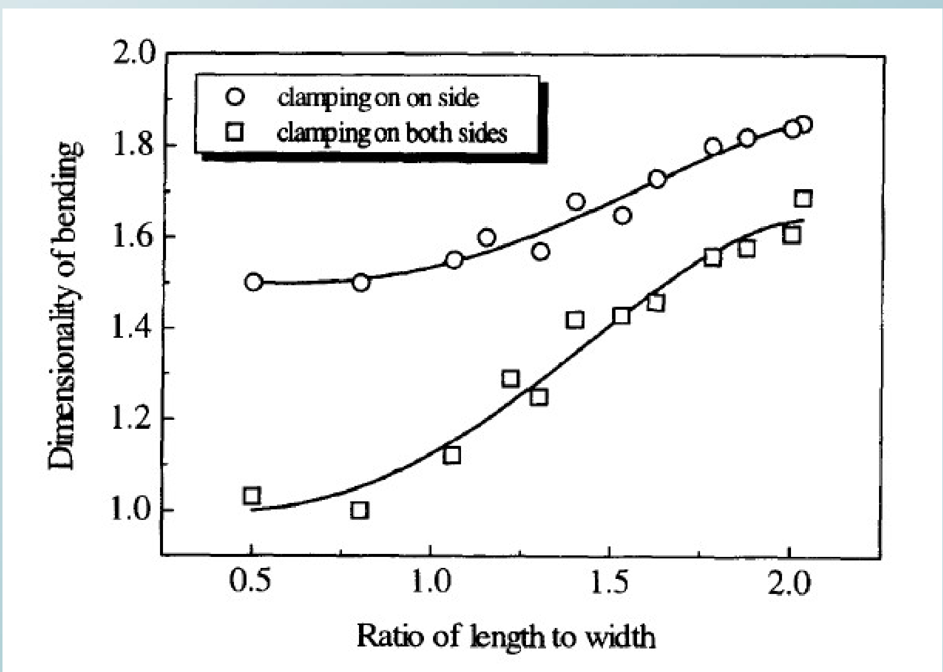

- Free-standing sample mounting

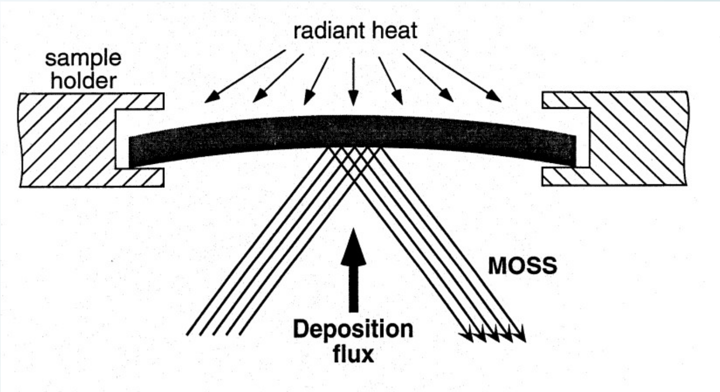

$\rightarrow$ Biaxial stress (2D bending)

from Ibach, Surf. Sci. Rep. 29 (1997) 193

MOSS: resolution and sensitivity

Resolution

There are two dominant sources of error in MOSS measurements.
- The first is the *noise* or error in the measurement of the beam spacing from a single sample.
- The second is determining the difference in the beam spacing that is due to stress in the film.

Reduction of noise during in situ curvature measurements by using multiple beams

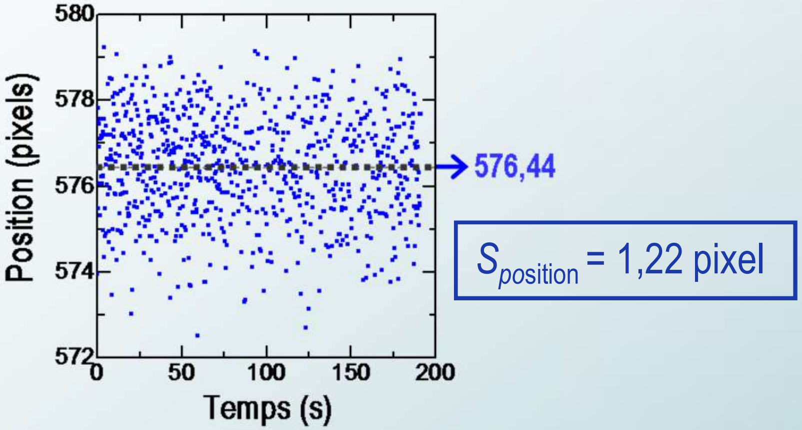

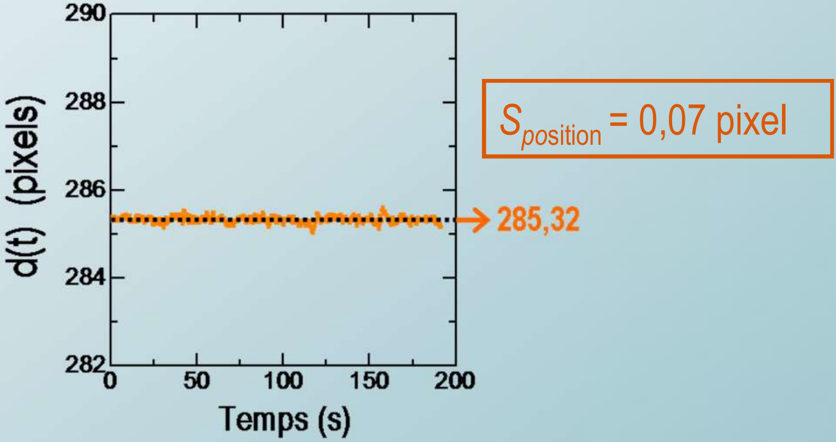

Stability of MOSS measurement with time

Note that averaging N points will reduce the noise by a factor of √N. So, e.g., averaging 25 points reduces the error on the average value of the beam spacing to 0.031 pixels. This yields a maximum resolvable *R* of 25 km

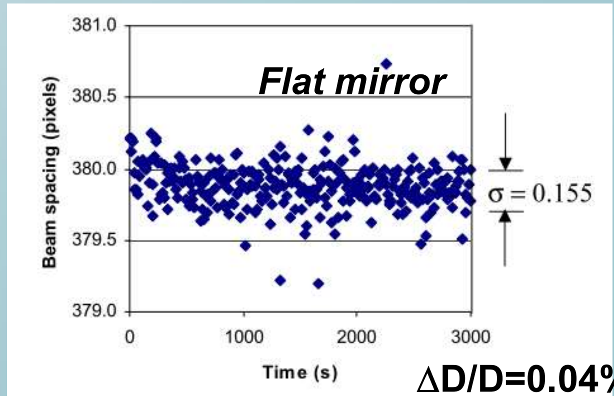

ΔD/D=0.04%

MOSS: resolution and sensitivity

Sensitivity

- Data acquisition averaged over 4 measurements of $\delta d/d_0$
- Acquisition rate: 1.25 Hz
- Typical relative incertitude in $\delta d/d_0$: 3.4×10^{-4}
- Corresponding sensitivity in curvature κ: 2.4×10^{-4} m^{-1}
  and film force F/w: 0.29 N/m

for h_s=200 μm

- for h_s=100 μm, the minimum detectable force is **0.12 N/m** (surface stress, adsorption)

σ_{min} = 0,5 GPa

σ_{min} = 10 MPa

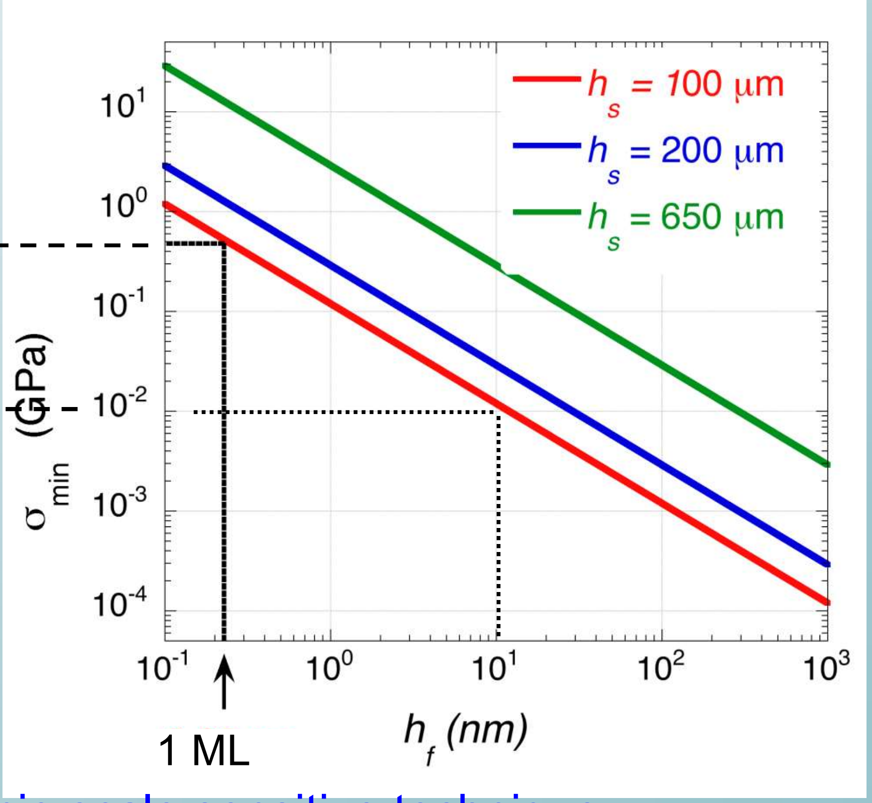

Because the curvature measures the product of stress and thickness, determination of the smallest stress that can be measured must be specified relative to the thickness of the film

Atomic-scale sensitive technique

MOSS: incertitudes of measurements

Incertitudes

- Substrate thickness

  $\Delta h_s = \pm 2\ \mu m$

- Film thickness

  $\Delta h_f / h_f = 1\%$ from XRR

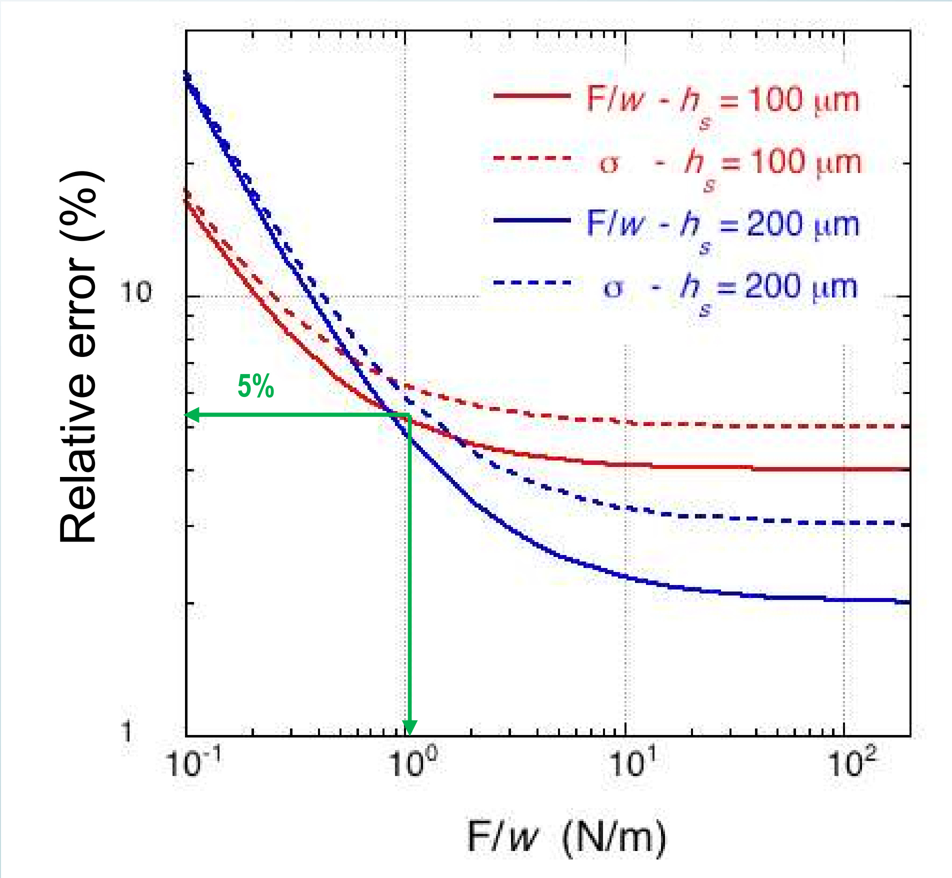

MOSS: experimental set-up

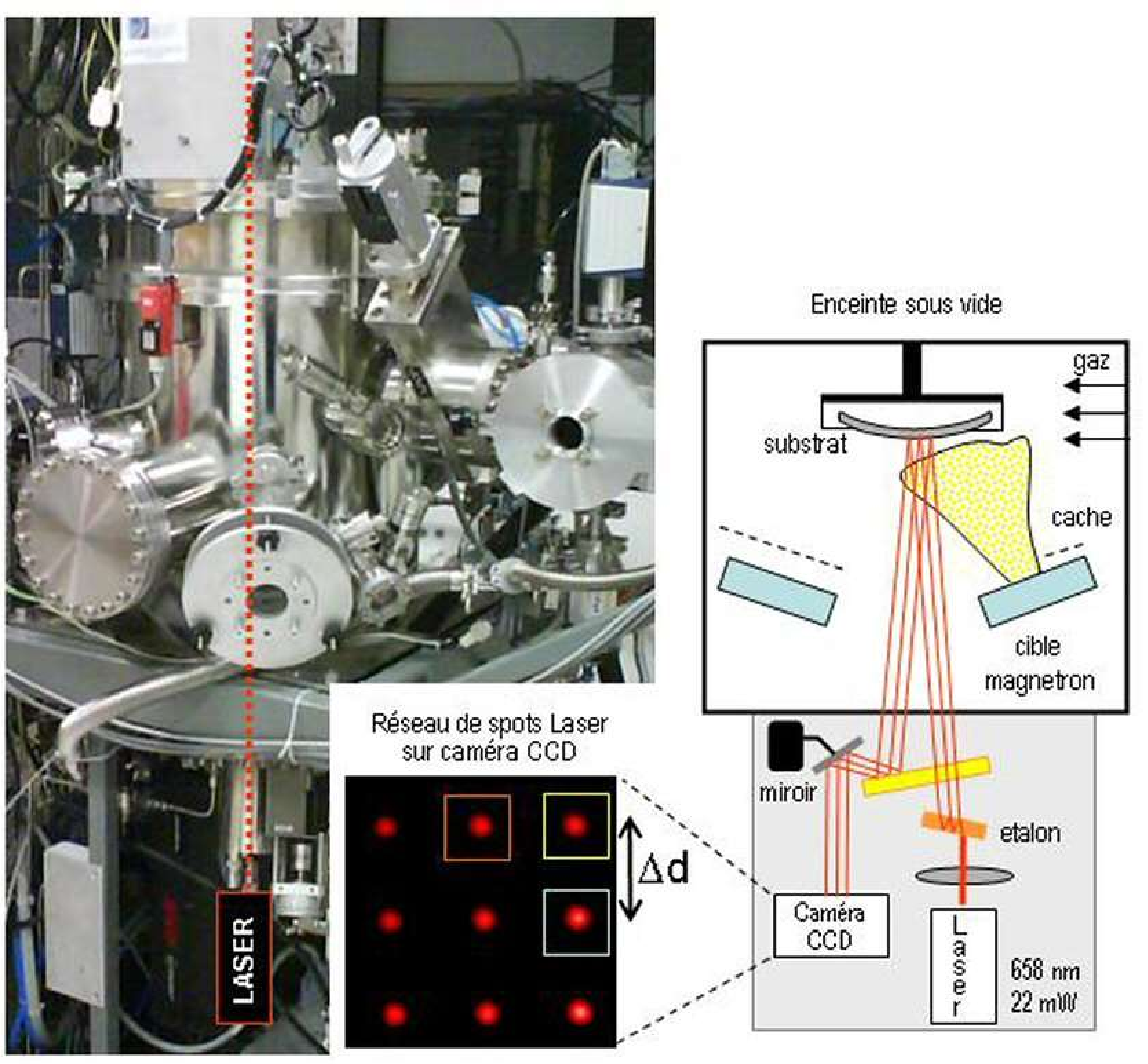

Easy implementation
- deposition chamber
- vacuum furnace
- Ion implantation

Holder for freestanding sample: the same simply rests face-down on a circulate plate

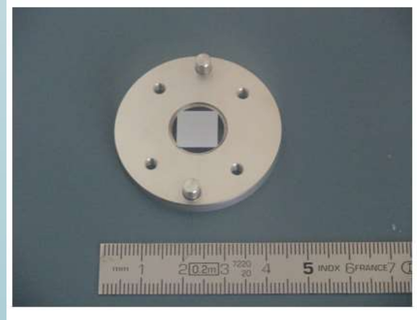

Resolution : ΔR ~ 2 km

What quantity is measured during MOSS acquisition?

Stoney equation

$$\boxed{F / w = \langle \sigma \rangle * t_f = \frac{1}{6} Y_s \, t_s^2 \, \kappa}$$

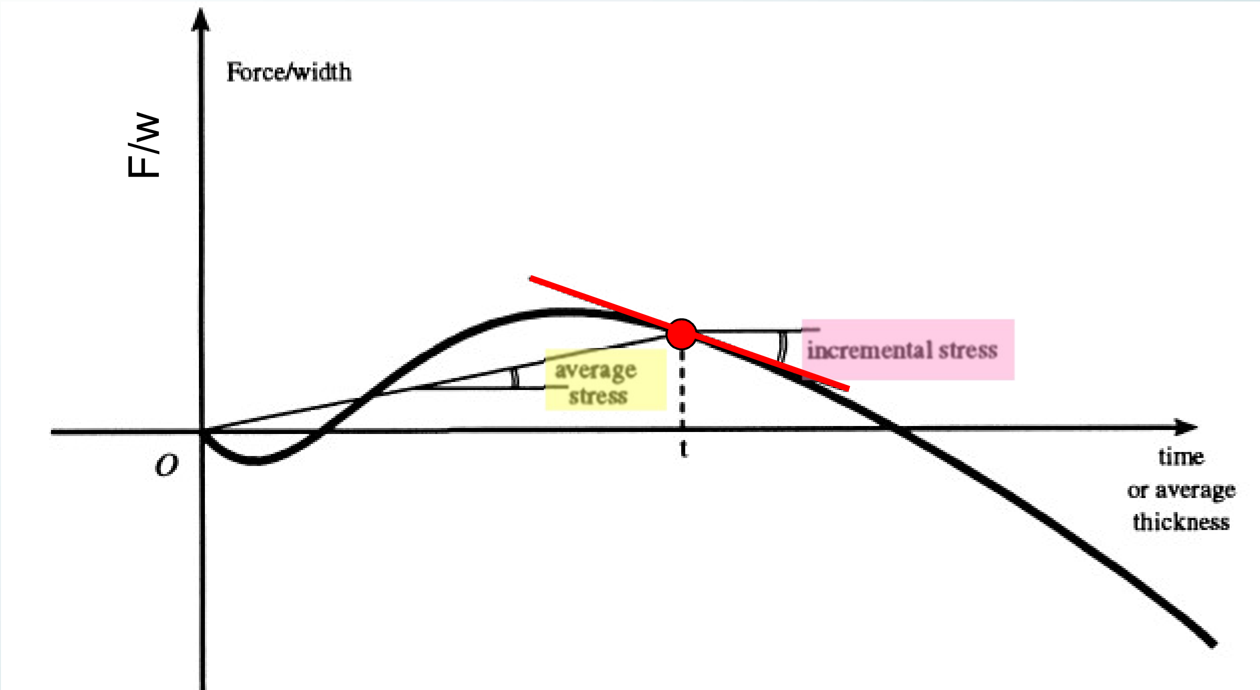

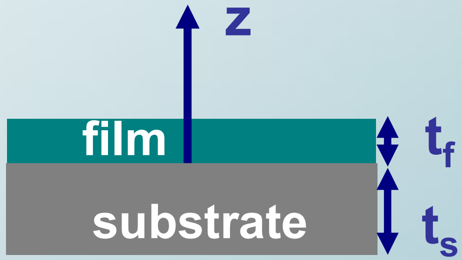

Spaepen, Acta Mater 48 (2000) 31

How to extract the average stress from real-time force data?

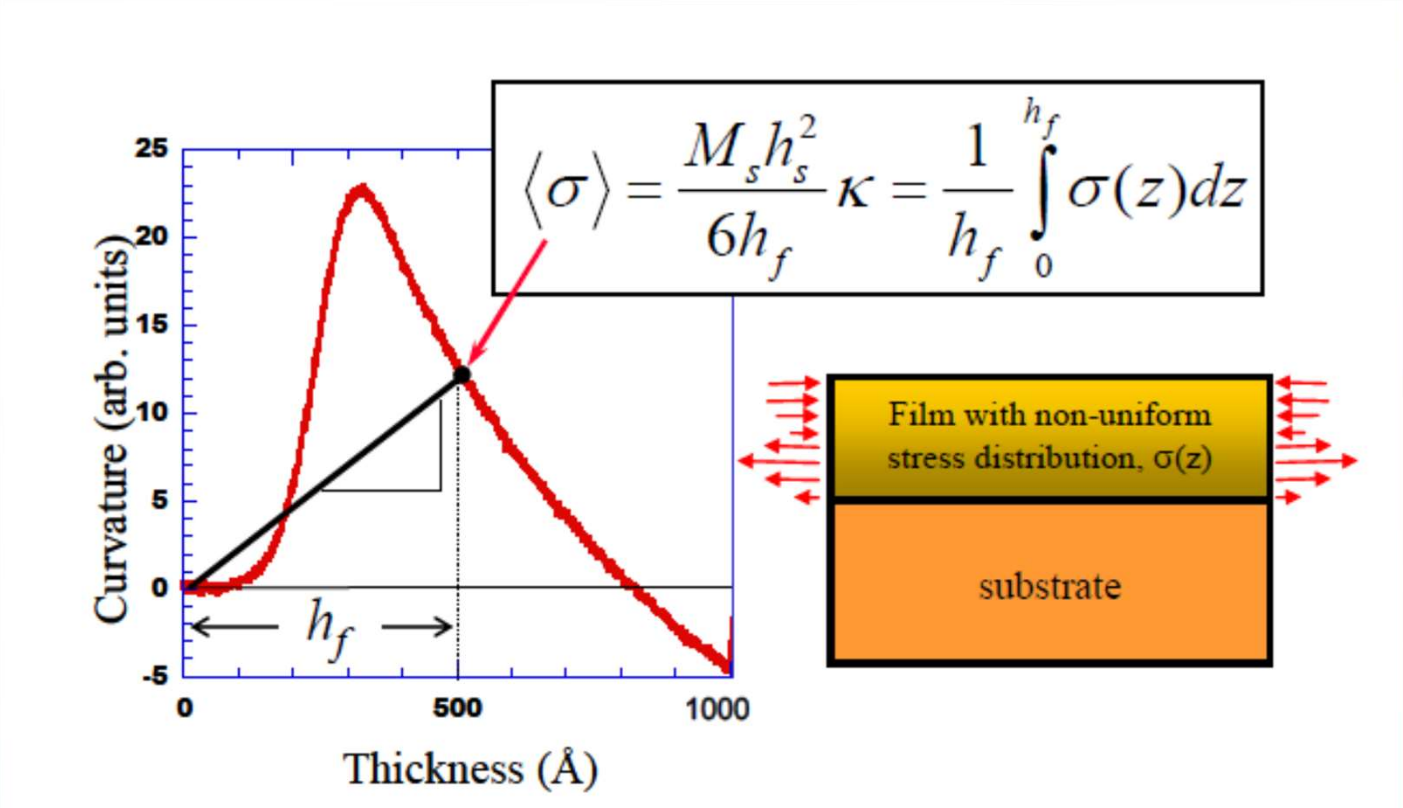

The average stress is obtained by integrating the stress distribution σ(z) over the thickness of the film

from Chason, Thin Solid Films (2012)

What do we learn from the time-derivative of the curvature ?

$$\frac{d\kappa}{dt} \propto \sigma(h_f,t)\frac{\partial h_f}{\partial t} + \int_0^{h_f} \frac{\partial \sigma(z,t)}{\partial t} dz$$

two terms !

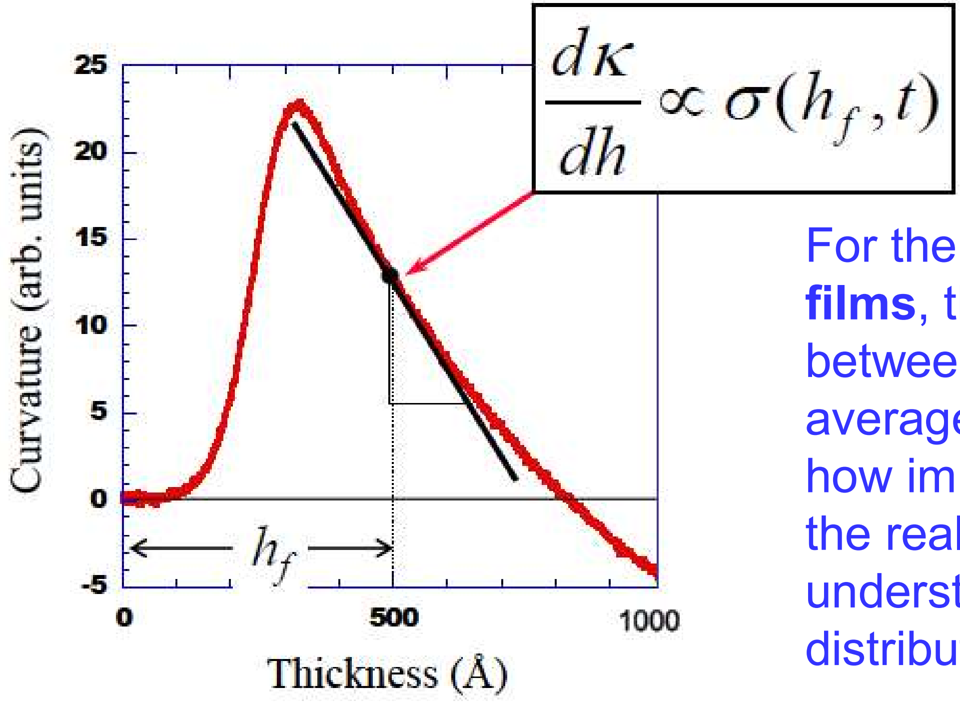

For the case of **polycrystalline films**, the large difference between incremental stress and average stress clearly shows how important it is to measure the real-time stress evolution to understand the stress distribution along the film depth

- **incremental** stress (or instantaneous stress), corresponding to the stress of additional topmost deposited layer
- **modification** of the stress state in the **buried layers**

Selected examples

Stress evolutions during 3D Volmer-Weber growth

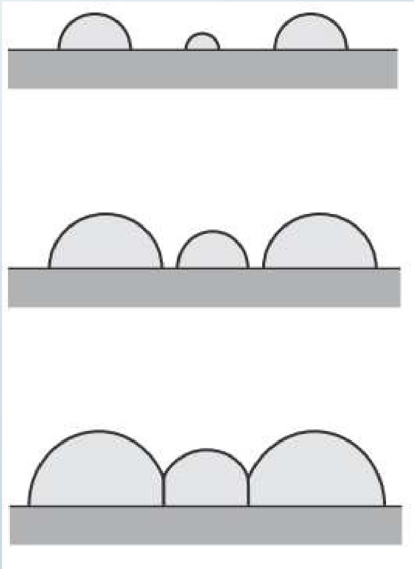

Volmer-Weber (3D) growth mode of high-mobility metal: Ag on Si

compressive-tensile-compressive (CTC) behavior
⇒ typical of high-mobility metals growing in Volmer-Weber mode

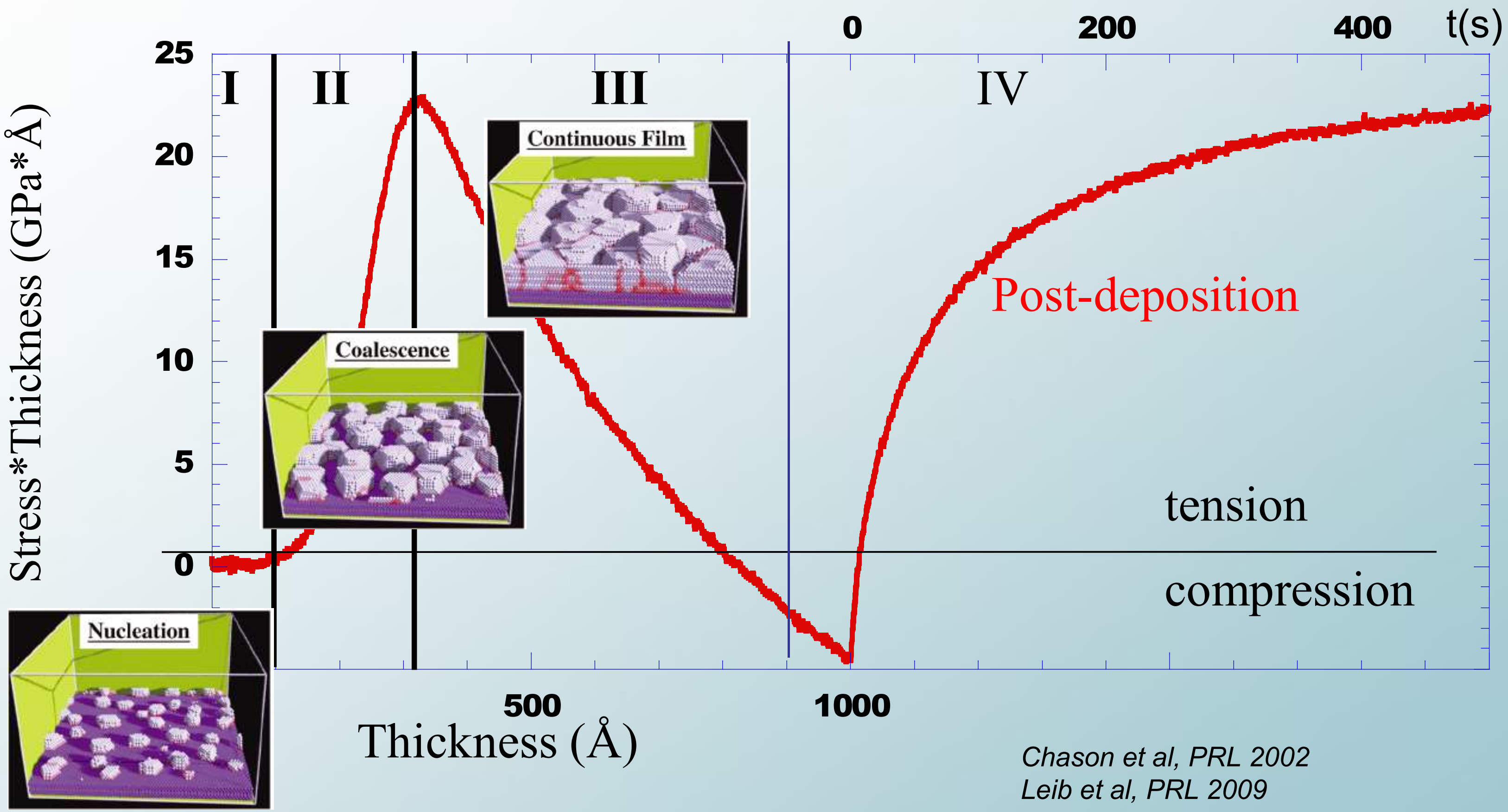

Chason et al, PRL 2002
Leib et al, PRL 2009

Floro et al. JAP (2001)
Abermann and Koch (1986)
Shull and Spaepen (1996)
Gonzalez-Gonzalez, PRL (2013)

- Reversible stress change upon growth interrupt

⇨ Spontaneous flow of excess atom at the GB ?

⇨ Morphological rearrangement ?

Archetypal stress evolution

Two archetypes of stress evolution

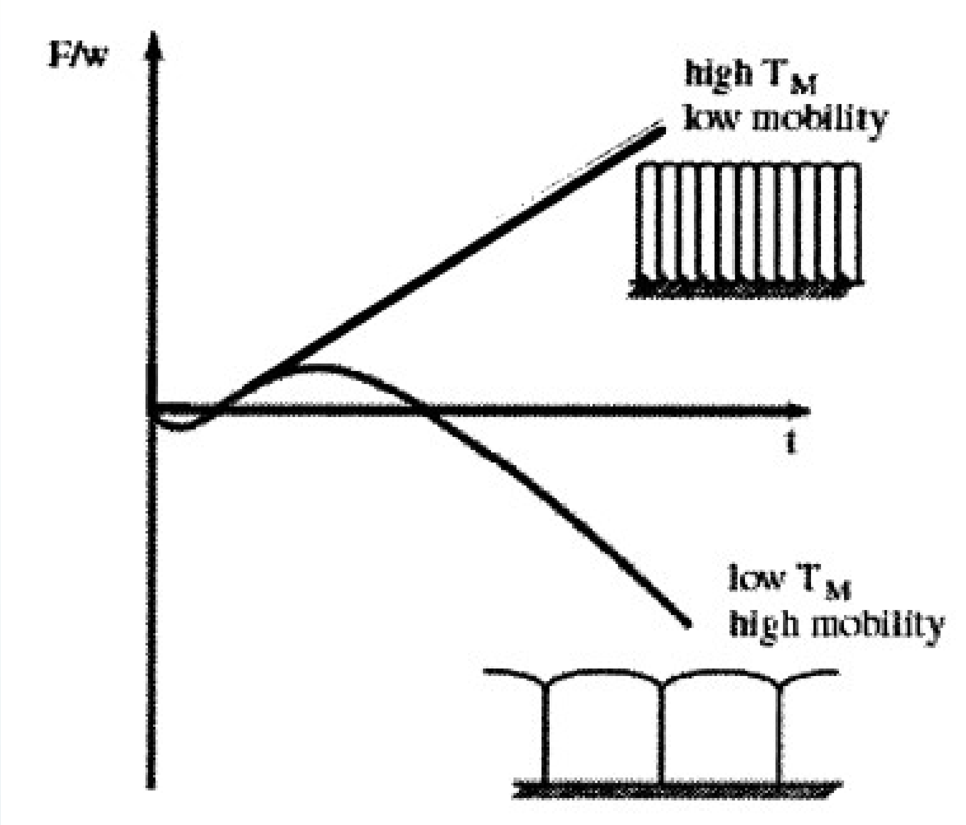

Co	1768 K
Fe	1811 K
Ti	1941 K
Mo	2896 K
Al	933 K
Ag	1235 K
Au	1337 K
Cu	1357 K

Schematic drawing for metal films grown by thermal evaporation

Characteristic CTC behavior

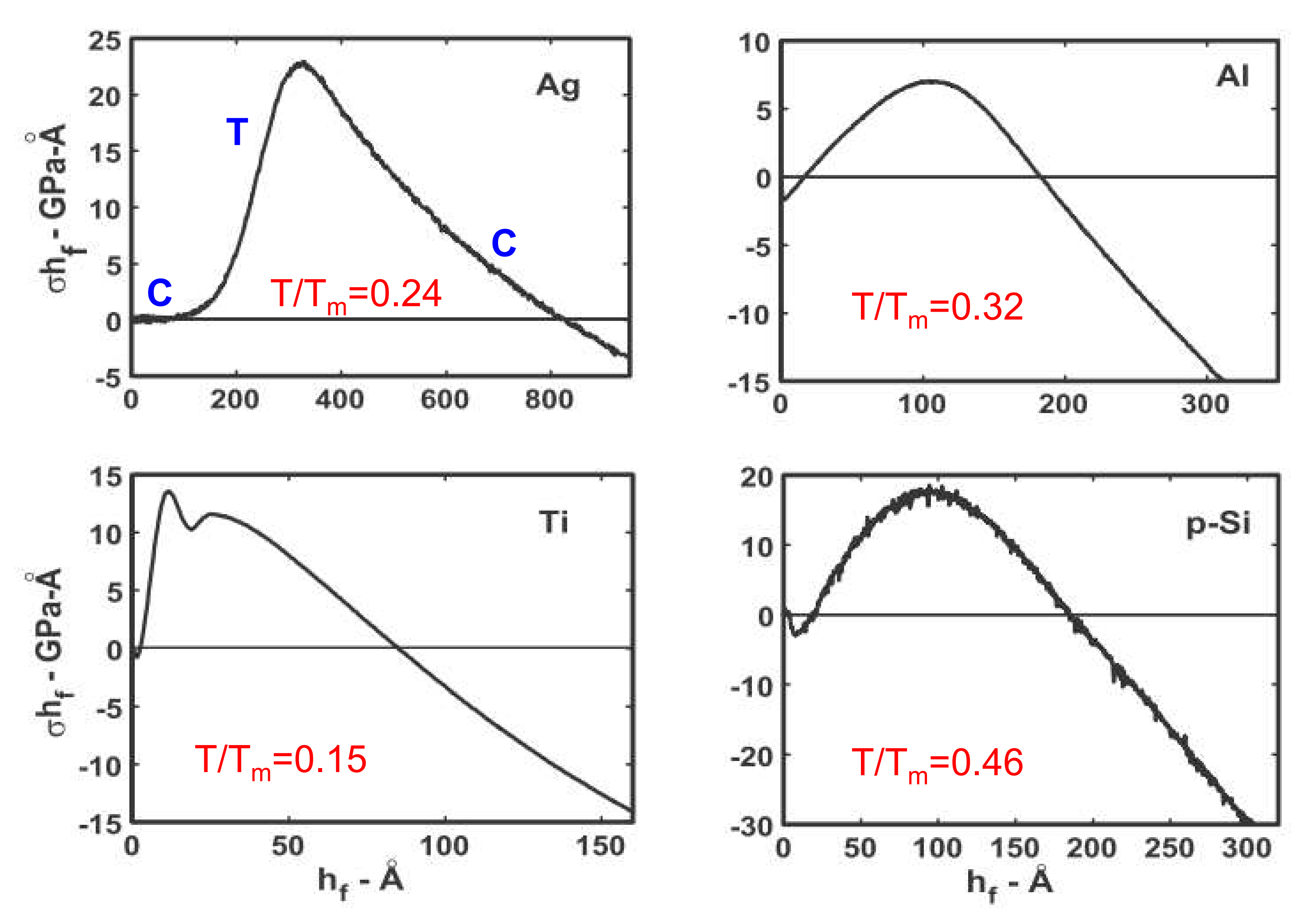

Floro et al., J. Appl. Phys. **89**, 4886 (2001)

Archetypal stress evolution

Depending on the material mobility (or homologous temperature T_s/T_m), the force evolution may be more complex

- For **intermediate** adatom mobility, like Ni or Pd evaporated films, a **stress turnaround** is observed in the later stages, where the instantaneous stress changes from compressive to tensile

- The turnaround thickness increases as the substrate temperature is increased or the deposition rate is decreased

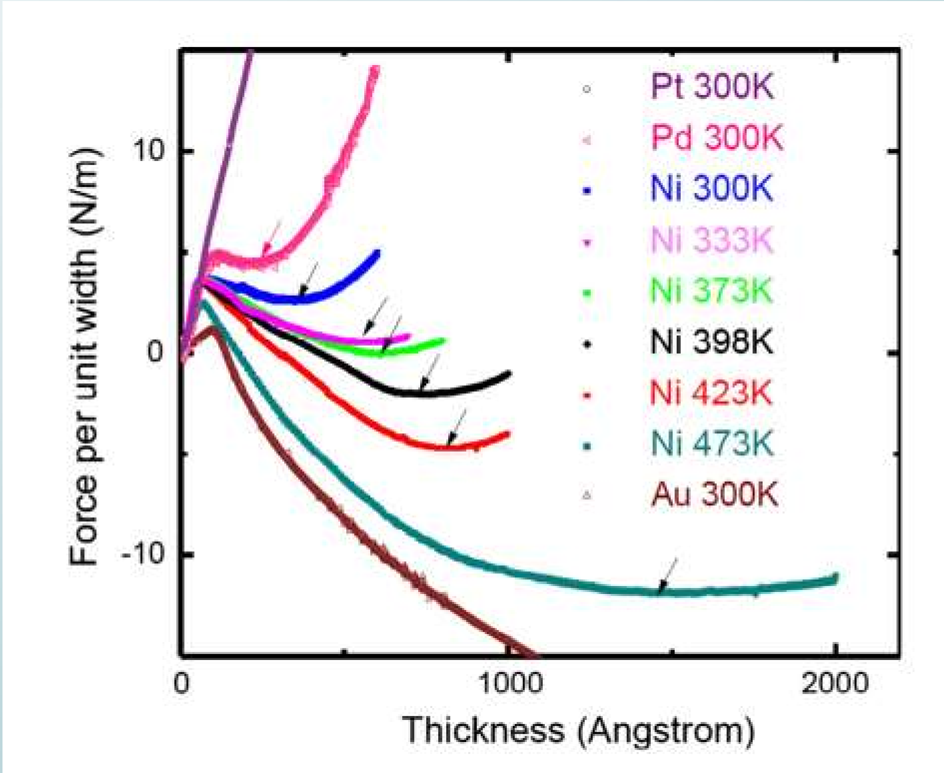

from H.Z. Yu, C.V. Thompson, Acta Materialia 67 (2014) 189

Stress evolution with material mobility

thermal evaporation

magnetron sputtering

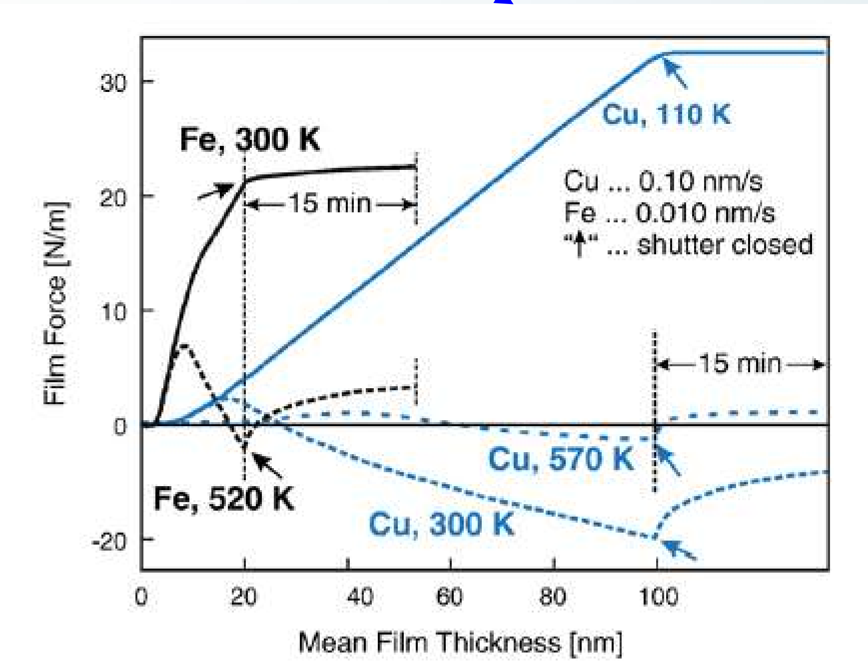

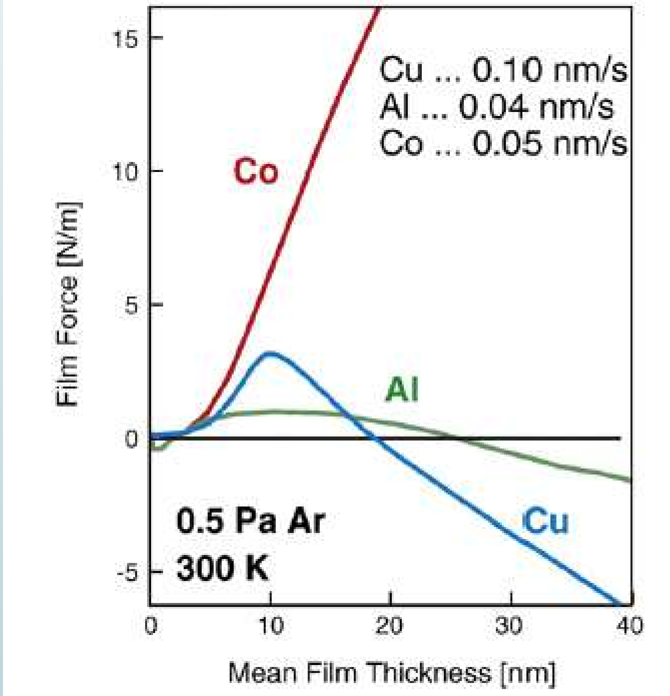

Koch, SCT 204 (2010) 1973

Similar stress evolutions suggest similar atomistic processes of stress build-up

What do we learn from the time derivative of the curvature ?

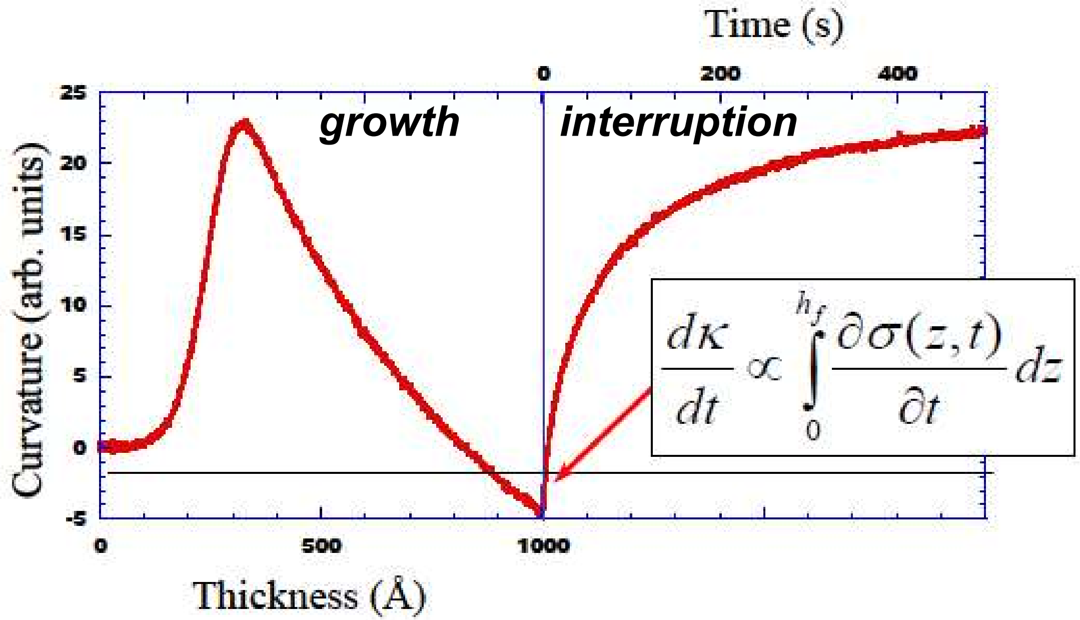

Figure 4. Change in curvature when growth is interrupted corresponds to changing stress in the layers that have already been deposited without the addition of new layers.

Example:
Cu sputter-deposition at different pressure

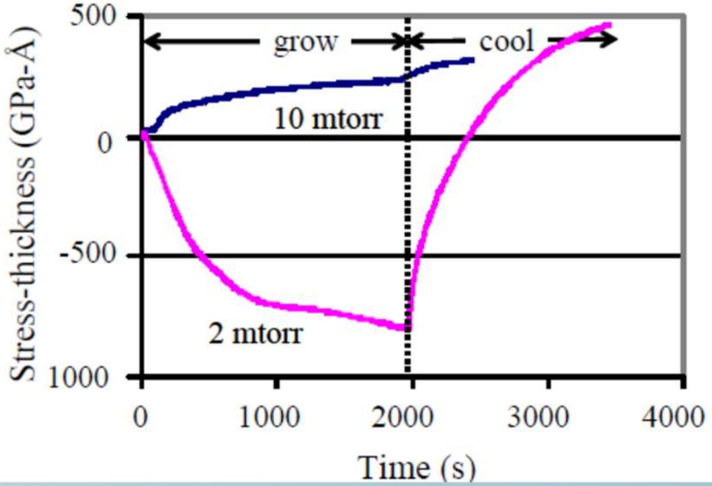

Possible reasons:

- a change in **temperature** can add a thermally-induced stress to all the layers of the film.
- **relaxation** processes (mechanisms discussed later)

Stage I: capillary-induced compressive stress

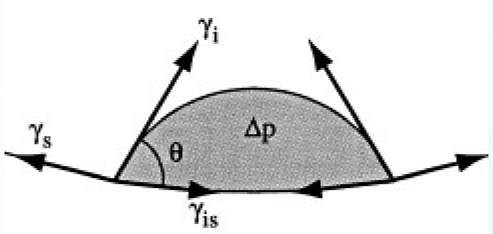

Densification of small island lattice due to surface stress f

For spherical solids

$$\boxed{\Delta P = P^{\alpha} - P^{\beta} = \frac{2f}{r}}$$

Laplace overpressure

\- $h < h_c$

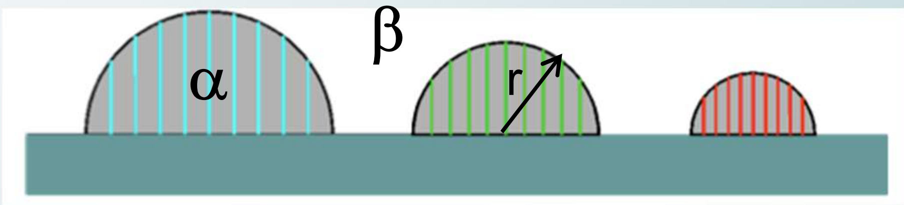

Densification :

$P = 2f / r$

\- $h > h_c$

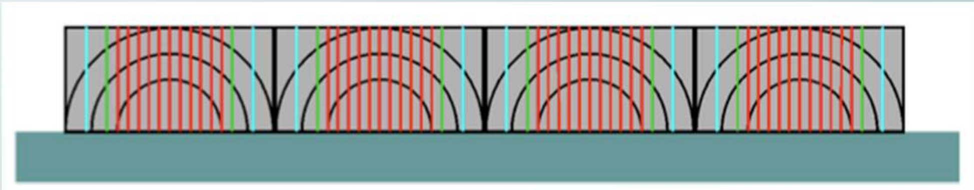

Local epitaxial growth

h_c= critical thickness at which the grains become firmly attached to the substrate, or «locked down», corresponding to radius R_{ld}

For $R>R_{ld}$

$$\epsilon_m = \frac{1-2\nu_f}{E_f}\left(\frac{2f}{R} - \frac{2f}{R_{ld}}\right)$$

$$\sigma = \frac{2f}{R_{ld}}\left(\frac{R_{ld}}{R} - 1\right)$$

$\sigma < 0$

Abermann et al., Thin Solid Films, 1979; Cammarata et al., J. Mat. Res. 2000

Stage I: capillary-induced compressive stress

- Mays et al. (1968) estimated the surface stress generated during the evaporative deposition of gold onto an amorphous carbon substrate in ultrahigh vacuum

- Using electron diffraction, the average lattice constant varied from 0.4075 nm to 0.4063 nm as the radius of curvature of the nanocrystal varied from very large values down to ~2nm.

- A value of *f* to be 1.175 N/m could be determined, which is comparable with the surface energy of gold: γ=1.4 J/m^2 ;

Stage II: attractive force during island coalescence

• Creation of grain boundaries during island coalescence induces tensile stress

Ag films on SiO_2

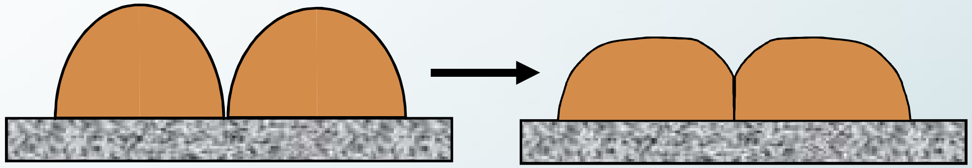

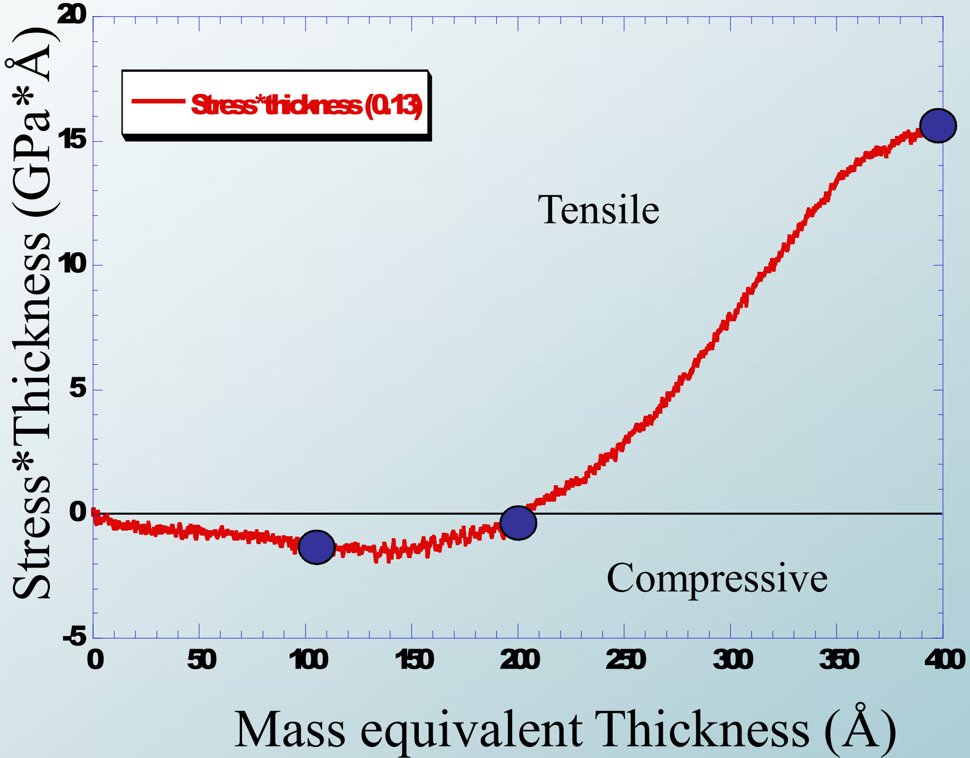

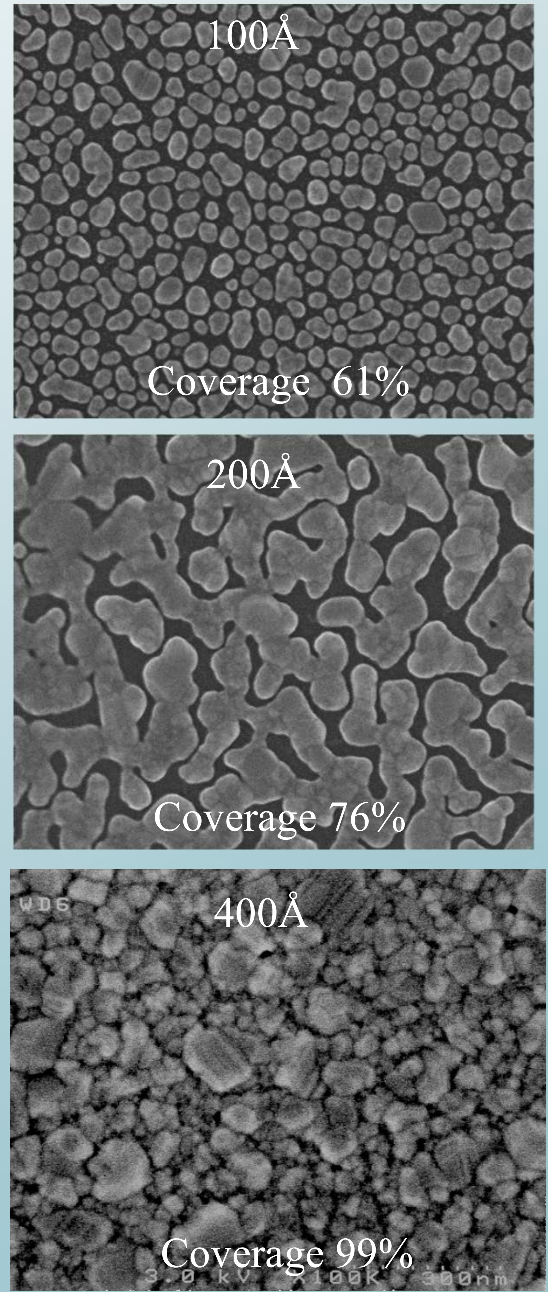

Courtesy of Eric Chason

Stage II: attractive force during island coalescence

- Polycrystalline metal films

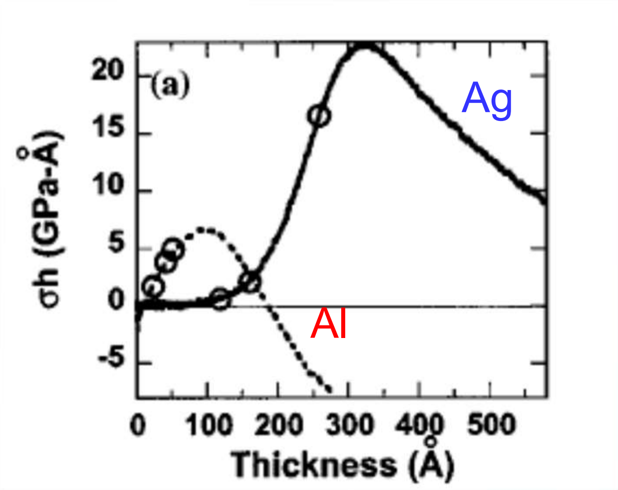

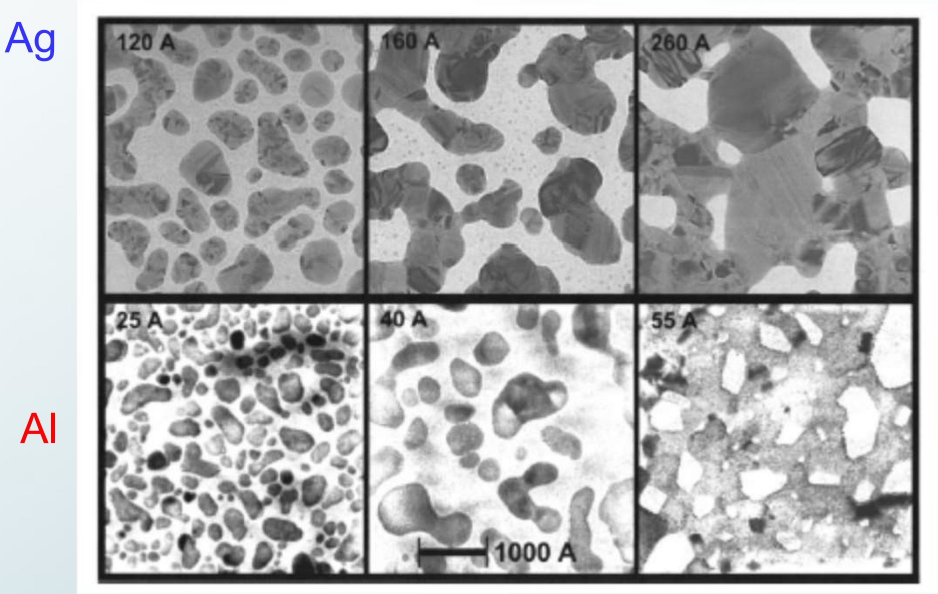

- Amorphous Ge films

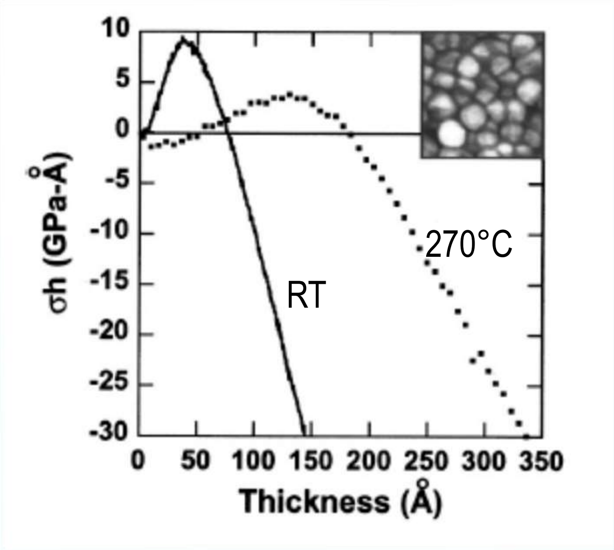

- Similar CTC behavior also observed for amorphous films, related to the VW growth
- By comparison with Ag, Al films develops tensile stress at the very begining of growth
- Increasing the substrate temperature shifts the tensile peak to larger film thickness -> larger islands formation

Floro et al., J. Appl. Phys. **89**, 4886 (2001)

Stage II: attractive force during island coalescence

- Polycrystalline Ag films (thermal evaporation)

In situ MOSS

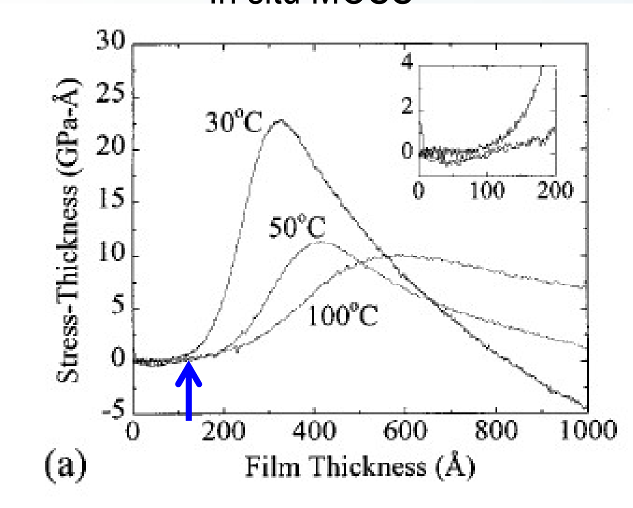

TEM image

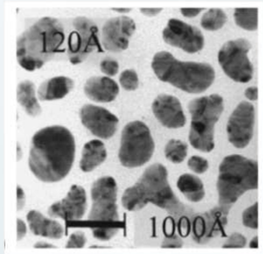

FEM-based simulations

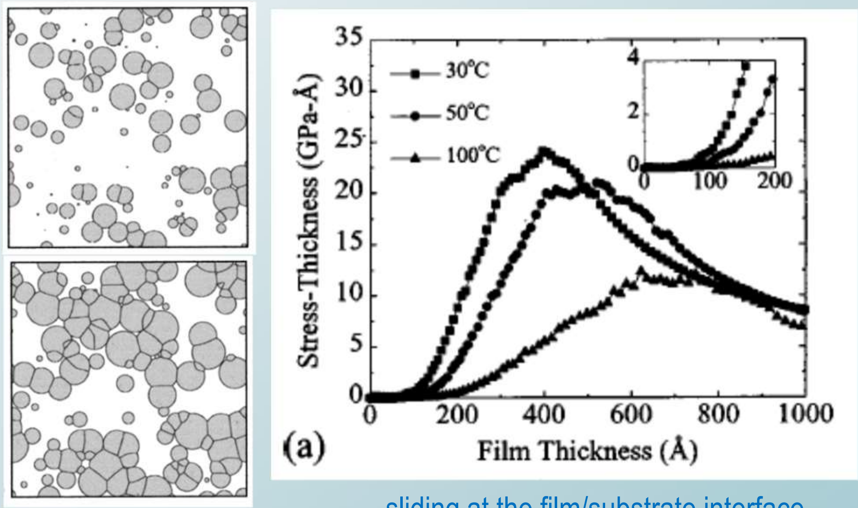

sliding at the film/substrate interface

- Even once numerous GB have formed (h~120 Å), the fim force remains very low
- The maximum in the tensile stress-thickness coincides with late channel stages, for which the fractional substrate coverages is ~0.95, i.e. just before film continuity
- The magnitude of the 'tensile maximum' decreases with increasing deposition temperature, due to larger grain size at film continuity, as supported by FEM calculations

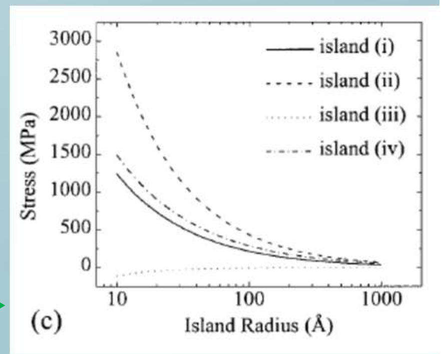

Seel et al., J. Appl. Phys. **88**, 7079 (2000)

Stage II: origin of tensile stress upon island coalescence

- Free surfaces convert to grain boundaries at expense of strain energy
- Driving force: surface energy gain: $\gamma_{gb} - 2\gamma_s < 0$

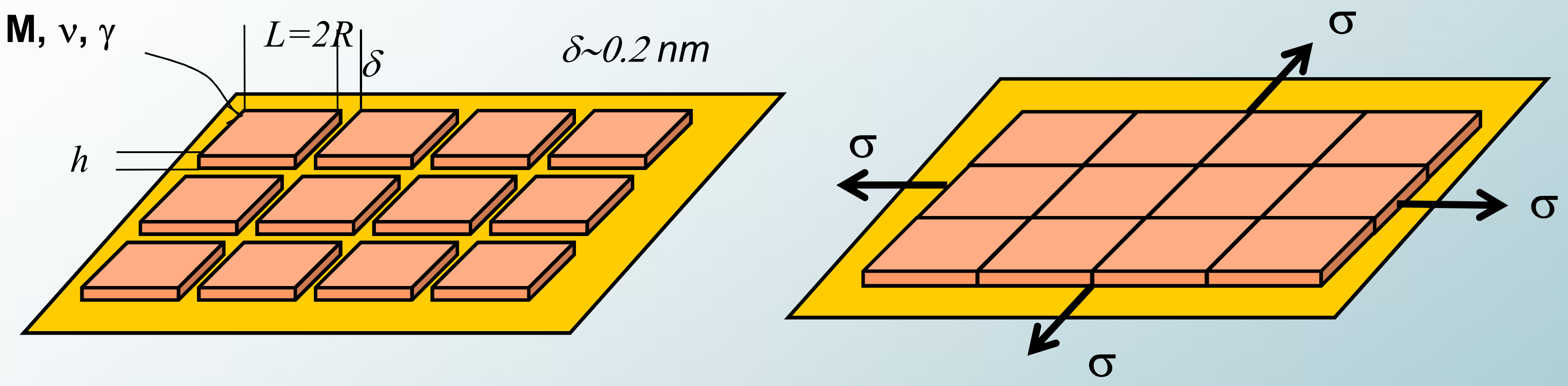

from R.W. Hoffman, Thin Solid Films 34 (1976) 185

Energy balance between

- Increase in strain energy
- Decrease in surface energy

$$\Delta E_{\text{strain}} = hL^2 \frac{\sigma^2}{\left(\frac{E}{1-\nu}\right)}.$$

$$\Delta E_{\text{interface}} = -4Lh\Delta\gamma$$

$$\Delta\gamma = \gamma_s - \frac{1}{2}\gamma_{gb} > 0$$

This model predicts a critical value for tensile stress

$$\boxed{\sigma_{crit} = 2\sqrt{\frac{Y_f \Delta\gamma}{L}}} \rightarrow \text{1-2 GPa!}$$

The dependence on $L^{-1/2}$ suggests that **finer-grained materials** will have **larger tensile stress** generated due to more grain boundaries formed per unit area of film

But this model largely overestimates experimental tensile stress values, and it considers an unrealistic geometry of grain boundary formation

Stage II: origin of tensile stress upon island coalescence

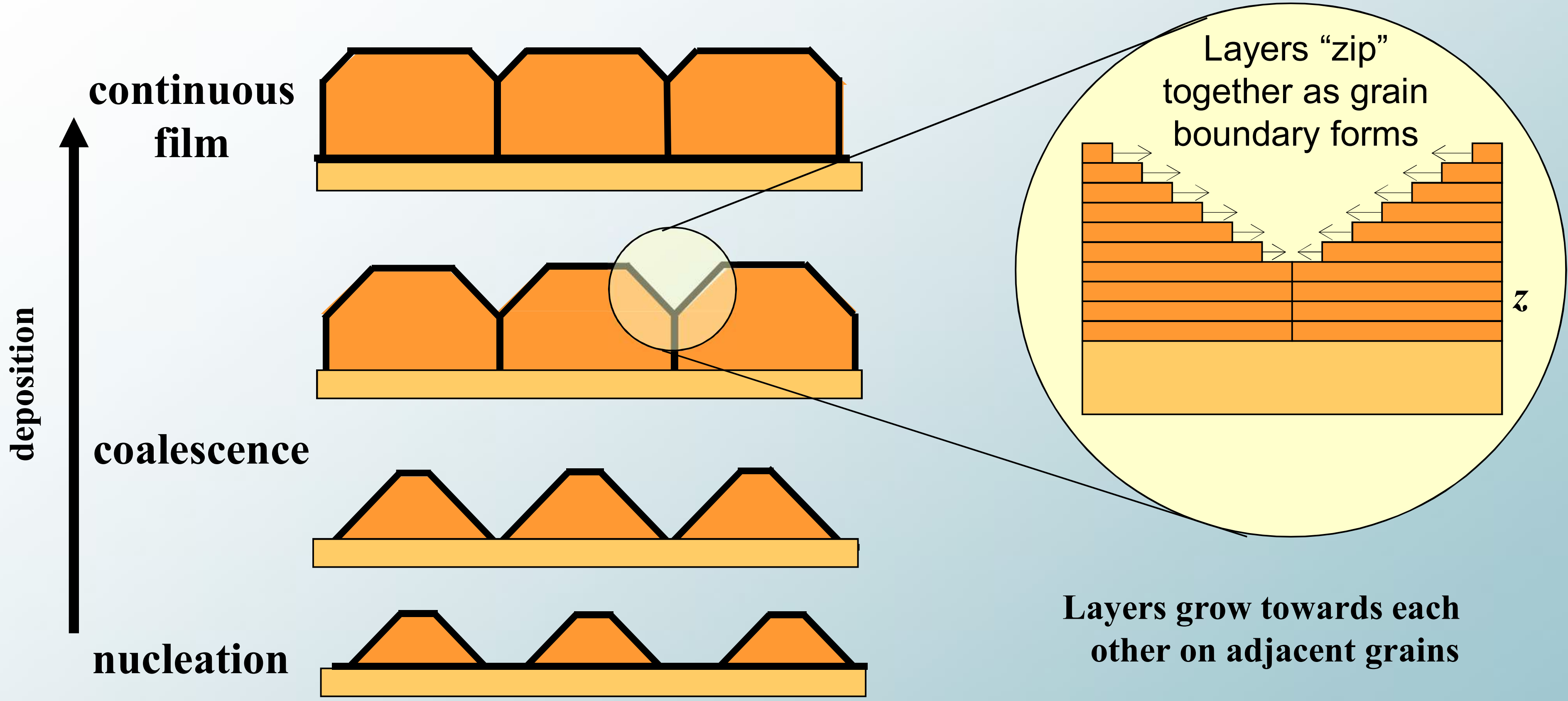

Layers grow towards each other on adjacent grains

Attractive force between atoms makes grain boundary "snap" closed, and creates residual tensile stress

Multilayers

Force evolution during growth of multilayered films

Example 1: Mo/Si multilayers

- Alternate tensile/compressive stress state during growth
- Complex stress evolution in Mo layers: interfacial effects and transient phenomenon
- Surface stress change of similar amplitude at both interfaces

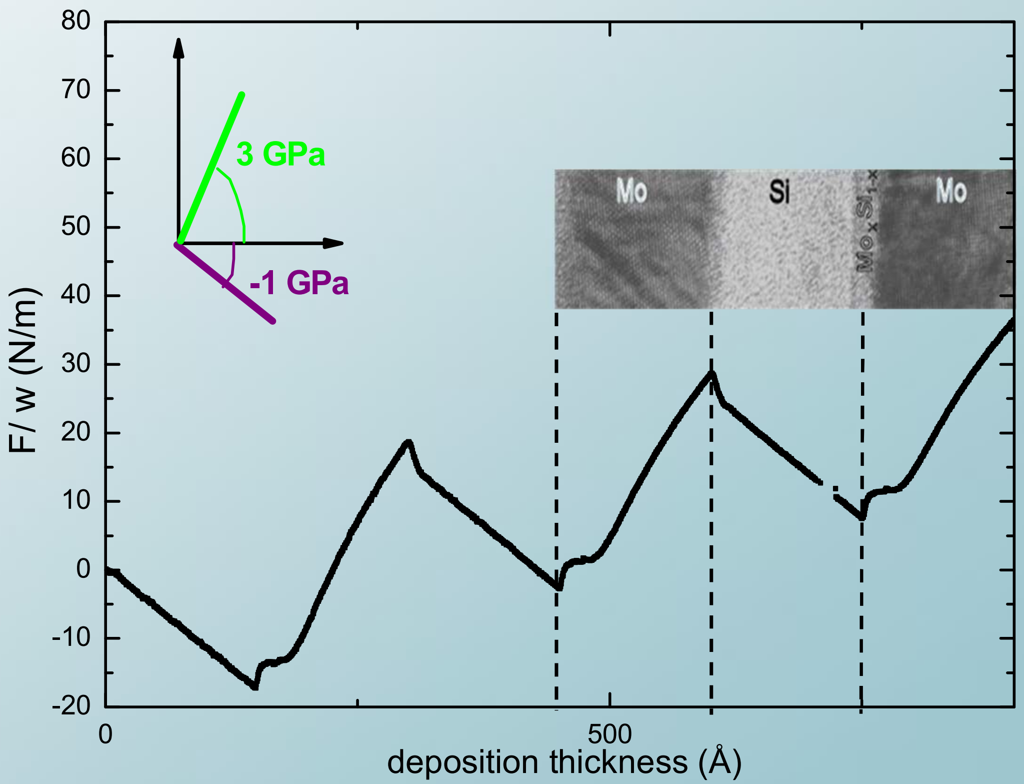

Force evolution during growth of multilayered films

Example 2: Pd/Si multilayers

- Both layers under compressive stress
- Complex stress evolution in Pd layers: interfacial effects
- Surface stress change of similar amplitude at both interfaces

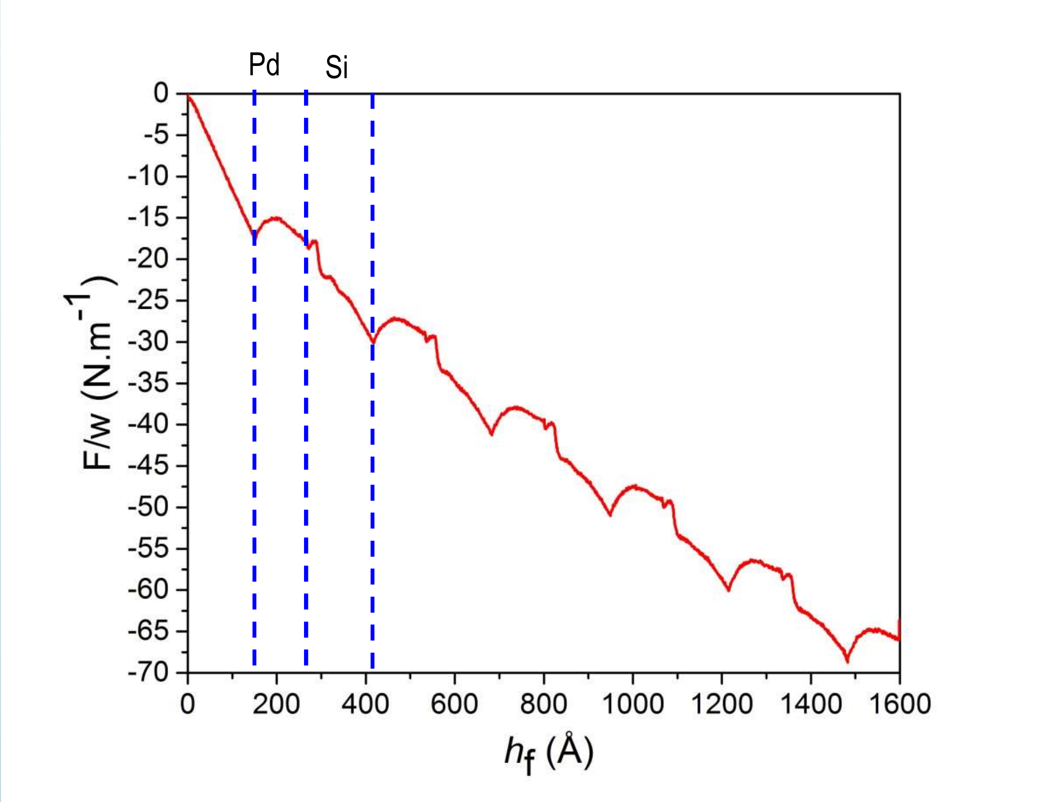

Epitaxial growth – Stress relaxation

Stress relaxation in strained layer heteroepitaxy

Stress comes from lattice mismatch

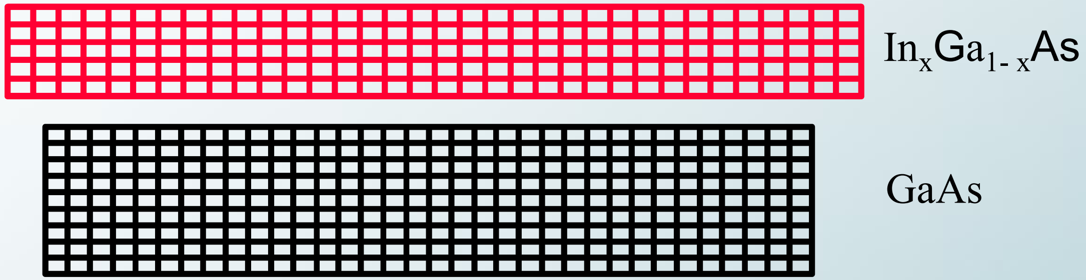

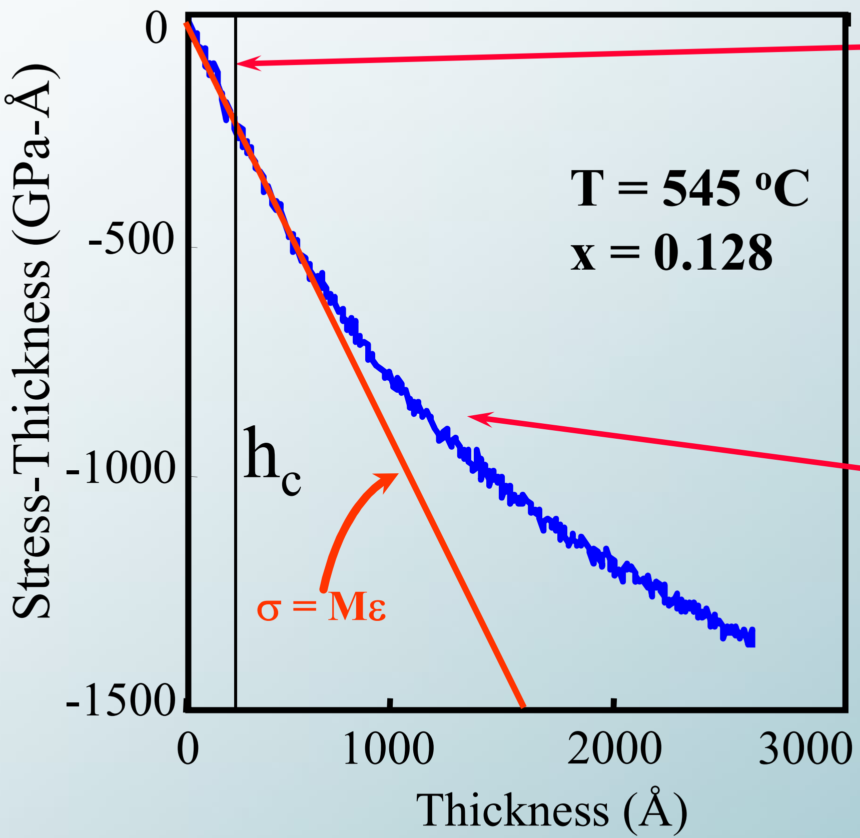

Below t_c, film is pseudomorphic

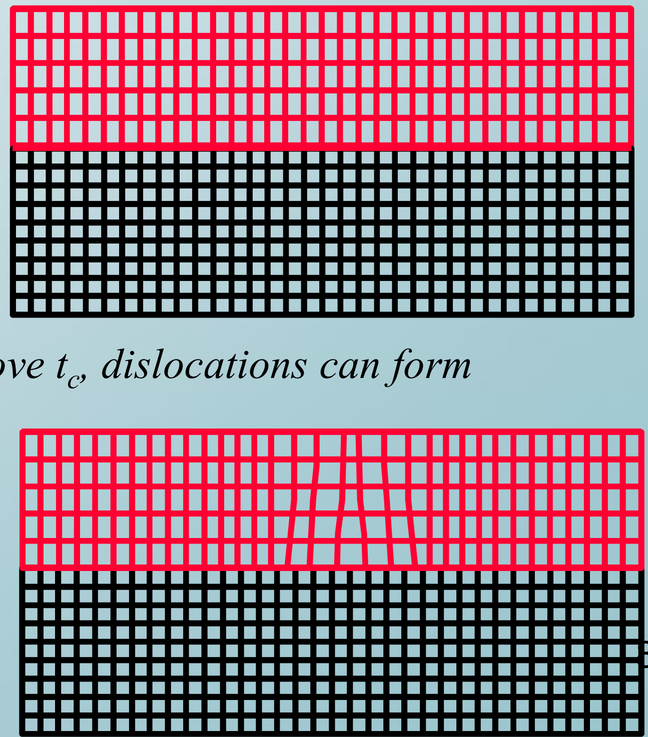

Above t_c, dislocations can form

Example: coherency stresses

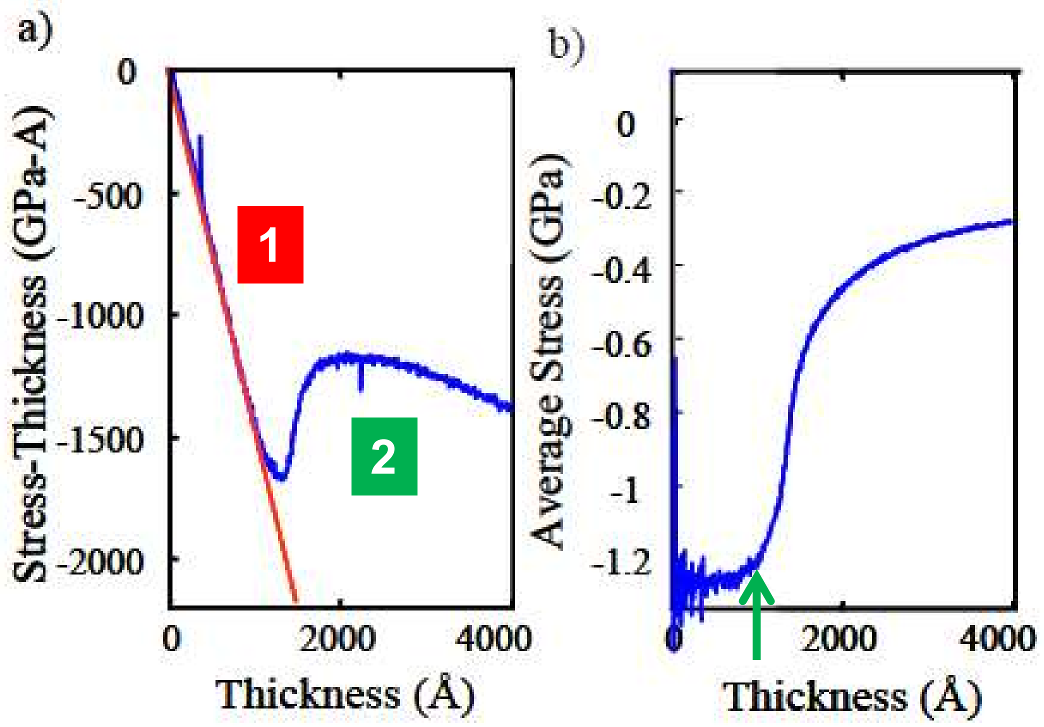

Figure 6. a) Evolution of curvature (converted to units of stress-thickness) in $In_{0.18}Ga_{0.72}As$ layers grown on GaAs(100). b) Average stress in the film calculated from the curvature.

from Beresford et al., J. Vac. Sci. Technol. B18, 1431 (2000).

1 compressive stress due elastic strain as layers growth pseudomorphically on GaAs substrate.

2 plastic relaxation due to the introduction of misfit dislocation above a critical thickness (↑)

Example: monitoring of QW growth

Growth of $In_xGa_{1-x}As$ quantum well (QW) on GaAs

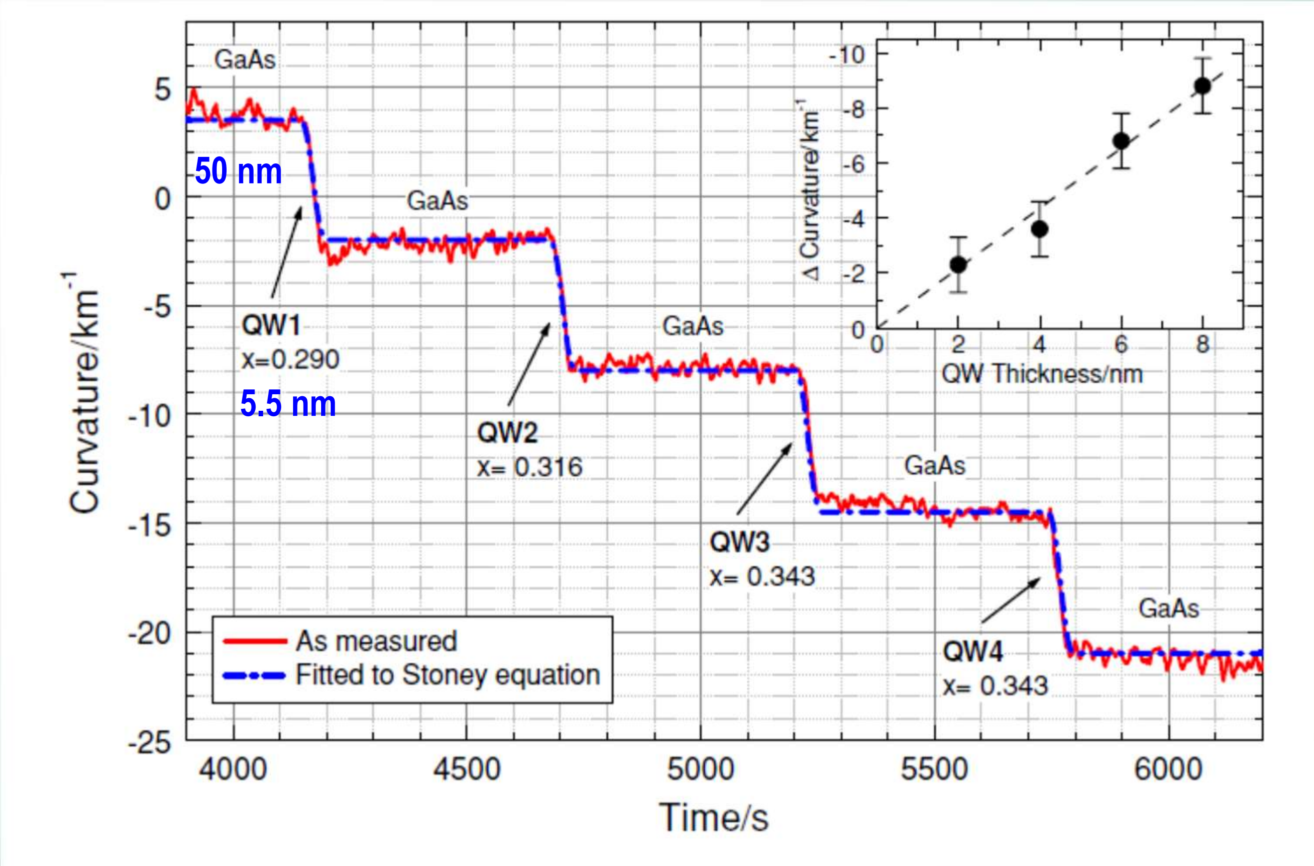

direct correlation between the curvature change and the indium content *x* can be obtained from Stoney equation

$$\Delta\kappa = -\frac{6h_{QW}}{h_s^2} \times \frac{a_{InAs} - a_{GaAs}}{a_{GaAs}}\, x$$

Zorn et al., Semicond. Sci. Technol. 21 (2006) L45–L48

Coupling with other *in situ* diagnostics

Coupling in situ MOSS and laser reflectance

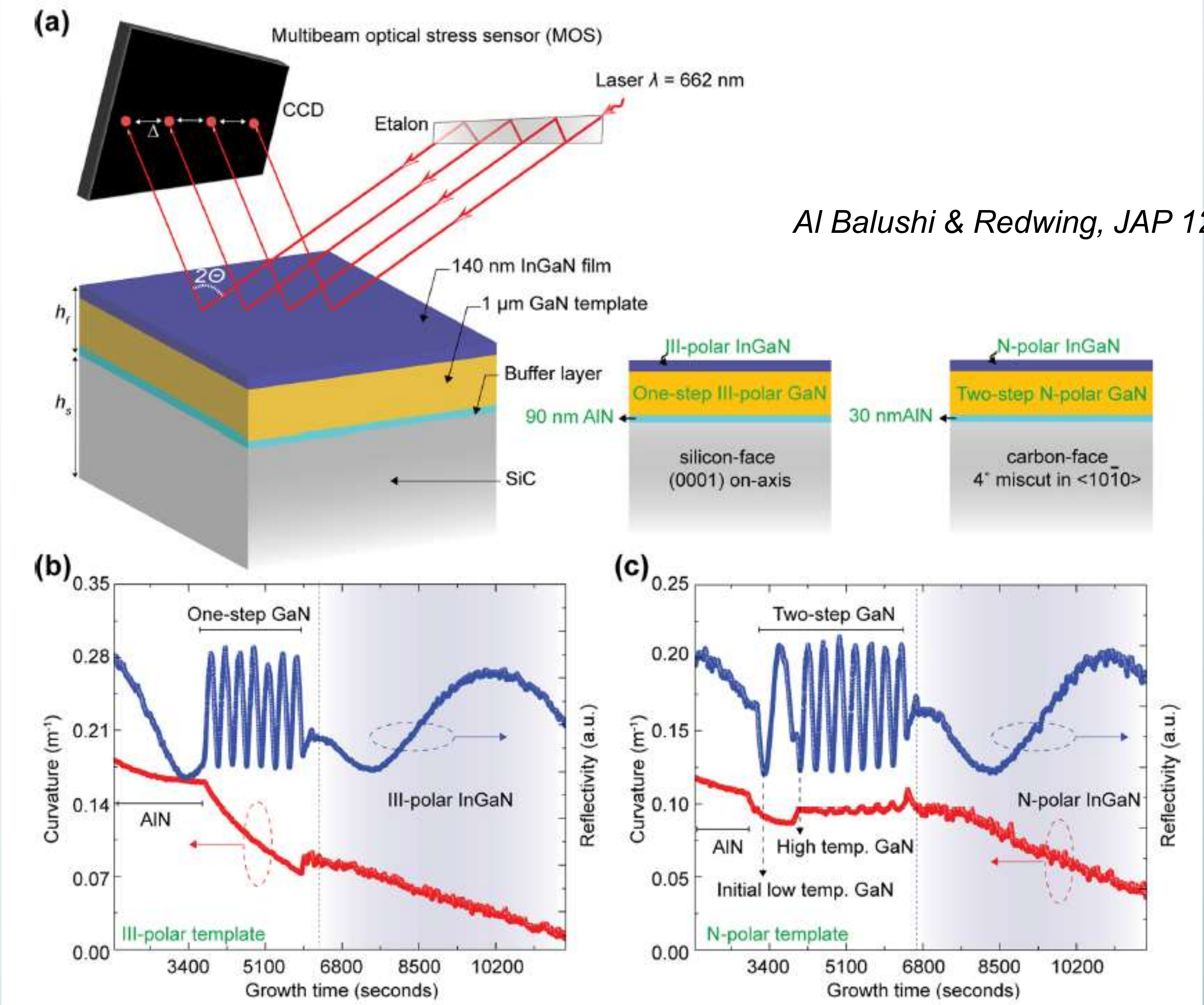

Al Balushi & Redwing, JAP 122, 085303 (2017)

- Film thickness h_f is determined from simultaneously collected oscillations in laser reflectance that results from Fabry–Perot constructive and destructive interferences during film growth
- This can also provide real-time monitoring of the morphological evolution and surface roughness of the films

Interface reactivity during Cu film growth

SDRS: principle of measurement

Surface differential reflectance spectroscopy

- Spectroscopic measurement: $\lambda \in [350 - 800 \text{ nm}]$
- Strong signal dynamic (signal to noise ratio: 1000:1)

$$\frac{\Delta R}{R_0}(t,\lambda) = \frac{R(t,\lambda) - R_0(\lambda)}{R_0(\lambda)}$$

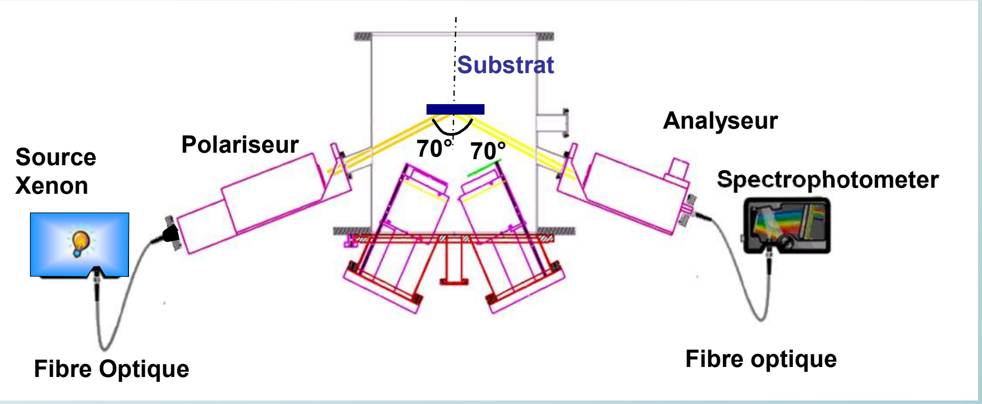

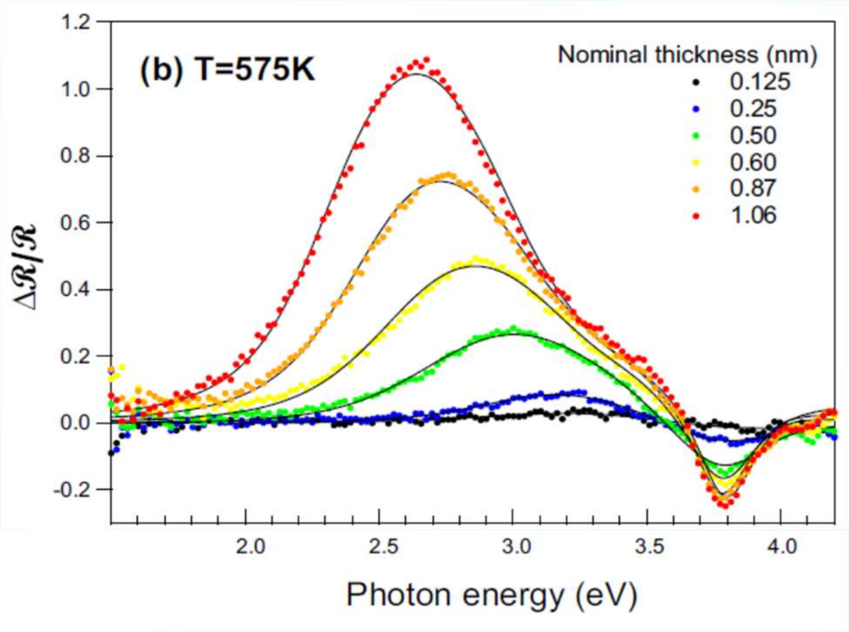

Possibility to fit SDRS data to extract morphological parameters, but needs a model

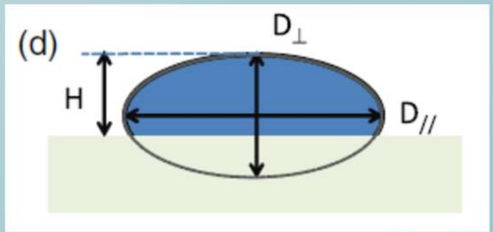

Grachev et al., J. Phys. D: Appl. Phys. ***46*** *(2013) 375305*

Four-point probe electrical resistance measurement setup

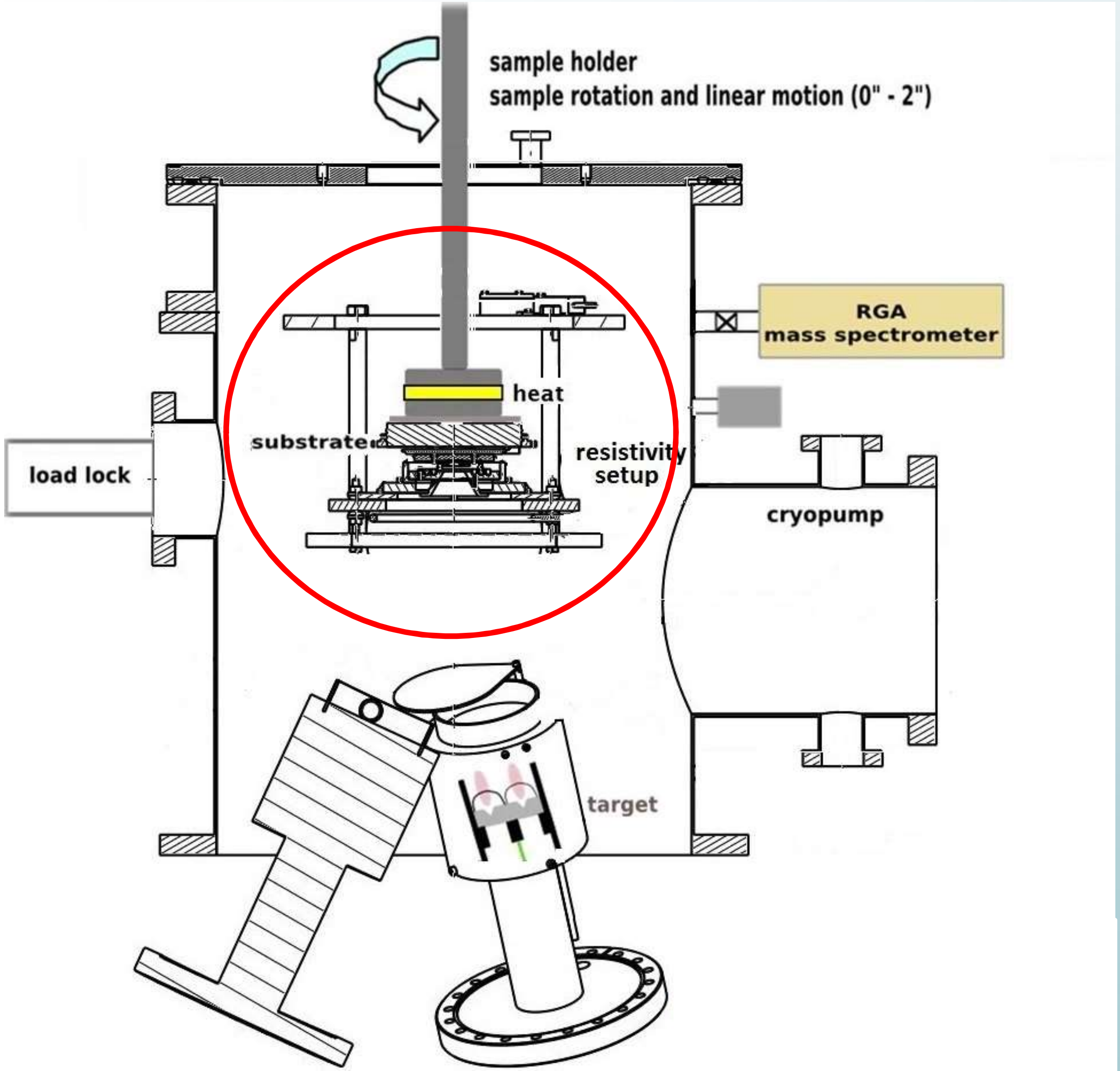

J. J. Colin et al., Rev. Sci. Instrum. 87 (2016) 023902

Four-point probe electrical resistance measurement setup

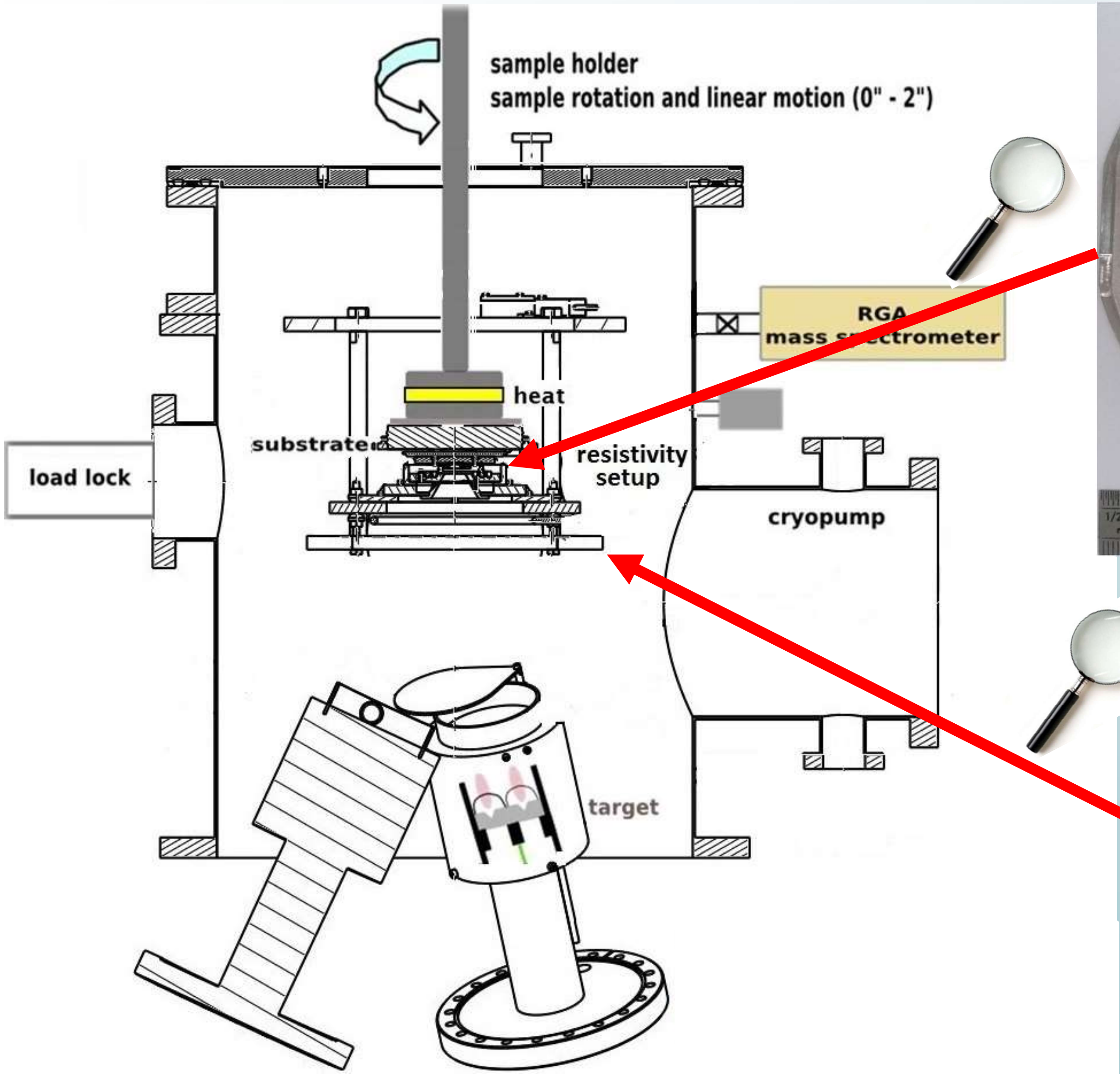

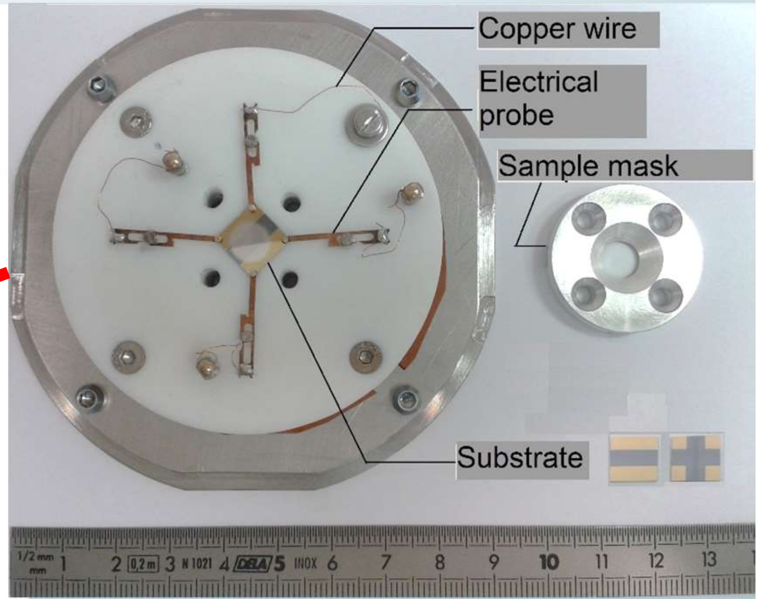

Specimen holder

Electrical collector

J. J. Colin et al., Rev. Sci. Instrum. 87 (2016) 023902

Electrical resistance evolution

Typical curve of resistance vs. time for metal growth on insulator

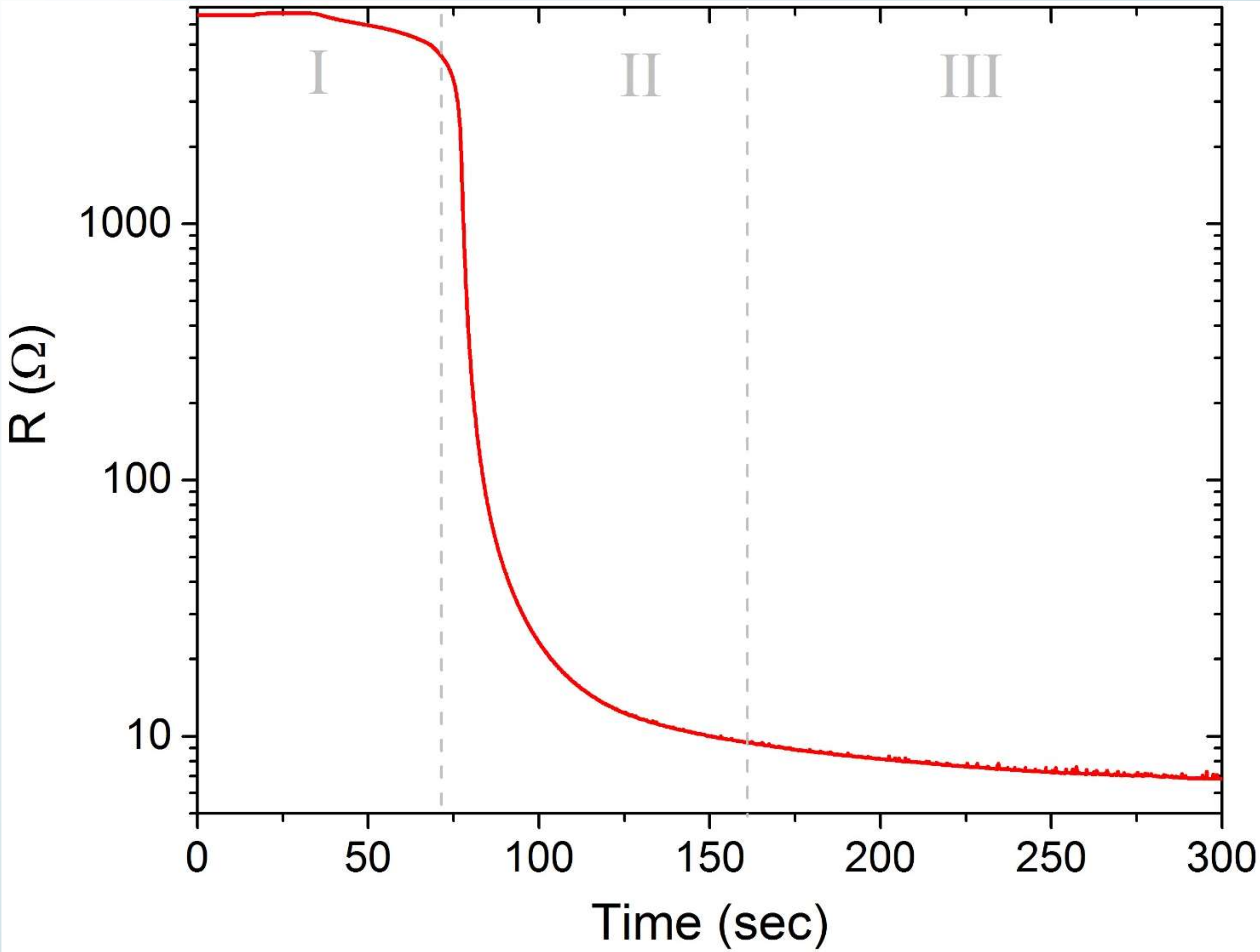

Resistance variation over several orders of magnitude

Acquisition rate: 10 Hz

Electrical resistance evolution

Typical curve of resistance vs. time for metal growth on insulator

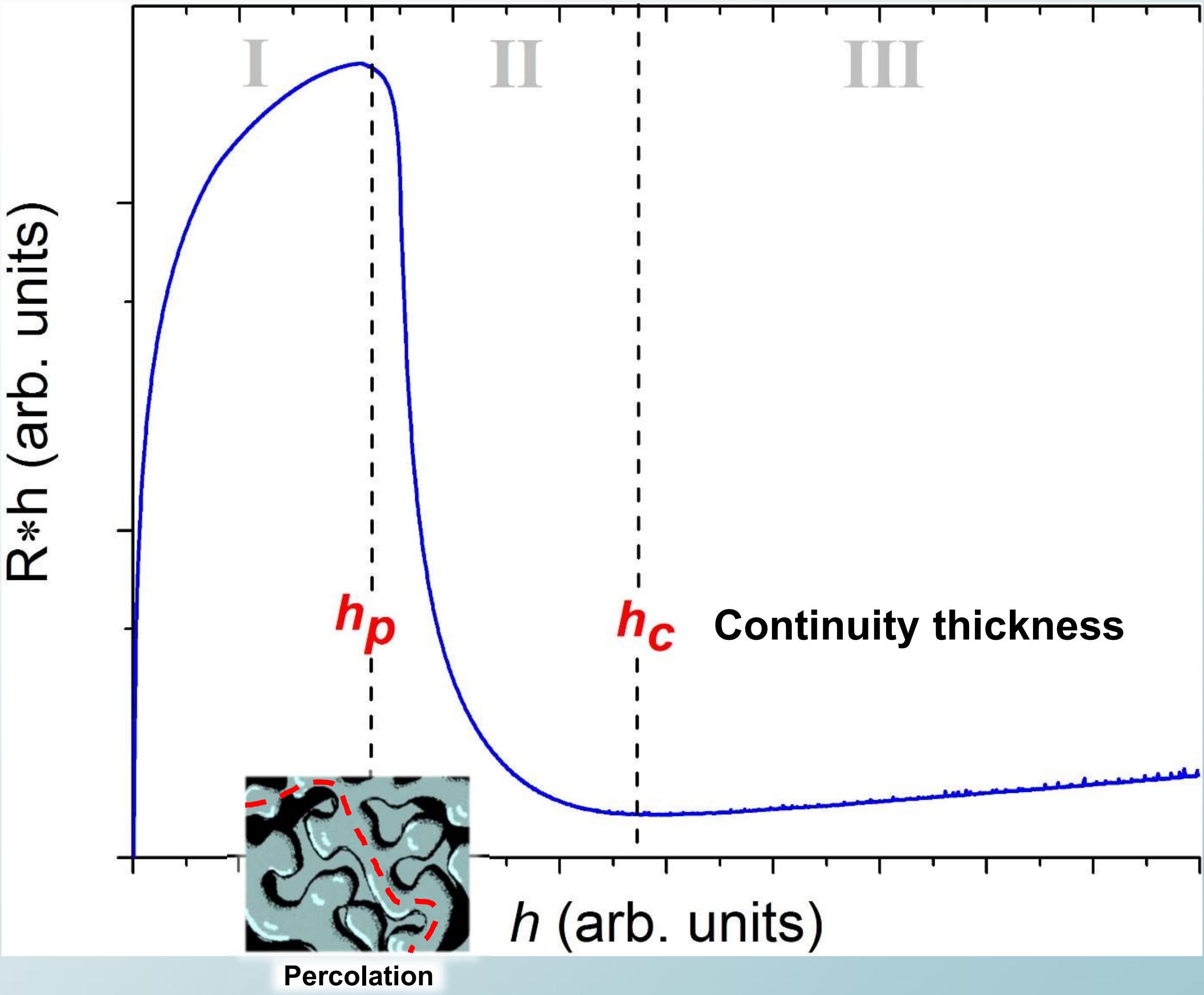

h_p: **Percolation thickness**

Coupling in situ MOSS, SDRS and resistivity

Cu film growth

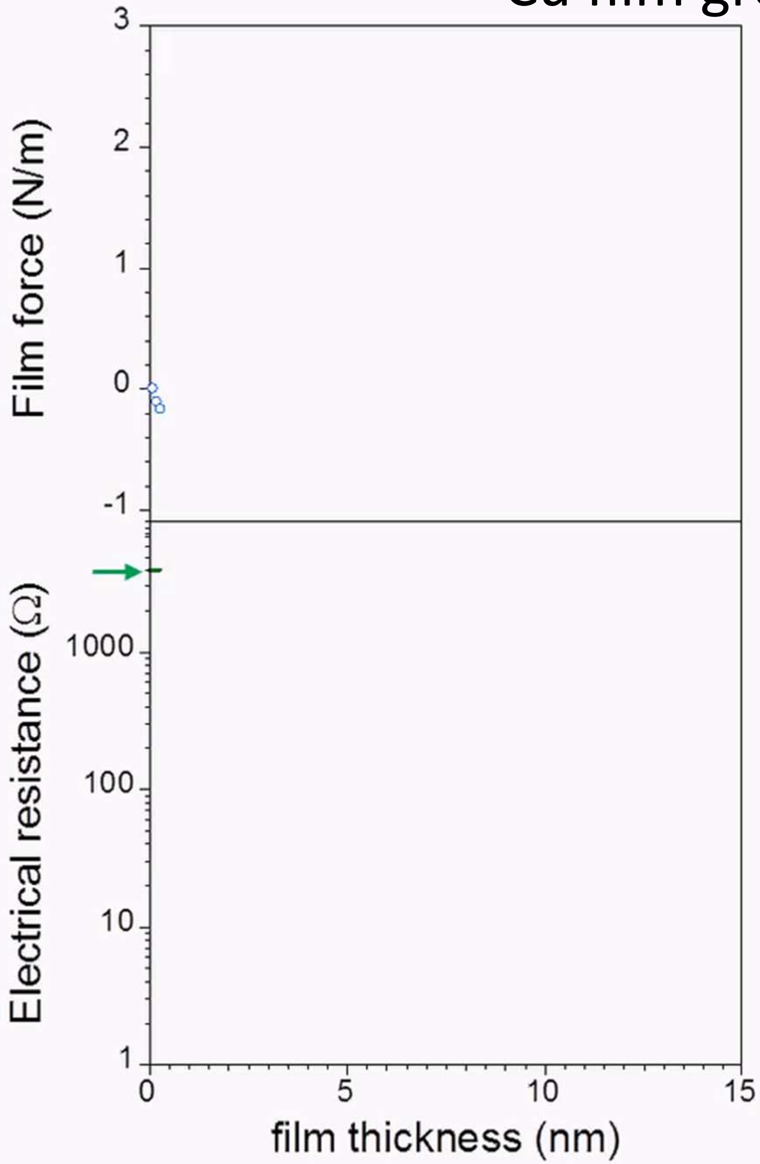

h= 0.3 nm

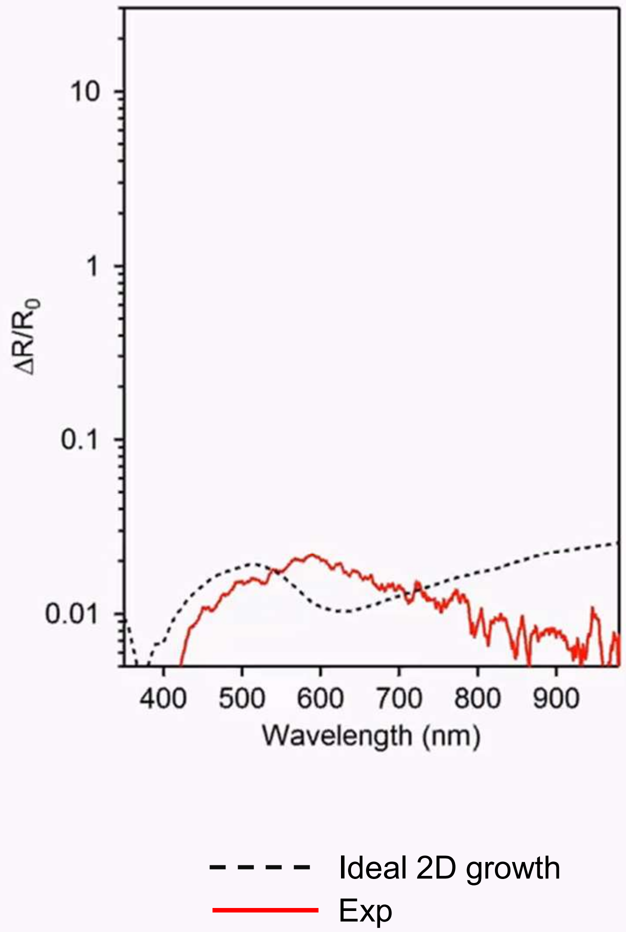

Cu on SiOx: growth characteristics

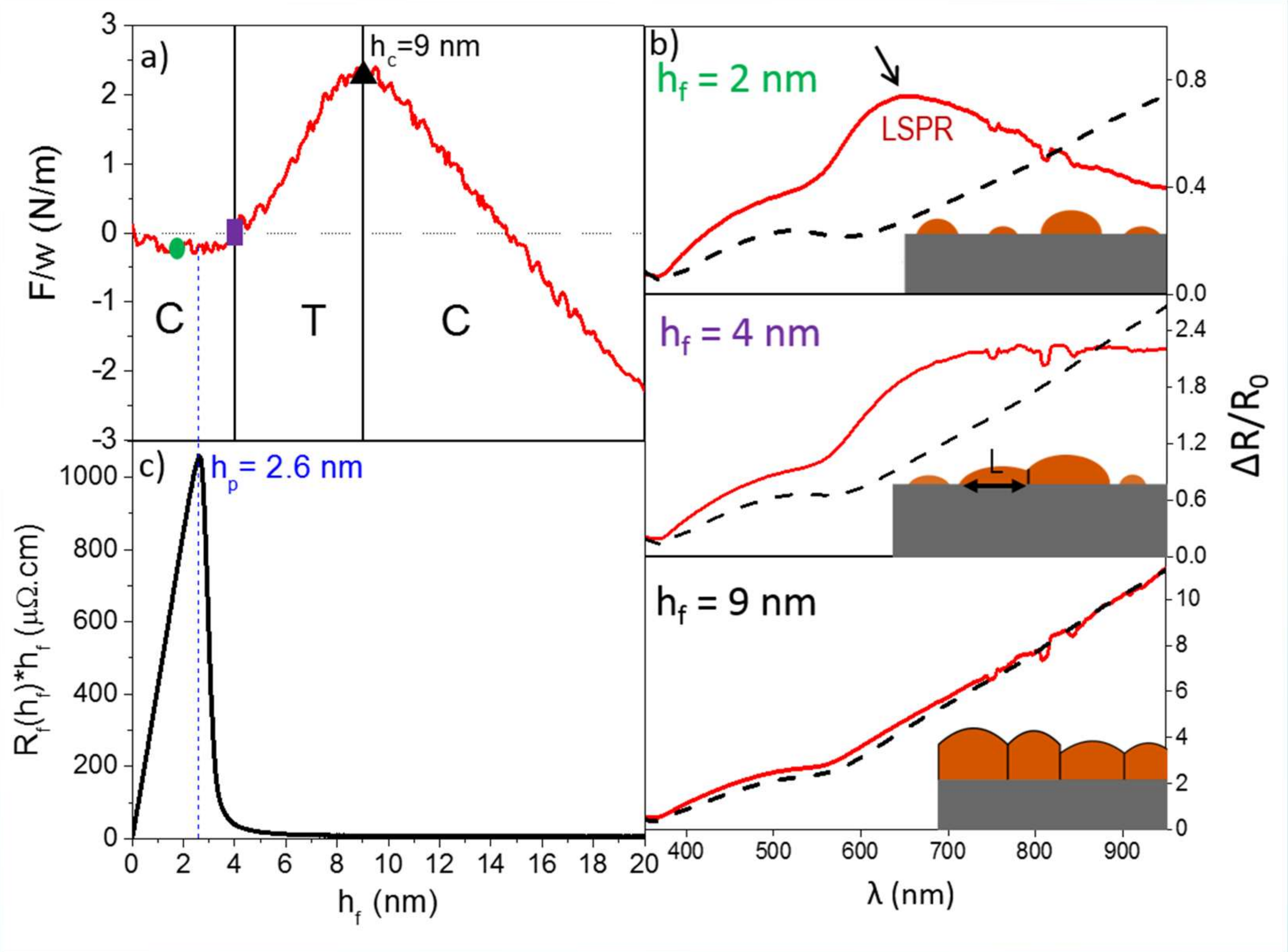

STEM-HAADF

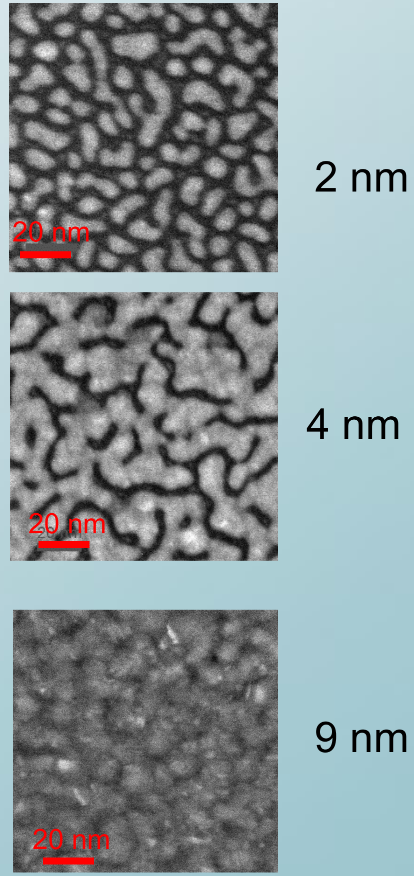

Comparison on SiOx and *a*-Ge

MOSS

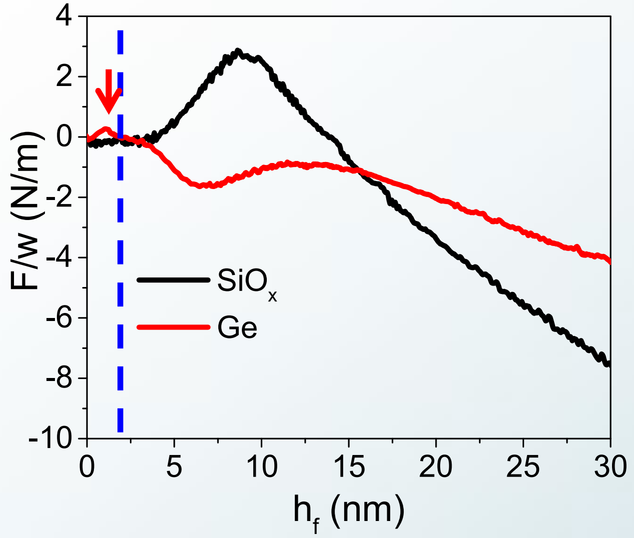

SDRS h_f=2 nm

SiO$_x$

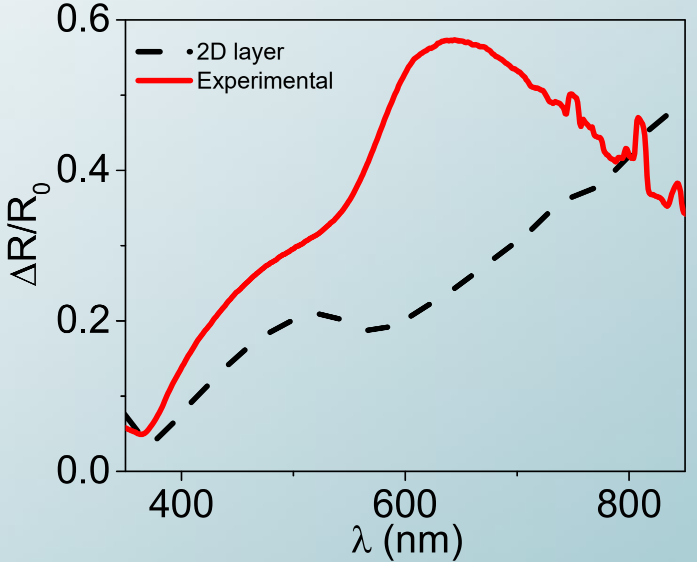

Resistance

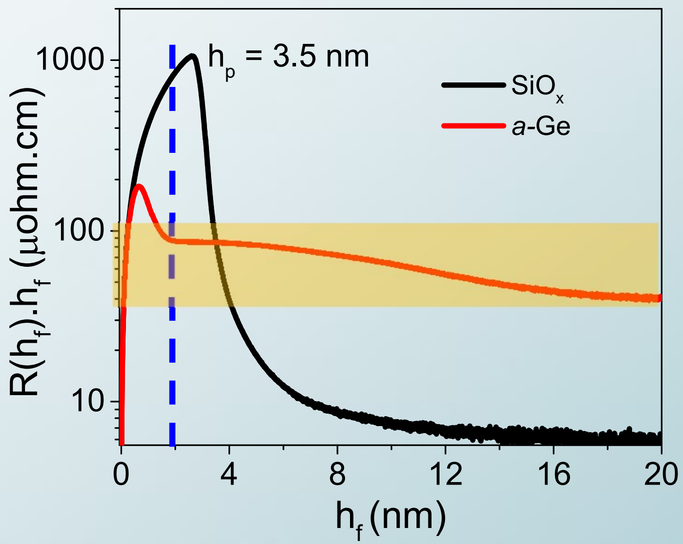

a-Ge

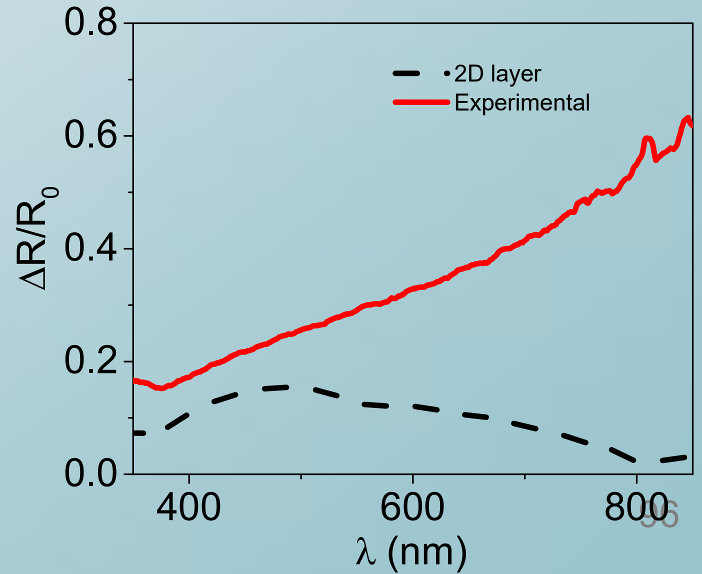

Segregation in Au/Ni multilayers

Coupling in situ MOSS and RHEED

Au/Ni multilayers

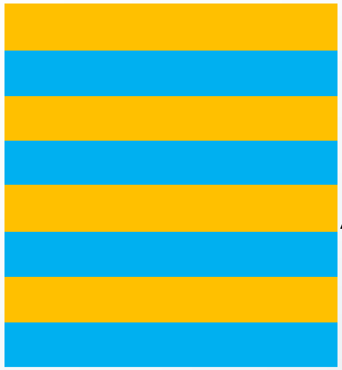

RHEED pattern

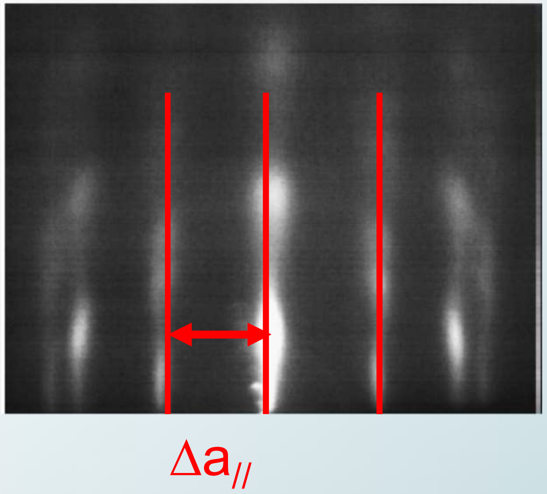

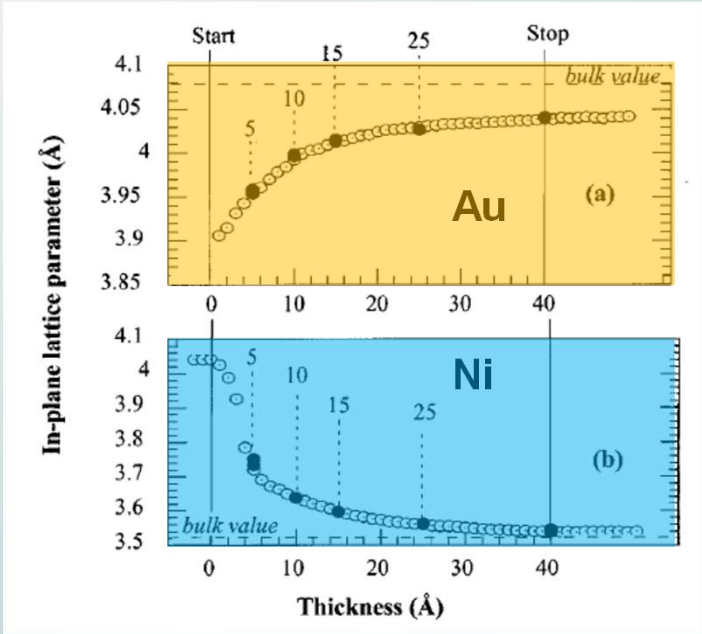

Wafer curvature

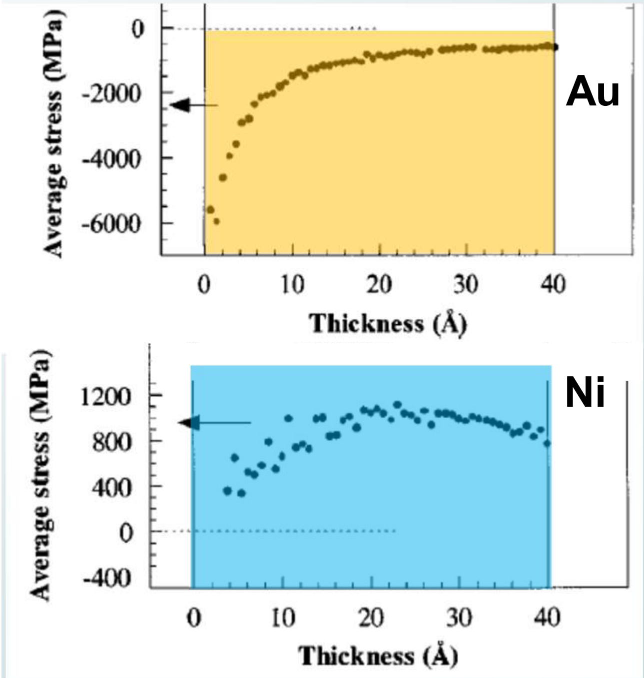

- Stress relaxation is observed in agreement with in-plane strain state for Au layers

- Opposite findings between stress and strain states in Ni layers
- *reason*: intermixed Ni(Au) layer due to surfactant character of Au

S. Labat et al., Applied Physics Letters 75, 914 (1999)

Coupling in situ MOSS and RHEED

determination of interface stress **f**

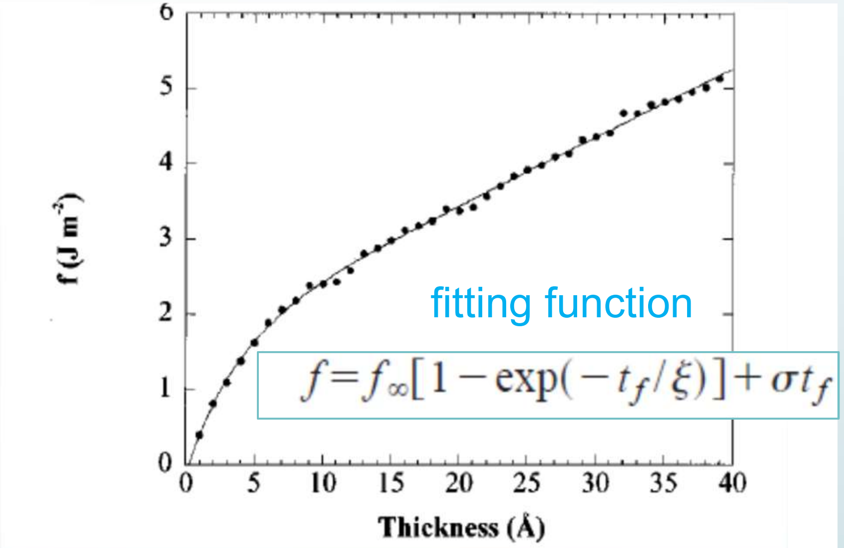

$$f = \langle \sigma_f \rangle \, h_f - Y_f \, \epsilon_f \, h_f$$

MOSS RHEED

determination of Au surface concentration $\mathbf{c_{Au}}$

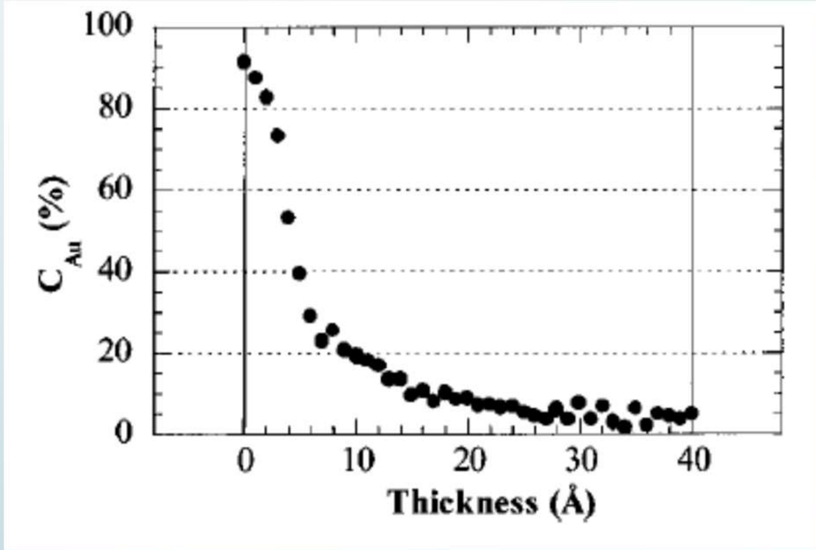

(surface stress has been neglected)

$$\Delta F = Y_{(x)} \, (a_{(x)} - a_{\parallel}) / \, a_{(x)} \, \Delta h_f$$

MOSS RHEED

S. Labat et al., Applied Physics Letters 75, 914 (1999)

Phase transformation in Mo/Si films

Coupling in situ MOSS, XRD and XRR

MPI beamline, ANKA synchrotron

SIXS beamline, SOLEIL synchrotron

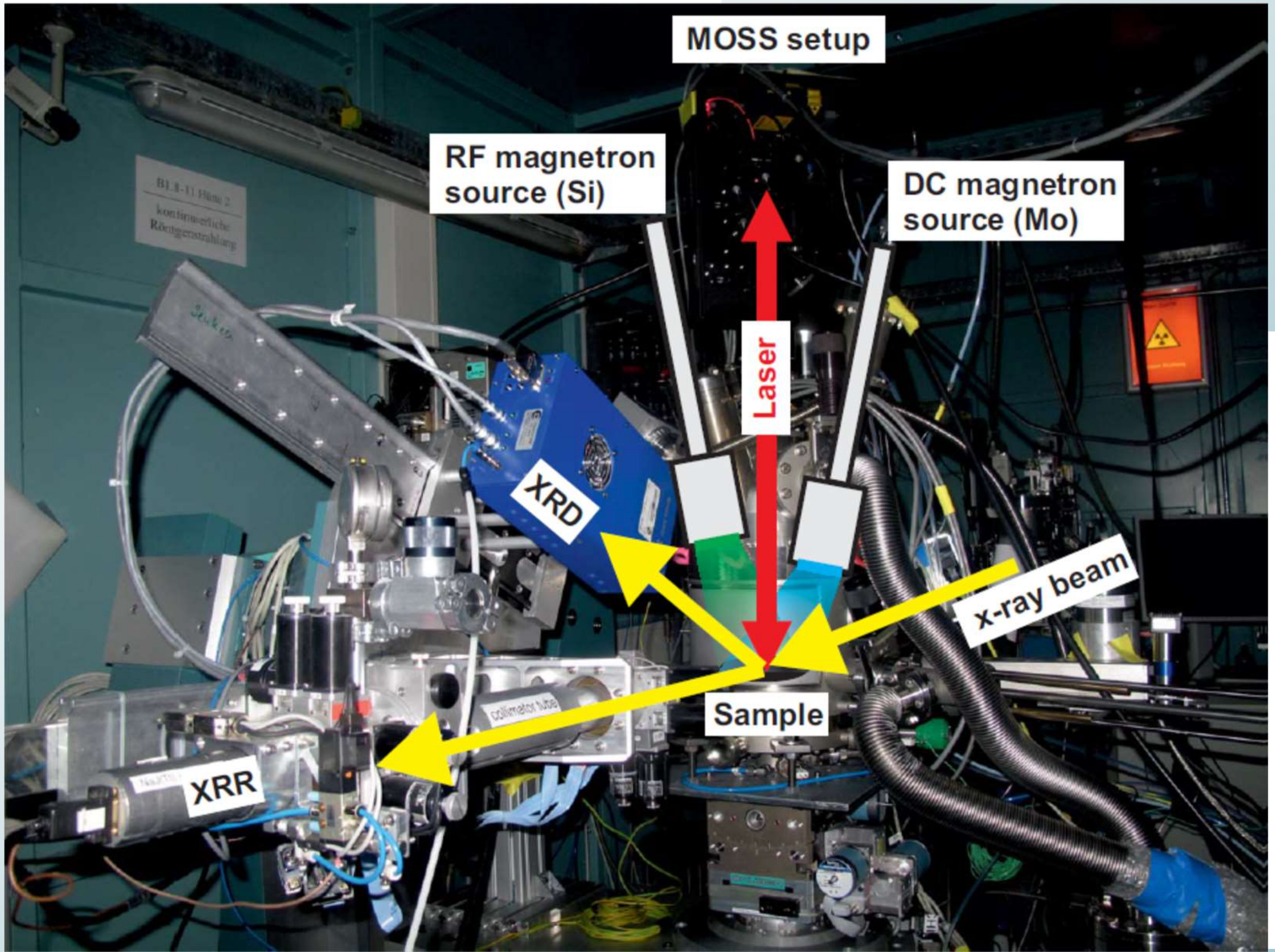

Collaboration B. Krause (KIT, Germany)

Coupling in situ MOSS, XRD and XRR

- **XRR signals**

Standard angular dependence

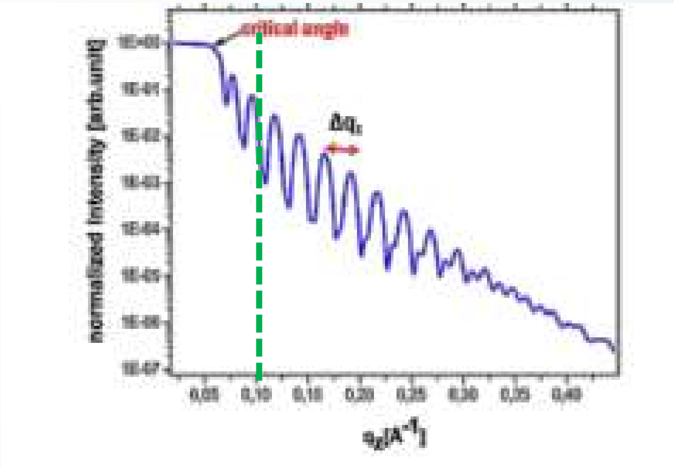

Time-dependence of XRR signal at fixed q position

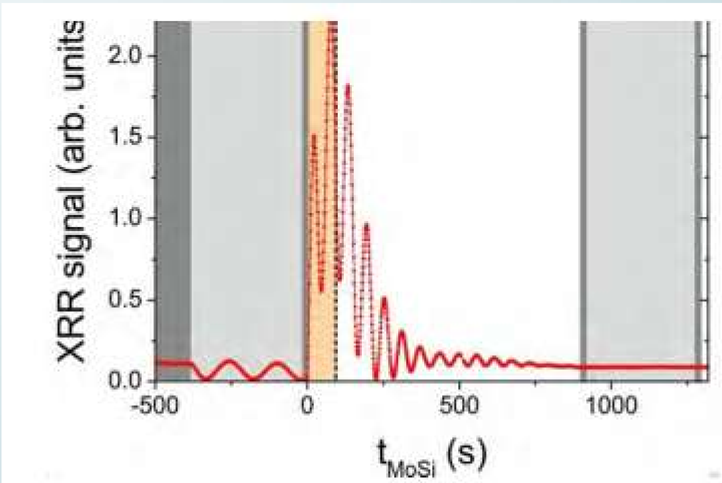

- **XRD signals**

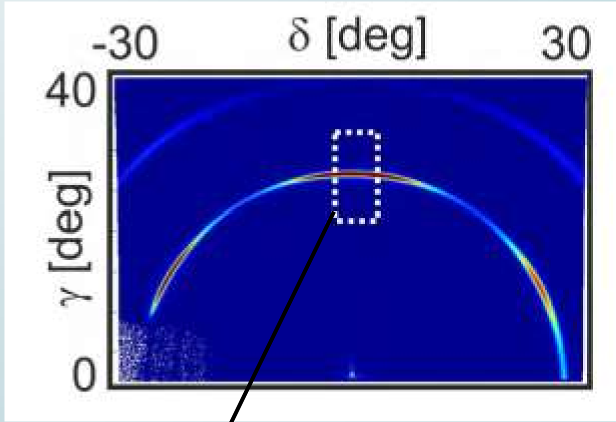

Time-dependence of reciprocal space XRD signal

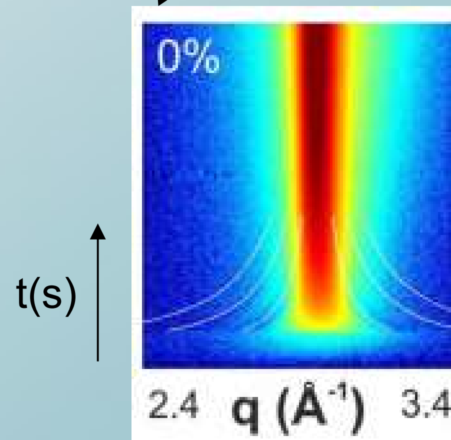

Coupling in situ MOSS, XRD and XRR

Case of pure Mo deposited on a-Si

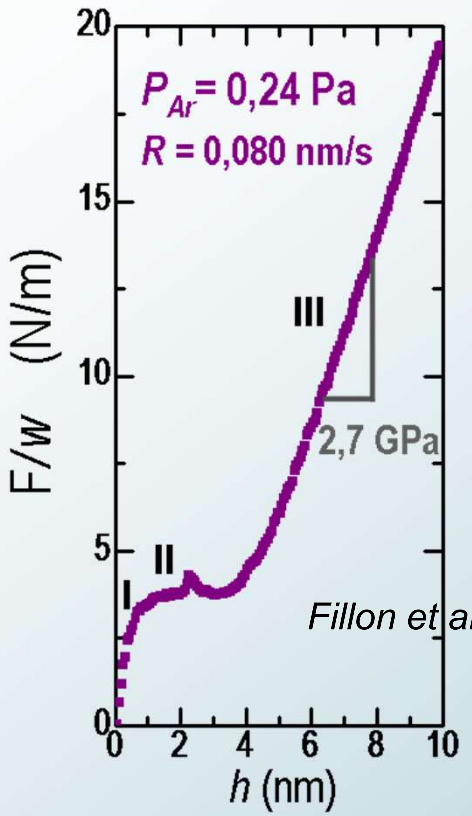

Fillon et al, PRL (2010)

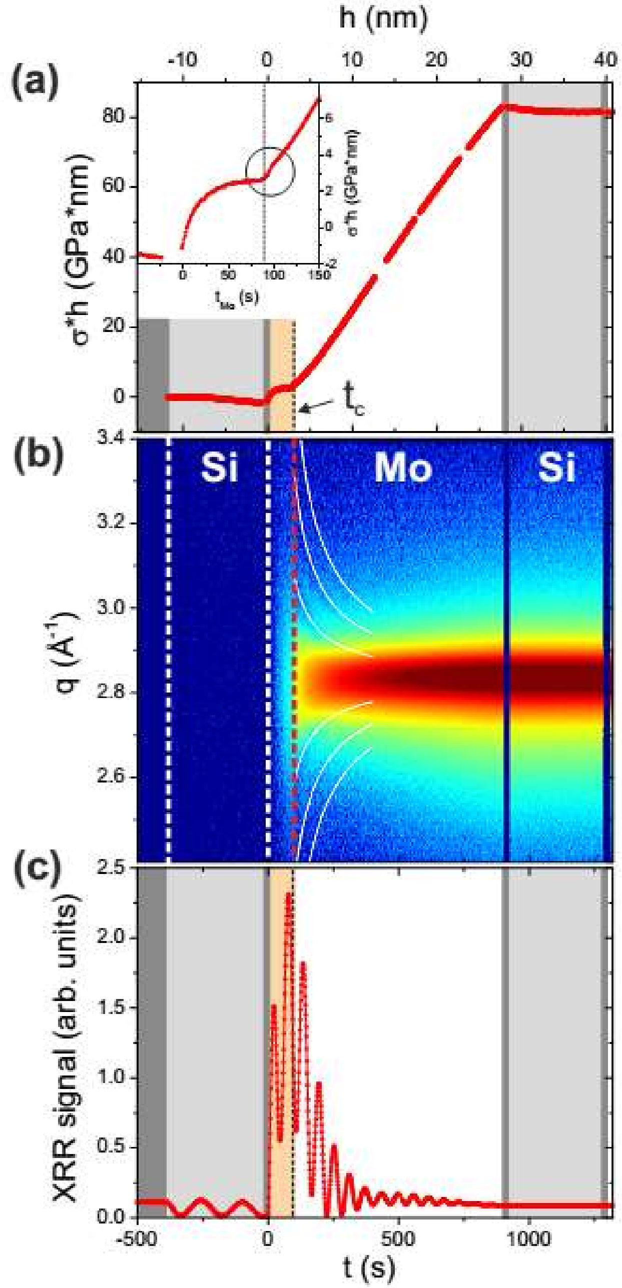

- Initial tensile rise due to change in surface stress
- Sudden tensile stress change after 90s concomittant with increase of XRD signal and decrease of XRR oscillations magnitude
- Steady-state tensile stress upon further growth

$Mo_{1-x}Si_x$ alloys deposited on a-Si

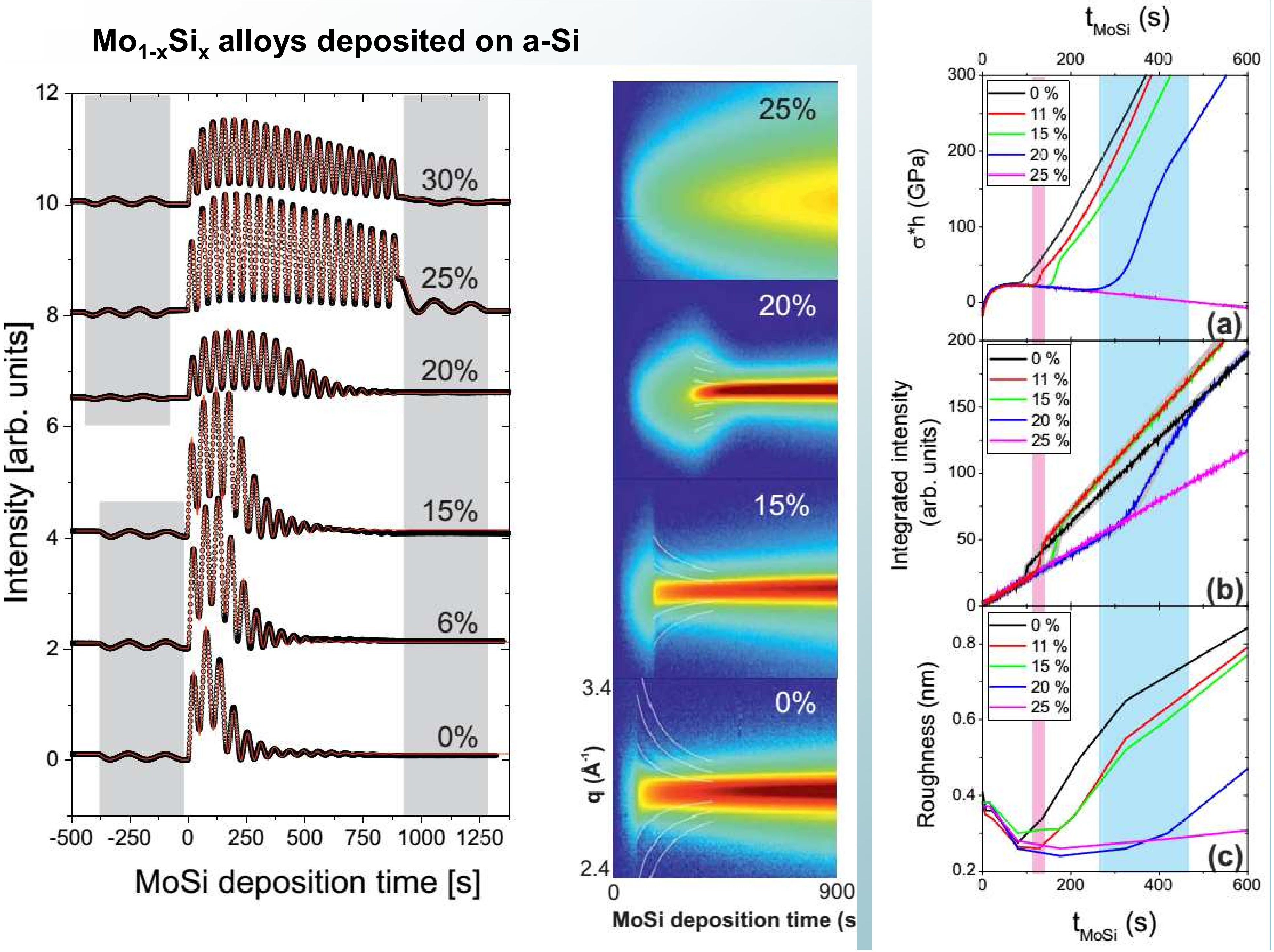

Conclusions

Tensile stress sources

- Grain growth : Chaudari
- Crystallite coalescence : Nix and Clemens
- Attraction between columns and voids formation

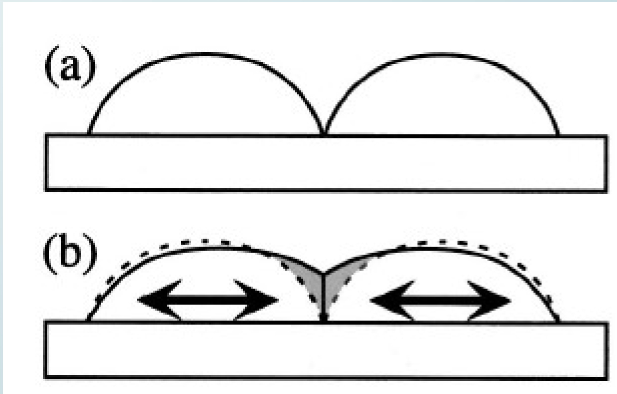

grain boundary « zipping » process

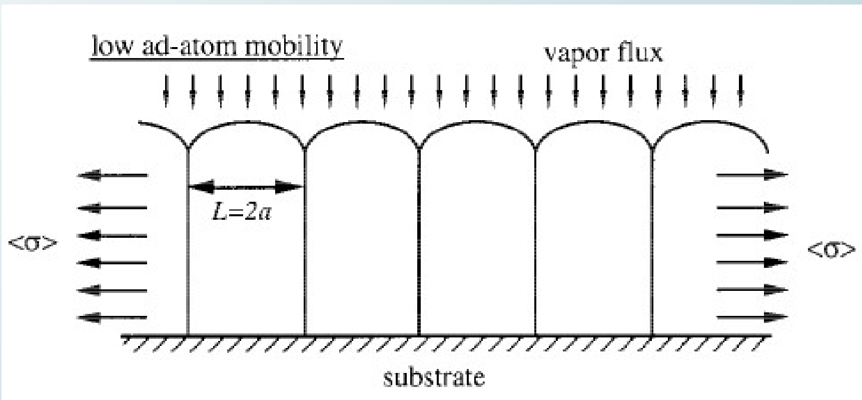

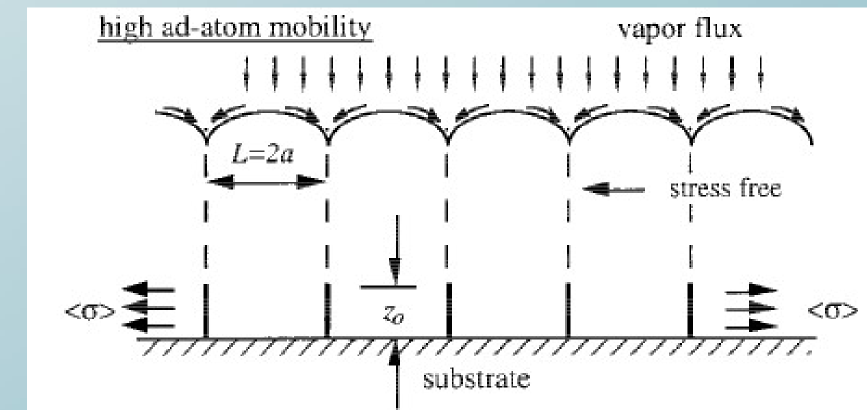

Atomistic mechanisms of stress generation in polycrystalline films

Compressive stress sources

- Laplace pressure (isolated island) and capillary-induced stress (continuous film)
- Incorporation of excess atoms at surface ledges : Spaepen
- Incorporation of excess atoms in GB due to $\mu_s > \mu_{GB}$: Chason
- Excess population of adatoms on the surface: Friesen
- “Atomic peening” mechanism

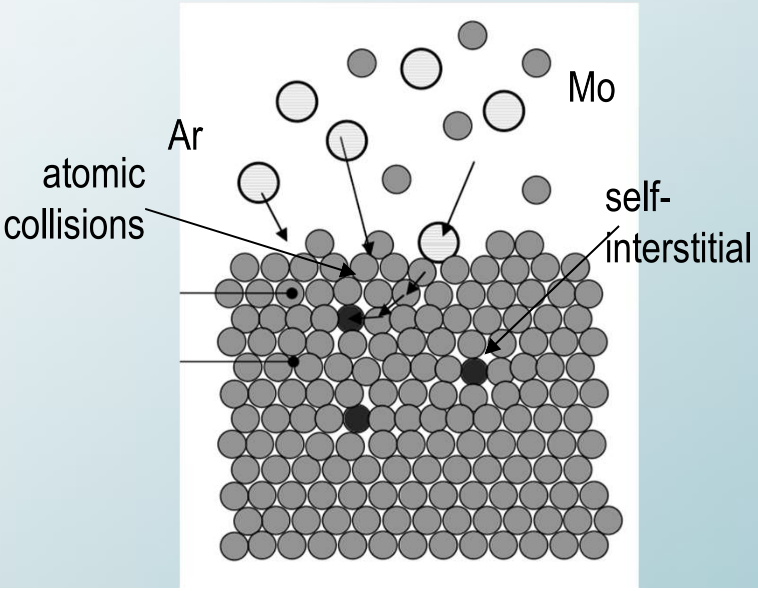

Some possible stress relaxation mechanisms

Relaxation kinetics are strongly dependent on deposition temperature and microstructural length scales

- Interfacial shear for weak film/substrate interaction
- Inclined shear: dislocations on inclined glide planes
- Viscous flow in amorphous materials
- Surface diffusion : morphological rearrangement, Ostwald ripening, flow of adatoms in the GB

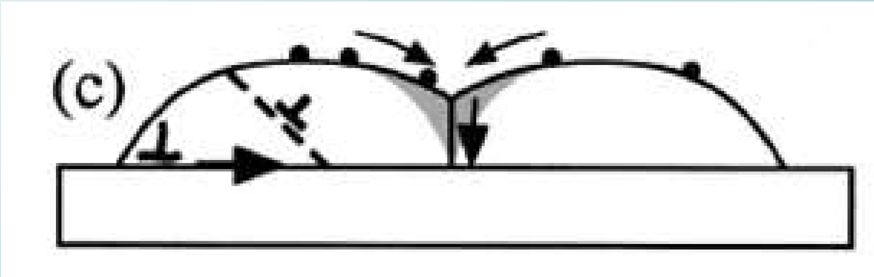

Floro et al., JAP 89 (2001) 4886

Conclusions

Wafer curvature laser deflectometry

- Non destructive, atomic-scale sensitive and time resolved technique
- Reflective material is required
- Macroscopic biaxial stress can be determined
- Limitations exist for film thickness/substrate ration > 0.5 %
- Ease implementation during thin film growth, thermal cycling, ion irradiation
- Possibility to implement during electrodeposition
- Coupling with other in situ diagnostics (RHEED, optical reflectance, ellipsometry,…) is possible

REVIEW ARTICLE

Journal of Vacuum Science & Technology A
36, 020801 (2018);

Review Article: Stress in thin films and coatings: Current status, challenges, and prospects

Grégory Abadias[a)]
Département de Physique et Mécanique des Matériaux, Institut Pprime, UPR 3346, CNRS-Université de Poitiers-ENSMA, SP2MI, Téléport 2, F86962 Futuroscope-Chasseneuil, France

Eric Chason[b)]
School of Engineering, Brown University, Providence, Rhode Island 02912-9104

Jozef Keckes[c)]
Department of Materials Physics, Montanuniversität Leoben and Erich Schmid Institute for Materials Science, Austrian Academy of Sciences, Leoben 8700, Austria

Marco Sebastiani[d)]
Engineering Department, University of Rome "ROMA TRE," Via della Vasca Navale 79, Rome 00147, Italy

Gregory B. Thompson[e)]
Department of Metallurgical and Materials Engineering, The University of Alabama, P.O. Box 870202, Tuscaloosa, Alabama 35487-0202

Etienne Barthel[f)]
Laboratoire Sciences et Ingénierie de la Matière Molle, ESPCI Paris, PSL University, Sorbonne Université, CNRS, F-75005 Paris, France

Gary L. Doll[g)]
Mechanical Engineering Department, The University of Akron, Akron, Ohio 44325-0406

Conal E. Murray[h)]
IBM T.J. Watson Research Center, Yorktown Heights, New York 10598

Chris H. Stoessel[i)]
Eastman Chemical Co., 3788 Fabian Way, Palo Alto, California 94303

Ludvik Martinu[j)]
Department of Engineering Physics, Polytechnique Montréal, Montreal, Quebec H3T 1J4, Canada

(Received 3 November 2017; accepted 9 February 2018; published 5 March 2018)

May 27-31, 2019, Nice, France

2019 E-MRS Spring Meeting

Symposium N: Nano-engineered coatings and thin films: from design to applications

Symposium Organizers:	Dr. K. Sarakinos, IFM Linköping (Sweden) Prof. G. Abadias, Institut Pprime (France) Prof. P. Patsalas, Univ. Thessaloniki (Greece)
Abstract submission deadline:	**January 15, 2019**

www.european-mrs.com/meetings/2019-spring-meeting